Title

Tuning Interactions Between Contaminants and Surfaces: Applications Ranging from Biological Treatment to Biofouling Prevention

Author

Ramos, Maria Pia

Publication Date

2022

Peer reviewed|Thesis/dissertation

UNIVERSITY OF CALIFORNIA

Los Angeles

Tuning Interactions Between Contaminants and Surfaces: Applications Ranging from Biological Treatment to Biofouling Prevention

A dissertation submitted in partial satisfaction of the

requirements for the degree Doctor of Philosophy

in Civil Engineering

by

Maria Pia Ramos

2022

ABSTRACT OF THE DISSERTATION

Tuning Interactions Between Contaminants and Surfaces: Applications Ranging from Biological Treatment to Biofouling Prevention

by

Maria Pia Ramos

Doctor of Philosophy in Civil Engineering

University of California, Los Angeles, 2022

Professor Shaily Mahendra, Chair

The fundamental understanding and control of the interactions that occur between surfaces and chemicals allows us to design materials with enhanced binding and reactive properties for various industrial, environmental, and clinical applications. However, understanding and optimizing these interactions can also be used to limit the attachment and accumulation of undesirable substances and organisms to surfaces which may otherwise hinder their successful operation. This dissertation describes research on the tuning and optimization of surfaces and operating conditions for different purposes ranging from biological treatment of

water and wastewater to the prevention of the undesired attachment of microbial biofilms to functional surfaces.

Modification of the surface of granular activated carbon (GAC) using the cationic polymer polydialydimethyl ammonium chloride (polyDADMAC) was studied as a strategy to improve the removal of the persistent environmental contaminant class per- and polyfluoroalkyl substances (PFASs). Specifically, complex water matrices were used in these studies to simulate challenging conditions that are environmentally relevant. Amending the surface with polyDADMAC concentrations as low as 0.00025% enhanced GAC's adsorption capacity for both short- and long-chained PFASs, even in the presence of competing ions. Regeneration with minimum disruption to the adsorbent's structure was achieved using low-power ultrasound, supporting the consideration of polyDADMAC-modified GAC was an effective, regenerable adsorbent for real environmentally relevant water conditions.

The relationships between the influent nutrient ratios in the context of wastewater treatment and the mechanisms responsible for biofilm formation were investigated. Wastewater treatment is an example of a scenario where biofilm formation may be either desirable or undesirable depending on the treatment system being employed. A comprehensive evaluation of the effect of Carbon/Nitrogen ratio in influent wastewater on biofilm characteristics and relevant mechanisms were studied. *Pseudomonas aeruginosa* was used as a model organism due to its widely understood biofilm formation pathways, as well as its prevalence in the environment, distribution systems, and in clinical settings. The development of a dual-species biofilm of *P. aeruginosa* and *N. winogradskyi* was also influenced by C/N, with increase in the relative abundance of the slower-growing *N. winogradskyi* above C/N=9. These results indicate that altering operational

parameters related to C/N may be relevant for mitigating or promoting biofilm formation and function depending on the desired industrial application or treatment configuration.

Despite the benefits of chemically- and biologically mediated surface modifications, microbial adhesion to surfaces can also be detrimental in the context of biofouling, which yields industrially relevant surfaces such as water treatment membranes less efficient or causes adverse patient health outcomes in clinical settings. In this context, a culture-independent biofilm quantification protocol was developed to accurately quantify cellular and extracellular components attached to medically relevant surfaces such as urinary catheters. The developed multipronged approach had validated efficacy as it was verified to accurately quantify biofilms of four pathogenic clinical isolates, two types of silicone catheters *in vitro* and indwelling catheters in patients.

Characterization and assessment of synthesized hydrogels made of a modified chitosan/ silver nanoparticle composites showed the potential of these material for antimicrobial and antifouling purposes. Three synthesis methods were compared in terms of their effects on the physical, mechanical, and antimicrobial capabilities of the hydrogels, and evaluation showed the potential for tuning the synthesis to yield materials with different physical and mechanical properties but equally promising antimicrobial and antifouling potential. This gives rise to the possibility of using these composites in a range of industrially relevant scenarios depending on the desired characteristics for use.

The quantitative understanding of factors impacting surface modifications and microbial attachment to surfaces will be valuable for improved water treatment systems as well as to limit or help guide biofilm formation on medically- and industrially relevant surfaces.

The dissertation of Maria Pia Ramos is approved.

Sanjay K. Mohanty

Jennifer Ayla Jay

Richard B. Kaner

Shaily Mahendra, Committee Chair

University of California, Los Angeles

2022

Table of Contents

List of Figures

List of Tables

Acknowledgements

First I would like to express my deep gratitude to my advisor and committee chair, Dr. Shaily Mahendra. Dr. Mahendra introduced me to the world of water treatment and microbiology. Her own passion for the field and her guidance has inspired me and contributed greatly to my academic advancement and research career. Professor Mahendra has supported me to pursue unique areas of research in ways that have helped me grow individually and professionally. I am grateful and inspired to bear witness to her enthusiasm, creativity and commitment to education. I would also like to thank my committee members Professor Sanjay Mohanty, Professor Jennifer A. Jay and Professor Richard B. Kaner. Each of them was an integral part of my PhD by providing important insights for my growth and education, and by helping me pursue distinct areas of my research through their guidance.

I would also like to thank other research mentors who have been integral to the development of the research in Chapter 4 and Chapter 6 as well as my own individual and professional growth throughout my PhD. In a collaboration with Dr. Eric M.V. Hoek I was introduced to the world of wastewater treatment and energy recovery, and have learned valuable lessons about the intersection of engineering and entrepreneurship that I hope to carry to my future career. Dr. Moshe Gottlieb of Ben Gurion University of The Negev has introduced me to the world of polymers and materials chemistry as a research mentor since my undergraduate days, and I am certain that I would not be where I am today without his support and mentorship.

I am also very grateful to my research collaborators for each project. Dr. Jens Blotevogel and Dr. Gregory Dooley for their help and guidance on everything PFAS. Also Drs. Poonam Kulkarni and David Adamson of GSI Environmental, as well as Jovan Popovic, Anthony Danko, John J. Kornuc, and Arun R. Gavaskar of US Navy for their research support.

I am very grateful to Dr. Kaner and his students Dr. Brian McVerry and Ethan Rao for introducing me to the world of surface chemistry and biofouling. This collaboration, which was one of the very first projects I started helping with in this lab, was inspiring for all my subsequent research as well as my future research and career, and also resulted in the research presented in Chapter 5. I would also like to thank all of the researchers I worked with at Ben Gurion University, Dr. Einat Chetrit, Nofar Yehuda, David Kogan, Dr. Einat Nativ-Rith Dr. Ariel Kushmaro, Dr. Ronen Berkovich for their support and collaboration in the research presented in Chapter 6. Thank you also to Dr. Ryo Honda of Kanazawa University for his guidance and research mentorship on wastewater treatment and bacterial biofilms, which was invaluable for the experimental design in Chapter 4.

I would like to thank Kshitija Shah and Kevin Clack for their endless collaboration and friendship throughout the development of the project presented in Chapter 4. Together we have faced and overcome many challenges, and I am excited to see where they will take the subsequent stages of that exciting research.

The work presented in this dissertation would not have been possible without the mentorship of previous Mahendra lab members Dr. Alexandra Polasko, Dr. Nicholas Johnson, and Dr. Yu Miao. Thank you for all of your initial guidance and for your kindness and continued support over the years, and thank you for inspiring me to follow in your footsteps in our lab. I would also like to thank other former and current Mahendra lab members Dr. Meng Wang, Dr. Shashank Kalra, Catherine Clark, Jerry Ngo and Ben Croze as well as Ivy Kwok, Yifan Gao, David Zgonc and Dr. Himadri Bose. Thank you also to my undergraduate research assistants Katerina Jowid and Drew Ferketic.

I would like to thank the UCLA Department of Life Sciences as well as the California NanoSystems Institute NanoScience Outreach Program for helping me strengthen my teaching skills and discover an interest in education and inclusion. Thank you to everyone in the Department of Civil and Engineering who has guided me through all the crucial administrative tasks necessary to successfully make it through UCLA. Thank you Dr. Vanessa Thulsiraj, Mimi Baik, Stacey Tran Fong, Helen Weary, Melissa Custodio, Dr. Ben Rossi, Dr. Eric Ahlberg.

This research was supported by United States Naval Facilities Engineering and Expeditionary Warfare Center (NAVFAC EXWC) [award # N3943018C2076], National Defense Center for Energy & Environment (NDCEE) [award # N3943019C2149], Oceankind, The National Philanthropic Trust, and UCLA Civil and Environmental Engineering Department. Additionally I would like to thank all the companies and organizations that have provided scholarships to help me through graduate school including, Eugene V. Cota-Robles, The Israeli Council for Higher Education, Innovations at The Nexus of Food, Energy, and Water Systems-Graduate Traineeship in Integrated Urban Solutions (NRT-INFEWS) funded by the National Science Foundation, and Hydrophilix.

Thank you to all my friends who have become family over all these years, and who have supported me through all the ups and downs. Thank you to my brother for your humor y por ser mi inspiración desde siempre. Lastly I would like to express my deepest gratitude to my parents. To my mom, nada de esto hubiera sido posible sin tu sacrificio y dedicación a mi, and to my dad muchas gracias por todo tu esfuerzo y apoyo en todo siempre. Nothing would be possible without your endless love and support throughout the years. Todo es gracias a ustedes y para ustedes.

Vita

EDUCATION

M.Sc. Environmental Engineering, University of California, Los Angeles 2019

B.Sc. Environmental Science, B.A. Public Policy Studies, The University of Chicago 2018

PUBLICATIONS

Ramos, P., Kwok, Ivy Y., Ngo, J., Zgonc, D., Miao, Y., Pornwongthong, P., Blotevogel, J., Mahendra, S. (2022). A, B, Cs of 1,4-dioxane removal from water: Adsorption, biodegradation, and catalysis.. Curr Opin Environ Sci Health. **29**: 100386. DOI: https://doi.org/10.1016/j.coesh.2022.100386

Ramos, P., Kalra, S. S., Johnson, N. W., Khor, C. M., Borthakur, A., Jassby, D., Kranmer, B., Dooley, G., Mohanty, S. K., Blotevogel, J., & Mahendra, S.(2022) Enhanced Removal of Per- and Polyfluoroalkyl Substances in Complex Matrices by polyDADMAC-Stabilized Granular Activated Carbon with Regeneration Potential. Environ Pollut **294**: 118603. DOI: https://doi.org/10.1016/j.envpol.2021.118603

Borthakur, A., Kumar, Das, T., Zhang, Y., Libbert, S., Prehn, S., **Ramos, P.**, Dooley, G., Blotevogel, J., Mahendra S., Mohanty S. "Rechargeable stormwater biofilters: In situ regeneration of PFAS removal capacity by using a cationic polymer, polydiallyldimethylammonium chloride" (2022). J Clean Prod **375**: 134244. DOI: https://doi.org/10.1016/j.jclepro.2022.134244

McVerry, B; Polasko, A; Rao, E., Haghniaz, R., Chen, D. He, N., **Ramos, P**., Hayashi, J., Curson, P., Wu, C-Y., Bandaru, P., Anderson, M., Bui, B., Sayegh, A., Mahendra, S., Di Carlo, D., Kreydin, E. Khademhosseini, A., Sheikhi, A., Kaner, R." A readily scalable, clinically demonstrated, antibiofouling zwitterionic surface treatment for implantable medical devices" (2022) Adv Mater. **24** (20): 2200254. DOI: https://doi.org/10.1002/adma.202200254

Finish, N., **Ramos, P.,** Borojovich, E. J.C. , Zeiri, O., Amar, Y., Gottlieb, M., , Characteristics of Zeolite Performance in Removal of Heavy Metals from Stormwater Runoff. (2022) SSRN. DOI: http://dx.doi.org/10.2139/ssrn.4089420

Polasko, A*. & **Ramos, P*.**, Rao, E., Kaner, R., & Mahendra, S. A Multipronged Approach for Systematic *in vitro* Quantification of Catheter-Associated Biofilms, (2021). J Haz Mat Lett**. 2:** 100032**.** DOI: https://doi.org/10.1016/j.hazl.2021.100032

Pica, N. E., Miao, Y., Johnson, N. W., **Ramos, P.,** Mahendra, S., & Blotevogel, J. "Bioelectrochemical treatment of 1,4-dioxane in the presence of chlorinated solvents: Design,

process, and sustainability considerations" (2020) ACS Sus Chem Eng. **9** (8): 3172–3182. DOI: https://doi.org/10.1021/acssuschemeng.0c08152

In Review:

Ramos, P., Chetrit, E., Yehuda, N., Kogan, D., Miao, Y., Nativ-Roth, E., Kushmaro, A., Berkovich, R. Mahendra, S., Gottlieb, M. "Physical and Antimicrobial Properties of Chitosan/Silver Nanoparticle Composite Hydrogels: Role of Crosslinker: (2022)

Submitted:

Ramos, P., Honda, R., Hoek, Eric M.V., Mahendra, S. "Carbon/Nitrogen Ratios Determine Biofilm Formation and Characteristics in Model Microbial Cultures" (2022)

In Preparation:

Johnson, N. W., Ngo, J., **Ramos, P**., Miao, Y., Popovic, J., Danko, A., & Mahendra, S. Bio-GAC flow-through column systems for the simultaneous removal of 1,4-dioxane and CVOCs in mixtures. 2022

PESENTATIONS

A Multipronged Approach to Clinical & Environmental Biofilm Quantification. Association of Environmental Engineering and Science Professors (AEESP). Summer 2022. Oral Presentation

Role of Crosslinker on Antimicrobial and Antifouling Hydrogels based on a Hydrophilic Chitosan Derivative Incorporating Silver Nanoparticles. Polymer Networks Group. Summer 2022. Oral Presentation

Enhanced Removal of Per-and Polyfluoroalkyl Substances in Complex Matrices by polyDADMAC-Stabilized Granular Activated Carbon. American Chemical Society. Spring 2021. Oral Presentation

A Multipronged Approach for Systematic in vitro Quantification of Catheter-Associated Biofilms. American Chemical Society. Spring 2021. Poster

HONORS AND AWARDS

2020 Israeli Council for Higher Education PhD Sandwich Research Fellowship

2019-2022 Eugene V. Cota Robles 4-year Graduate Fellowship

2019-2020 Hydrophilix Industry-Sponsored Research Fellowship

2019 National Science Foundation Innovation at The Nexus of Food, Energy, and Water Systems- Graduate Traineeship in Integrated Urban Solutions.

Chapter 1: Introduction and Objectives

1.1 Objective and Scope

The overall objective of this work was to engineer, characterize, and assess chemical and biological surface modifications for applications ranging from water and wastewater treatment, such as in the removal of per- and polyfluoroalkyl substances (PFASs) or chemical oxygen demand (COD) and nutrients (nitrogen, phosphorous) to removal and prevention of biofilm formation on medically or industrially relevant surfaces such as catheters, drinking water distribution systems, or water treatment membranes. Several converging lines of research under this overall theme were carried out in this dissertation, whose specific objectives are detailed below:

Objective 1: To optimize and evaluate a surface modification of granular activated carbon (GAC) using the cationic polymer polydialydimethyl ammonium chloride (polyDADMAC) to improve the adsorptive removal of per- and polyfluoroalkyl substances (PFASs).

Objective 2: To assess the impact of growth media nutrients such as the carbon/nitrogen ratio on biofilm formation by *Pseudomonas aeruginosa* in the context of water and wastewater treatment.

Objective 3: To develop a culture-independent and reproducible biofilm quantification methodology for use in the quantification of attached microorganisms in clinical and environmental settings.

Objective 4: To engineer, synthesize, and evaluate antimicrobial hydrogels for the prevention of bacterial biofilm formation with applications in a range of industrial scenarios.

1.2 Dissertation Overview

This dissertation is organized into seven chapters. A general outline and contextualization of the research is presented in Chapter 1. Chapter 2 describes the background and current published research on surface modifications for water and wastewater treatment in terms of per- and polyfluoroalkyl substances (PFASs) and 1,4-dioxane, biofilm use and complications in wastewater treatment, biofilm quantification and biofilm prevention strategies. Subsections of this chapter have been or will be published as literature reviews, specifically the background on 1,4-dioxane has been included with the permission of *Current Opinion in Environmental Science and Health* (Ramos et al., 2022), and an extension on the PFAS background will be submitted to be published in a special issue of *Current Opinion in Chemical Engineering*. Chapter 3 contains results of an optimization and evaluation of a surface modification of granular activated carbon (GAC) using the cationic polymer polydialydimethyl ammonium chloride (polyDADMAC) to improve the adsorptive removal of per- and polyfluoroalkyl substances (PFASs). This work is included with permission from *Environmental Pollution* (Ramos et al., 2021). The assessment of the impact of feedwater nutrients such as the carbon/nitrogen ratio on biofilm formation by *Pseudomonas aeruginosa* in the context of water and wastewater treatment is detailed in Chapter 4. A subsection of this work has been submitted for publication in *International Biodeterioration and Biodegradation*. Chapter 5 delves into the development of a culture-independent and reproducible biofilm quantification methodology for use in the quantification of attached microorganisms in clinical and environmental settings and is included with the permission of *Journal of Hazardous Materials Letters* (Polasko and Ramos et al., 2021).The design, synthesis, and evaluation of antimicrobial hydrogels for the prevention of bacterial biofilm formation with applications in a range of industrial scenarios is detailed in Chapter 6, this work has been submitted for publication in *ACS Sustainable Chemistry and Engineering.* A summary of key

results along with their significance for environmental engineering and future research in these areas is included in Chapter 7.

1.3 References

Ramos, P., Kwok, Ivy Y., Ngo, J., Zgonc, D., Miao, Y., Pornwongthong, P., Blotevogel, J., Mahendra, S. (2022). A, B, Cs of 1,4-dioxane removal from water: Adsorption, biodegradation, and catalysis.. Curr Opin Environ Sci Health. **29**: 100386. DOI: https://doi.org/10.1016/j.coesh.2022.100386

Ramos, P., Kalra, S. S., Johnson, N. W., Khor, C. M., Borthakur, A., Jassby, D., Kranmer, B., Dooley, G., Mohanty, S. K., Blotevogel, J., & Mahendra, S.(2022) Enhanced Removal of Per- and Polyfluoroalkyl Substances in Complex Matrices by polyDADMAC-Stabilized Granular Activated Carbon with Regeneration Potential. Environmental Pollution **294**: 118603. DOI: https://doi.org/10.1016/j.envpol.2021.118603

Polasko, A*. & **Ramos, P*.**, Rao, E., Kaner, R., & Mahendra, S. A Multipronged Approach for Systematic *in vitro* Quantification of Catheter-Associated Biofilms, (2021). Journal of Hazardous Materials Letters**. 2:** 100032 **(*co-first authors)**

Chapter 2: Literature Review

2.1 Surface Modifications for Improved Water and Wastewater Treatment

2.1.1 Surface Modifications for Enhanced Contaminant Removal

The modification of functional surfaces has long been studied as a means for achieving improved removal of contaminants by membranes (Hu et al. 2020, Senthil Muthu Kumar et al. 2021), biochar (Dai et al. 2019, Liu et al. 2021), activated carbon (Ochoa-Herrera and Sierra-Alvarez 2008, Chularueangaksorn et al. 2014), ion-exchange resins (Chularueangaksorn et al. 2014, Gagliano et al. 2020) metal oxides (Heck et al. 2019), and other widely used water treatment materials. The need for surface modifications arises from fouling or other surface competition effects by biological and non-biological agents, which are phenomena that are especially relevant in environmental contexts because of the inherent complexities of the treated water matrices. In some cases, surface modifications not only allow materials to overcome limitations, but they actually improve their performance by introducing additional beneficial interactions. Examples of this which are relevant to this dissertation include bioaugmentation of adsorbents for the removal of recalcitrant contaminants such as 1,4-dioxane (Myers et al. 2018) (Simmer et al. 2020, Ramos-Garcia et al. 2022), or functionalization of adsorbents with charged polymers for effective removal of pollutants such as nitrate (Cho et al. 2011), heavy metals (Cho et al. 2011), and PFASs (Aly et al. 2018, Aly et al. 2019) .

2.1.2 Per- and polyfluoroalkyl substances and 1,4-dioxane

Per- and polyfluoroalkyl substances (PFASs) are a class of compounds consisting of fully or partially fluorinated carbon chains with different end groups including sulfonate, carboxylate, alcohol, and sulfonamide (Kwiatkowski et al. 2020) . Their chemical structure provides them with extremely low surface tension and unique hydrophobic and oleophobic traits, while also rendering them extremely difficult to break down through either physicochemical or biological methods. These amphiphilic properties and chemical stability make them highly mobile and persistent in groundwater (Caló and Khutoryanskiy 2015) leading to their detectable presence in as much as 70 percent of the water sources of some states in the United States (Hatton et al. 2018). PFASs are commonly used as surfactants, in water-, soil-, oil- and stain-resistant coatings for clothing, leather and paper among other products, as well as in paints, adhesives, polishes, waxes, and most importantly in fire-fighting foams (Barzen-Hanson et al. 2017, EPA 2019). PFASs have been detected essentially everywhere in the world, in the environment, wildlife, rainwater and in human tissues (Cordner et al. 2021, Pfotenhauer et al. 2022). There are concerns over the toxicological effects of PFASs in both humans and in wildlife as some have been designated as possible human carcinogens, while also having suspected endocrine or developmental effects (DeLuca et al. 2021, Espartero et al. 2022)

1,4-Dioxane is a widespread emerging contaminant of concern (CoC), with 22% of public water systems tested containing levels above the U.S. EPA's published reporting limit of 0.07µg/L according to the UCMR 3 (2013-2015) data summary (Mohr et al. 2020, ITRC 2021). Historical sources of 1,4-dioxane in water result from its disposal and uses in varnishes, cosmetics, paints, antifreeze, dyes, greases, waxes, and aircraft de-icing liquid as well as in polymers processing (McElroy et al. 2019, Mohr et al. 2020, Hossein et al. 2022). 1,4-Dioxane's environmental fate and transport is facilitated by its hydrophilicity and low volatility, which

allow it to rapidly mix with groundwater and develop large contaminant plumes following its release into the subsurface (ITRC 2021). 1,4-Dioxane exhibits poor sorption to soils, further facilitating its downgradient migration and long-term persistence (ITRC 2021). Due to its use as a stabilizer for 1,1,1-trhichloroethane (1,1,1-TCA), 1,4-dioxane co-occurs environmentally with toxic chlorinated volatile organic compounds (CVOCs) such as trichloroethene (TCE), 1,1-dichloroethene (1,1-DCE), cis-1,2-dichloroethene (cDCE), and vinyl chloride (VC) (Adamson et al. 2017, Polasko et al. 2021, Adamson et al. 2022).

The concern regarding both contaminants has made their regulation an area of increasing interest in the public health sector. The U.S EPA has established a drinking water health advisory level for total perfluorooctane sulfonate (PFOS) and perfluorooctane carboxylate (PFOA) at 0.02 and 0.004 parts per trillion, respectively (EPA 2022). There is no federal regulation in place for 1,4-dioxane's presence in water, however the Unmonitored Contaminant Monitoring Rule (2013-2015) has set a limit of 0.07µg/L (ITRC 2021).

2.1.3 Adsorption of PFASs and 1,4-Dioxane

PFAS-impacted water is difficult to remediate due to the compound's unique chemical and transport characteristics. Conventional adsorbents such as granular activated carbon (GAC) and ion exchange resins can effectively remove long-chain PFASs from water (Ochoa-Herrera and Sierra-Alvarez 2008, Chularueangaksorn et al. 2014, Du et al. 2014). However, they are less effective at removing short-chain PFASs, especially ones with carboxylate moieties, and are also negatively affected when they are used in complex water matrices containing co-occurring competing ions (Kothawala et al. 2017, Maimaiti et al. 2018, Ross et al. 2018, Westreich et al.

2018, Zhang et al. 2019). Co-occurring inorganic ions have complex effects on PFAS adsorption through factors such as competitive adsorption, electrical double-layer compression, divalent cation bridging, and salting out effects (Du et al. 2014). Additionally, the exhaustion of attachment sites on GAC by PFASs, natural organic matter (NOM), or other competing ions may increase the cost of GAC-based treatment process (Kothawala et al. 2017). Therefore, it is important to develop strategies that are effective at removing PFASs when the cumulative loading of dissolved salts and NOM is high so that the materials can be used to effectively treat real environmental waters.

Despite its low octanol-water partition coefficient and high water miscibility, appreciable water-mediated adsorption of 1,4-dioxane has also been demonstrated and comprehensively described and modeled (Myers et al. 2018, Liu et al. 2019). Norit™ brand 12-40 mesh size granular activated carbon (GAC) has been shown to be effective over a range of concentrations, with maximum capacity around 35 mg/g, best described by the Toth isotherm model for heterogenous systems (Myers et al. 2018). It was also demonstrated that zeolites can adsorb 1,4-dioxane, outperforming GAC with capacities ranging from about 64 mg/g (ZSM-5) g to 85 mg/g (TS-1) (Chen et al. 2019, Liu et al. 2019). ZSM-5 is a widely used hydrophobic zeolite with three active sites, including differently shaped channels and channel intersections, which serve as adsorption sites (Liu et al. 2019). It was shown to rapidly adsorb 1,4-dioxane despite its critical diameter (5.6 Å) being slightly smaller than that of 1,4-dioxane (Liu et al. 2019). Titanium Silicate-1 (TS-1) is a zeolite with high capacity and rapid kinetics for 1,4-dioxane adsorption, owing to a combination of hydrophobic interactions on its inner surface and hydrogen bond formation with hydroxyl groups on its outer surface. Overall, adsorption of 1,4-dioxane onto

zeolites is governed by a combination of hydrophobic interactions, hydrogen bonding, molecular volume, and polarizability (Chen et al. 2019, Liu et al. 2019).

Adsorption has inherent drawbacks when used as a strategy for removal of toxic recalcitrant contaminants such as PFASs and 1,4-dioxane since it doesn't alter the compounds' structures or detoxify them in any way but instead only transfers the contamination from the aqueous to the solid phase, from which subsequent desorption raises liability concerns. Additionally, concerns over proper disposal or additional regeneration costs need to be considered (Myers et al. 2018, Chen et al. 2019, Liu et al. 2019). As a result, it is of interest to develop improved adsorption-based treatment strategies such as those relying on surface modifications that can result in favorable synergisms that may allow mitigation of the detrimental effects of complex water matrices or facilitate the detoxification of contaminants by localizing effects such as biodegradation to surfaces (Myers et al. 2018). Understanding the feasibility of adsorbent regeneration through various strategies is beneficial from sustainability perspectives as this may allow longer lifetimes, resulting in less waste generated.

2.1.4 Strategies for Improving Adsorbents for PFASs and 1,4-Dioxane

Adsorption of PFASs onto GAC can exhaust the attachment sites which limits its useful lifespan, resulting in the generation of large quantities of exhausted solid waste containing high concentrations of the adsorbed contaminants (Cho et al. 2011, Merino et al. 2016). Conventional regeneration processes for spent adsorbents saturated with PFASs include chemical and thermal regeneration (Merino et al. 2016, Watanabe et al. 2018, Gagliano et al. 2020). Chemical regeneration requires the use of organic solvents, which generate a secondary waste stream that requires further treatment (Merino et al. 2016, Gagliano et al. 2020). Thermal regeneration often

requires extreme temperatures, especially when saturated with PFASs, which can cause a decrease in adsorption potential because of the collapse of micropores, leading to losses in surface area (Hamdaoui et al. 2005, Watanabe et al. 2018). Ultrasonic treatment of sorbents has been used for regenerating GAC saturated with chlorinated volatile organic compounds (Lim and Okada 2005), *p*-chlorophenol (Hamdaoui et al. 2003, Hamdaoui et al. 2005), and many other contaminants (Rege et al. 1998, Schueller and Yang 2001). Ultrasonic treatment of GAC works by localizing thermal effects at the interface where the contaminant is adsorbed (Breitbach and Bathen 2001, Breitbach et al. 2003), as well as by the generation of high-speed micro jets that produce high pressure shock waves at the surface (Hamdaoui et al. 2003). This localization of energy at the surface may prevent some of the negative effects of thermal regeneration, where the effects of the energy reach beyond the surface. Consequently, ultrasonic regeneration may be explored as a viable strategy for regeneration of GAC saturated with various contaminants including PFASs.

In the case of 1,4-dioxane, bioaugmentation has been studied as a surface modification strategy to achieve better results than either adsorption or biodegradation alone (Myers et al. 2018, Johnson et al. 2020). CB1190 bioaugmented GAC (bioGAC) achieved one order of magnitude greater 1,4-dioxane removal from water as compared to reactors with abiotic GAC (Myers et al. 2018). BioGAC may be viewed as a synergistic treatment technology, employing abiotic removal of CVOCs –some of which are inhibitory to 1,4-dioxane metabolism (Mahendra et al. 2013, Zhang et al. 2016, Polasko et al. 2021) combined with the biological degradation of 1,4-dioxane (Myers et al. 2018). Additionally, BioGAC mitigates the leaching concerns of conventional GAC systems as CB1190 degrades desorbed 1,4-dioxane at the solid-liquid interface, effectively regenerating the GAC sorbent (Myers et al. 2018).

2.1.5 Surface-Mediated Wastewater Treatment Strategies

Wastewater treatment relies on several types of surfaces which can be optimized for either improved fouling control for increased efficiency or for enhanced microbial attachment for contaminant biodegradation. Two important examples of wastewater treatment processes that rely on these different surface optimizations include biofilm-based treatment strategies such as trickling filters (Petrovich et al. 2017) as well as abiotic-biotic strategies such as membrane bioreactors (Saidulu et al. 2021) . Both processes are alternatives to the conventional activated sludge wastewater treatment processes and have benefits depending on the contexts in which they are used due to the unique microbial community structures which they foster (Ye et al. 2011, Panchavinin et al. 2019).

Biofilm-based reactors include trickling filters, moving bed biofilm reactors, membrane biofilm reactors, rotating biological contactors, and passive aeration simultaneous nitrification/denitrification biofilm reactors, but can be generally considered to be reactors in which microbial cells are retained as a biofilm which may either be strictly attached or attached to free moving carrying materials (Saidulu et al. 2021). Attached-growth bioreactors are often used in wastewaters with difficult-to treat characteristics (i.e., different from average municipal wastewater in that the organic carbon, nutrient, or pollutant loading rate is very high) because treating these waters with conventional activated sludge processes would require very large spaces and large amounts of aeration energy (Saidulu et al. 2021). Attached-growth treatment systems have the capacity to simultaneously remove organic carbon (BOD and COD), as well as inorganic nutrients (nitrogen, phosphorous) because the biofilms that grow on support surfaces contain both oxic and anoxic zones. This is because oxygen gradients develop, across the depth of the biofilm structure, each fostering different groups of microorganisms with different

metabolic capabilities (Saidulu et al. 2021). Attached growth systems are currently mostly designed for specific treatment purposes such as pretreatment or posttreatment of water with high influent COD, nutrients, or high concentrations of emerging contaminants such as dyes or varnishes (Forbis-Stokes et al. , Abdelfattah et al. 2020). Understanding the process of biofilm formation in these complex conditions and communities is important for enhancing the effectiveness of the treatments as well as aiding in the design and implementation of more successful technologies going forward.

2.1.6 Current State of Wastewater Treatment Process and Future Directions

Current estimates have determined that only 48% of wastewater is treated globally, however the level of treatment varies and does not result in the same level of water quality everywhere in the world (Jones et al. 2021). Conventional wastewater treatment processes are energy intensive and emit large amounts of greenhouse gases from the metabolisms of aerobic and anaerobic bacteria which are used in the conventional activated sludge process or in anaerobic digestion respectively. These processes rely on a linear economy model rather than a closed loop circular economy and are not sustainable long term, while their operating intricacies and economic burden pose a barrier to access for inexperienced or resource-limited areas (Sheik et al. 2014). The burden of climate change is pushing a shift in municipal wastewater treatment from an end-of-pipe treatment towards one where there is integrated energy and resource recovery. This means that rather than being a source of pollution wastewater treatment is moving towards being a source of energy, nutrients, and clean water.

Overcoming the challenges of the conventional activated sludge process may rely on the use of membrane bioreactors (MBRs), as these systems have been deemed to be promising due to their very high removal efficiencies for solids, microorganisms, and pollutants due to their

facility for independent control of hydraulic retention time (HRT) and solids retention time (SRT) (Zeng et al. 2015). MBRs with the use of a single aerobic stage are effectively able to remove 90-95% of the influent dissolved organic matter from wastewater but are not able to remove nitrogen and phosphorous (Vinardell et al. 2020). Wastewater treatment plants must employ biological processes containing multiple redox stages for nitrogen and phosphorus removal to effectively meet discharge standards and prevent negative ecological effects such as eutrophication in the receiving water bodies (Vinardell et al. 2020). Biological nitrogen removal traditionally is only able to achieve 75% removal under optimum conditions (Vinardell et al. 2020), while phosphorous removal is even more limited at 60-70% in ideal conditions (Nguyen et al. 2020, Vinardell et al. 2020). These limitations are due to the complexities of alternating between aerobic and anaerobic conditions to enrich specific microbial communities for the different transformation stages (Verrecht et al. 2008, Nguyen et al. 2020, Vinardell et al. 2020). Additionally, conventional biological nitrogen removal may result in the release of nitrous oxide (N_2O), which is a potent greenhouse gas with a global warming potential about 300 times that of carbon dioxide (Griffis et al. 2017).

Limitations of conventional biological removal have been overcome both in lab-scale and full-scale systems by using microalgae, because these organisms rely on nitrogen and phosphorous as essential nutrients for their metabolism and growth (Nguyen et al. 2020). The design of MBRs relying on microalgae has been suggested as a promising solution to the issue of nutrient removal, however the technology readiness is still in the process of development and optimization (Nguyen et al. 2020).

The widespread application of MBRs is limited to an important extent by the issue of membrane fouling (Yeon et al. 2009, Meng et al. 2017, Hong et al. 2019). Membrane fouling is

linked to several factors such as temperature, HRT, SRT, biomass physical characteristics and microbial community composition, influent conditions, and membrane physical and chemical characteristics (Meng et al. 2017, Vinardell et al. 2020). Membrane fouling in MBRs is currently controlled by aeration/gas sparging (Verrecht et al. 2008, Vinardell et al. 2020), however this is considered the highest energy expense during an MBR operation..

2.2. Surface Modifications for Prevention of Undesired Microbial Attachment

2.2.1 Biofilms and Surfaces

Biofilms are complex microbial communities which attach to surfaces and become encased in an exopolymeric substance which yields them with protective qualities such as increased resistance to stressors such as shear, nutrient limitation, heavy metals, or antibiotics (Joshi et al. 2021). In the first stage of biofilm formation, planktonic cells adhere to a surface. In stage two, the adhered cells begin to secrete the extracellular polymeric substance (EPS) and become attached to the surface irreversibly, resulting in increased cell aggregation. The third stage involves biofilm maturation and the development of a layered community with an increasingly complex architecture, which is important for nutrient exchange. In stage four the biofilm community is fully mature and reaches its maximum cell density. The final stage involves the release of cells from the mature biofilm, which can go out and attach to new surfaces (Crouzet et al. 2014, Vasudevan 2014). The extracellular polymeric substance (EPS) is a complex material composed of a mixture of polysaccharides, lipids, proteins, nucleic acids (extracellular-DNA), small molecules, and cellular debris. Each of the constituents serves an important purpose such as providing structural support, entrapping nutrients, and providing additional protection against antimicrobials and antibiotics (Crouzet et al. 2014, Vasudevan 2014). EPS is essential because it is also responsible for enabling cell-to-cell chemical signaling

based communication, known as quorum sensing, and also facilitates horizontal gene transfer (Joshi et al. 2021).

2.2.2 Problematic Biofilms in Clinical Settings and Biofilm Quantification

Biofilms are a leading cause of infections, especially those initiated on medical tubing. Additionally, biofilm formation is a significant mechanism for providing virulence to harmful pathogens such as *Staphylococcus aureus*, *Escherichia coli*, and *Pseudomonas aeruginosa*. It has been estimated that as much as 80% of human infections are the direct consequence of biofilms (Davies 2003, Verderosa et al. 2019). Chronic infections are associated with microbial growth in the form of adhered colonies surrounded by a large exopolysaccharide matrix, which is used to establish biofilms (Roy et al. 2018). Biofilms are less susceptible to host defenses such as macrophage phagocytosis and can become resistant to antibiotics, resulting in reduced treatability (Bjarnsholt 2013). Medical tubing is a prime target for biofilm formation and is often the cause of severe infections, especially because it serves as a hiding place for microbes where the immune system is less effective (Trevisani et al. 2005, Stickler 2014). For example, urinary catheter tubing is associated with over 75% of urinary tract infections, which are the most commonly acquired hospital infections (HCAIs). It has been estimated that HCAIs have an annual cost of approximately $11 billion (Romling et al. 2014). Despite the widespread implications of biofilms and biofouling, there is currently no ‘gold standard’ available to evaluate the presence of microbial biofilms from medical tubing in order to assist in the diagnosis and prevention of clinical infections (Percival et al. 2015). Current standard methods typically target: 1). Viable cells via plate counting or flow cytometry 2). Total biomass via optical density 3). Extracellular polymeric substances via resazurin dye, crystal violet dye, or Live/Dead staining or 4). Cellular activity via ATP quantification (Stepanović et al. 2000,

Feneley et al. 2015, Doll et al. 2016, Singh et al. 2017, Stepanović et al. 2017). Successful detection by these assays is limited by factors such as small-colony variants, non-culturable microorganisms and false positives resulting from the inability to differentiate between live and dead cells. In addition, even though these tests are widespread, they are rarely performed together and even when they are, the limitations listed above prevent an accurate characterization and quantification of the biofilm being studied (Stepanović et al. 2000, Feneley et al. 2015, Doll et al. 2016, Singh et al. 2017, Stepanović et al. 2017).

2.2.3 Antimicrobial Surface Modifications and Hydrogels

Just as it is essential to accurately quantify and identify biofilms attached to surfaces, it is also important to design surfaces with the ability to prevent attachment of microbes in the first place. Fouling propensity depends mainly on surface properties, such as surface energy, wettability, and micro-texture, which means that modifying the structure of surfaces provides an avenue for preventing fouling (Maan et al. 2020). Three main types of antifouling surfaces exist: (1) Fouling resistant surfaces prevent adhesion by allowing the formation of a strongly hydrated layer, which provides a physical and free energy barrier that makes attachment more difficult. (2) Fouling-release surfaces allow weak adhesion but enable easy removal of adsorbed material with limited mechanical force or shear. (3) Fouling-degrading surfaces kill attached bacteria and other microorganisms due to the incorporation of bactericidal functionalities (Maan et al. 2020). Common modifications that exist in order to provide these characteristics include modifying the surface chemistry, surface architecture, or surface topography(Maan et al. 2020).

Hydrophilic surface modifications are a common kind of surface chemistry modification for antifouling purposes. Within this group, some modifications can be based on zwitterionic compounds, while other are based on non-zwitterionic hydrophilic compounds(Maan et al.

2020). Zwitterionic polymers contain oppositely charged anionic and cationic groups along their chain. Repulsive forces between the polymer's chains themselves induce the formation of highly hydrated layers which are responsible for preventing biofouling (Maan et al. 2020). Since these hydrated layers are formed by the electrostatic forces within the polymers themselves, they are stronger and more stable compared to those induced by non-zwitterionic hydrophilic polymers (Maan et al. 2020). The antifouling ability of zwitterionic and other hydrophilic surfaces is the result of the formation of this layer of high hydration. More specifically, the tightly bound water layer forms a permanent hydration layer that serves as a physical barrier, which at the same time makes attachment thermodynamically unfavorable by creating an energetic barrier. This energetic barrier is created because the only way for attachment to occur would be to first dehydrate the surface and in doing so reconfigure a system which already has high conformational entropy (Yeh et al. 2014, Maan et al. 2020). In addition, if antimicrobial moieties are incorporated inside the antifouling coatings, microbes can be killed upon settlement.

Chitosan is a natural polysaccharide derived from the polymer chitin (Zou et al. 2015, Xie et al. 2018). It is one of most prevalent natural polymers, second only to cellulose(Elieh-Ali-Komi and Hamblin 2016). It is a material of great interest in many industrial areas because of its biodegradability, biocompatibility, nontoxicity, and antimicrobial abilities(Elieh-Ali-Komi and Hamblin 2016). Its antimicrobial properties are due to its overall positive charge in acidic conditions, since the presence of its polycation can have detrimental interactions with microbial cell walls(Elieh-Ali-Komi and Hamblin 2016). However this activity is limited to acidic conditions, since this as well as its water solubility are limited to conditions when the cationic charge is present as a result of low pH. However it is possible to modify the structure of chitosan in order to overcome this limitation by reacting it with other compounds depending on the

desired properties of the resulting material (Lim and Hudson 2004, Zou et al. 2015, Elieh-Ali-Komi and Hamblin 2016). Many studies have reported a simple modification of chitosan into the derivative N-(2-hydroxy-3-trimethylammonium)propyl] chitosan chloride (HTCC). HTCC is a quaternary ammonium compound, which means that it has a permanent positive charge at neutral pH, making it water soluble and antimicrobial under these conditions(Roberts and Taylor 1989, Zou et al. 2015).

Hydrogels are crosslinked networks of hydrophilic polymers(Caló and Khutoryanskiy 2015), and have widespread industrial applications such as in wound dressings, drug delivery, agriculture, water and wastewater treatment and many more(Alcântara et al. 2020). They are able to absorb significant amounts of water within their structure without the dissolution of the crosslinked network (Caló and Khutoryanskiy 2015). Previous studies have shown that it is possible to form hydrogels from HTCC at neutral pH (Zou et al. 2015), likely as a result of the increased hydrophilicity of chitosan upon this modification. Thus the first objective of this project was to synthesize hydrogels from HTCC using three different hydrogels and assessing any differences in some of the properties of the resulting hydrogels such as hydrophilicity and swelling potential.

Chapter 3: Enhanced Removal of Per- and Polyfluoroalkyl Substances in Complex Matrices by polyDADMAC-Coated Regenerable Granular Activated Carbon

3.1 Introduction

Per- and polyfluoroalkyl substances (PFASs) are a class of compounds consisting of either fully or partially fluorinated carbon chains with different end groups including sulfonate, carboxylate, alcohol, and sulfonamide moieties (Kwiatkowski et al. 2020). Their amphiphilic properties and chemical stability makes them highly mobile and persistent in groundwater (Kwiatkowski et al. 2020), leading to their detectable presence in as much as 70 percent of the water sources in some states (Hatton et al. 2018). In addition to having bioaccumulation potential, PFASs have associated toxicity effects (Houde et al. 2006), (Lau et al. 2007), (Hekster et al. 2003). As a result, the U.S EPA has established a drinking water health advisory level for total perfluorooctane sulfonate (PFOS) and perfluorooctane carboxylate (PFOA) at 0.02 and 0.004 parts per trillion, respectively (EPA 2022), and has declared PFASs as hazardous waste (EPA 2019). However, PFAS-impacted water is difficult to remediate (Kwiatkowski et al. 2020). Conventional adsorbents such as granular activated carbon (GAC), ion exchange resins, and polymers can remove long-chain PFASs from water (Ochoa-Herrera and Sierra-Alvarez 2008), (Du et al. 2014), (Chularueangaksorn et al. 2014). However they can be less effective at removing short-chain PFASs, especially those with carboxylate moieties, and are negatively affected by complex environmental matrices containing co-occurring ions (Ross et al. 2018), (Zhang et al. 2019), (Maimaiti et al. 2018), (Westreich et al. 2018), (Kothawala et al. 2017). Recent developments in fabricating successful adsorbents for short-chain PFASs in the presence of competing ions, such as different kinds of biochar, (Liu et al. 2021) have the drawback of requiring high energy inputs to fabricate.

Co-occurring inorganic ions have complex effects on PFAS adsorption through factors such as competitive ion exchange, electrical double-layer compression, divalent cation bridging, and salting out effects (Du et al. 2014, Vo et al. 2021). Natural organic matter (NOM) can block GAC's pores or adsorb competitively onto GAC, increasing electrostatic repulsions (Kothawala et al. 2017). Exhaustion of attachment sites on GAC by PFASs and NOM can increase the cost of GAC-based treatment process. Thus, it is important to develop strategies that are effective at removing PFASs when the cumulative loading on NOM and dissolved salts is high, as well as to regenerate the adsorption capacity of spent GAC.

GAC primarily removes PFASs by hydrophobic interactions, which become less effective for short-chain PFASs. In that case, adsorption of anionic PFASs can be enhanced by the addition of cationic polymers such as poly diallyldimethylammonium chloride (polyDADMAC) (Aly et al. 2019), (Aly et al. 2018), (Liu et al. 2020). PFASs can adsorb onto polymer-modified GAC by both hydrophobic and electrostatic interactions (Aly et al. 2019). Quaternary ammonium functional groups, such as those present in polyDADMAC, are particularly effective modifiers for removing anionic species such as perchlorate (Xu et al. 2011), chromium (Cho et al. 2011), and PFASs (Liu et al. 2020), (Aly et al. 2018), (Aly et al. 2019). The aggregation of cationic polymer at the interface between the sorbent's surface and the bulk liquid can enhance the sorbent's adsorption capabilities (Leyva-Ramos et al. 2008), (Xu et al. 2011), (Cho et al. 2011). However in some cases, the modification with cationic polymers has decreased the adsorption capacity of GAC for the removal of other contaminants, likely as a result of the polymer masking sorption sites in GAC's interior (Cho et al. 2011), (Leyva-Ramos et al. 2008). Previous studies have selected one concentration of polymer (Liu et al. 2020), (Aly

et al. 2018), (Aly et al. 2019). Thus, the critical concentration of polymer beyond which an increase in the polymer dose would decrease PFAS adsorption is unknown.

The effect of competing ions naturally present in water on the effectiveness of polymer-modified GAC has not yet been studied. Natural organic matter such as humic acid adsorbs competitively onto unmodified GAC via hydrophobic interactions, in addition to blocking internal pores (Gong et al. 2016), (Vu and Wu 2020), (Kothawala et al. 2017). We hypothesized that PFAS adsorption onto polyDADMAC-GAC will be less sensitive to humic acids, as PFAS adsorption does not rely solely on hydrophobic interactions in the presence of the cationic polymer.

Adsorption of PFASs onto GAC can exhaust the attachment sites which limits its useful lifespan, resulting in the generation of large quantities of exhausted solid waste containing high concentrations of the adsorbed contaminants (Merino et al. 2016), (Cho et al. 2011). Conventional regeneration processes for spent adsorbents saturated with PFASs include chemical and thermal regeneration (Gagliano et al. 2020), (Merino et al. 2016), (Watanabe et al. 2018). Chemical regeneration requires the use of organic solvents, which generate a secondary waste stream that requires further treatment (Merino et al. 2016, Gagliano et al. 2020). Thermal regeneration often requires extreme temperatures, especially for PFASs, which can cause a decrease in adsorption potential because of the collapse of micropores, leading to losses in surface area (Hamdaoui et al. 2005), (Watanabe et al. 2018). Ultrasonic treatment of sorbents has been used for desorbing contaminants from GAC saturated with chlorinated volatile organic compounds (Lim and Okada 2005), *p*-chlorophenol (Hamdaoui et al. 2005), (Hamdaoui et al. 2003), and many other contaminants (Rege et al. 1998), (Schueller and Yang 2001). Ultrasonic treatment of GAC works by localizing thermal effects at the interface where the contaminant is

adsorbed (Breitbach and Bathen 2001), (Breitbach et al. 2003), as well as by the generation of high-speed micro jets that produce high-pressure shock waves at the surface (Hamdaoui et al. 2003). This localization of energy at the surface may prevent some of the negative effects of thermal regeneration, where the effects of the energy reach beyond the surface. Regeneration of polyDADMAC-GAC saturated with PFASs using ultrasound has not yet been evaluated and was therefore explored here as a viable method for regeneration.

In this chapter, the critical concentration range for polyDADMAC modification to increase the adsorption capacity of GAC was estimated, along with an evaluation of the material's adsorption capacity in complex water matrices with high dissolved salts and humic acid concentrations. Finally, an examination was performed in order to gage at the potential of ultrasonic treatment to desorb PFASs as to allow regeneration of spent GAC by simple reamending with polyDADMAC. Short-chain PFASs such as perfluorobutanoic acid (PFBA), perfluorobutane sulfonic acid (PFBS), and perfluorohexane sulfonic acid (PFHxS) were used in synthetic complex water matrices to examine the potential of this technology in challenging scenarios. The study in this chapter began with a low level of complexity to understand fundamental processes and mechanisms at play, however future investigations should address the performance of this material and regeneration strategy in the presence of more complex PFAS mixtures including precursor compounds and newer replacement products, such as Gen-X.

3.2 Materials and Methods

3.2.1 Effect of polyDADMAC dose

To evaluate the impact that the polyDADMAC dose used to modify GAC had on GAC's surface properties, five grams of activated carbon were added to a 100 mL solution containing polyDADMAC at different concentrations (0.00025% to 1% in deionized (DI) water) in glass

bottles. The range was selected based on previous evaluations of optimal coating of GAC for removal of environmental contaminants (Cho et al. 2011) and taking into consideration the molar mass of polyDADMAC. Because of its high molecular weight, which indicates long chains, polyDADMAC would likely mask more entries in GAC at elevated concentrations. (Cho et al. 2011), (Leyva-Ramos et al. 2008).

The GAC and polyDADMAC mixtures were placed in a shaker at 120 rpm for 5 h at 30°C. After modification, GAC particles were retrieved by centrifugation and dried in an oven at 100°C for 24 h (Cho et al. 2011). GAC samples were dried in order to ensure a consistent mass in all experiments and considering that adsorbents are packaged in the dry state for field and experimental uses. Surface areas of the GAC samples modified with different polyDADMAC doses were determined by the Brunauer-Emmett-Teller (BET) equation using a TrisStar II 3020 Surface Area Analyzer with analytical triplicates to assess whether different polyDADMAC doses resulted in surface area changes. Fourier-transform infrared spectroscopy (FTIR) spectra of the modified and unmodified GAC and the ATR-FTIR spectrum of polyDADMAC were obtained using a JASCO Model 420 FTIR to examine the effect that modifying GAC with polyDADMAC had on surface functional groups.

3.2.2 Effect of competing ions

Effectiveness of adsorption and sorbent capacity of the polyDADMAC-GAC was tested in the presence of both NOM (in the form of humic acid) and increasing ionic strength, individually and in combination, to represent a range of scenarios where GAC can be exhausted or adsorption of PFASs on GAC can be affected by prolonged exposure to humic acid and saline water. Simulated groundwaters were prepared with three concentrations of humic acid (5 mg/L, 15 mg/L, and 45 mg/L) and/or two ionic strengths (0.02 M and 0.2 M), in DI water. The humic acid

concentrations were selected based on the average NOM concentrations reported in Canada's Guidance on Natural Organic Matter in Drinking Water, 2019 (2019). The methods outlined by Knobel et al. (Knobel et al. 1989) and Smith et al. (E. J. Smith 2002) were used to prepare the 0.02 M ionic strength solution (**Table 3.2A**). The high ionic strength solution (0.2 M) was designed to mimic the groundwater chemistry at a site in Southern California; both solutions contained a mixture of monovalent and divalent ions (**Table 3.2B**). High concentrations of HA and salinity ions were set to simulate complex scenarios such as high cumulative loading per gram of GAC as in the case of long-term exposure to dilute waters.

Table 3. 1 Water Chemistry Ions for Synthetic Groundwater #1 (0.02 M Ionic Strength

Characteristic	Groundwater 1
Calcium (mg/L)	49.0
Magnesium (mg/L)	9.8
Sodium (mg/L)	15.3
Potassium (mg/L)	4.1
Chloride (mg/L)	24.0
Sulfate (mg/L)	58.1
Carbonate (mg/L)	60.3
Nitrate	6.2
pH	6.7

Table 3. 2 Water Chemistry Ions for Synthetic Groundwater #2 (0.2 M Ionic Strength)

Characteristic	Groundwater 2
Calcium (mg/L)	1145.0
Magnesium (mg/L)	581.4
Sodium (mg/L)	3202.9
Chloride (mg/L)	3283.7
Sulfate (mg/L)	1955.5
Nitrate (mg/L)	11.0
pH	6.70

Humic acid solutions 5 mg/L, 15 mg/L, 45 mg/L prepared with Sigma-Aldrich humic acid had a pH of 7.90 Solution of 1:1 15 mg/L ionic strength and 0.02M ionic strength had a pH of 7.20

3.2.3 Adsorption Experiments

PFAS stocks were prepared using high-purity methanol in a 70:30 ratio of methanol to DI water at 1 g/L. Aliquots from each PFAS stock were added individually to each vial and this was sampled as the starting concentration. To evaluate relative performance of polyDADMAC-GAC in different solution matrices, 0.2 g of polyDADMAC-modified GAC or unmodified GAC were placed in 30 mL of solution containing the desired ionic matrix. Each reactor was spiked with 1 mg/L each PFBA, PFBS, PFOS, PFOA, and PFHxS. The prepared solutions were replaced by DI water in the control experiments. The mixture of five PFASs was selected to understand the behavior in mixed systems with greater competition. Zeta potential of polyDADMAC and humic acid were measured (BrookHaven Instruments, Holtsville, NY) to elucidate role of surface charge electrostatic interactions between the cationic polymer, humic acid, and PFAS in the mixed system. Zeta Potential and Mobility measurements were collected for a solution of 0.00025% polyDADMAC, a solution prepared with a 1:1 ratio of 0.00025% polyDADMAC and

5mg/L humic acid at pH 7.90, and humic acid solutions at pH 2.80, 5.90, 8.70. Measurements were obtained using a ZetaPlus instrument (BrookHaven Instruments, Holtsville, NY)

To evaluate the effect of polyDADMAC dose for GAC modification on adsorption capacity, 0.2 g of GAC coated with polyDADMAC (0-1% by weight) were mixed with 30 mL solution containing 1 mg/L each of PFOA and PFOS at ionic strength of 0.2 M; A polyDADMAC concentration for modification was selected based on the effect of different doses. Two long chain PFASs were chosen to carry out this assessment in a scenario where adsorption is known to be effective, as to better gage at any potential effects of modification. These results were used to inform subsequent experiments.

To investigate the adsorption isotherm behavior of PFASs onto GAC modified with the selected polyDADMAC dose, adsorption isotherm experiments were carried out by equilibrating 0.2 g of adsorbent with 30 mL of solutions of PFBA or PFOA at varying concentrations in DI water. PFASs were selected to obtain isotherm data on one long chain and one short chain PFAS, with minimum competition as to model the adsorption behavior of individual PFASs effectively.

All reactions were carried out in 50 mL high-density polypropylene tubes and allowed to equilibrate for 96 h in a shaking incubator at 120 rpm and 30 °C. All initial concentrations were measured analytically to ensure accurate quantifications of adsorption capacity. All conditions were tested in triplicate to ensure statistically significant results.

The possibility of polyDADMAC leaching via the process of PFASs adsorption was evaluated because of detrimental implications that this could have on environmental health. Hach Total Nitrogen (TN) Kits were used (Method 10072, Persulfate Digestion Method, detection

limit 2 mg/L) to detect nitrogen in reactors where polyDADMAC-modified GAC had been allowed to equilibrate with the mixed PFAS systems presented above for 13 months.

3.2.4 Regeneration of contaminated GAC

Regeneration potential of GAC was assessed by first evaluating desorption, followed by assessing re-adsorption potential. Desorption of PFASs from polyDADMAC-modified GAC was assessed using high-frequency ultrasound at two frequencies (700 kHz, 900 kHz). Here, 6.6 g of GAC which had been previously modified with 0.00025% polyDADMAC according to the specifications above (five grams per every 100 mL) was incubated with 1 L of DI water containing 1 mg/L each PFBA and PFOA for 96 h in a shaking incubator at 120 rpm and 30 °C. A sample of the supernatant was collected and the saturated GAC was placed in an oven at 100 °C for 24 h to dry. Drying was performed to ensure that a consistent mass of GAC was placed in the ultrasound unit in order to maintain the same GAC to liquid ratio in the sonicator during replicates. Saturated dried GAC was then mixed with 200 mL of DI water in 1-L high-density polyethylene bottles. The mixture was poured into the reactor and sampled as the starting point. The bench-scale sonication reactor unit was custom-built by PCT Systems, Inc. (San Jose, California) (S1.3). The power selected for these experiments was 15.8 W, based on findings that the structure of GAC is preserved as long as the power used was less than 38 W per every 90 mL of liquid (Hamdaoui et al. 2005).

The sonolysis reactor unit (maximum volume 2 L) was made of polypropylene and equipped with a cooling coil made of stainless steel. Experiments were performed at 700 kHz and 900 kHz for two hours in a high purity Argon (99.999%) atmosphere. An initial 30 minutes of Argon sparging (5.7×10^{-2} m^3 h^{-1}) was allowed to occur before the reactor was started to allow argon to saturate the environment. After this sparging period, the reactor was kept airtight, and the

temperature was held at 5°C using a recirculating water bath for the entire duration of the sonication.

Five mL of sample were collected every 20 min using a sterile 1-mL polypropylene syringe, diluted with high-purity methanol for sample preparation, and stored in polypropylene tubes at 4°C until analysis. For control, another batch of saturated polyDADMAC-GAC was prepared in the same way, and the slurry was placed on a stir plate rotating at 120 rpm for the same duration (120 min) and sampled at the same frequency (20 min). At the end of 120 min, the GAC was recovered and placed in an oven at 100 °C to dry for 24 h in preparation for re-saturation experiments. Samples were dried to ensure consistent mass of GAC in replicates of these experiments.

To test the potential of the modified GAC to be reused, samples were placed in a 1 L solution of 1 mg/L each PFOA and PFBA in DI water and allowed to react for 96 h as before. The solution was sampled upon preparation as well as after 96 h to assess the adsorption capacity of the GAC after sonication at different frequencies. Once the optimum frequency for desorption of the PFASs was determined, the potential for regeneration of the polyDADMAC-GAC was tested by re-modifying with 0.00025% polyDADMAC following a round of sonication and drying.

Total fluoride was measured in the sonicated samples after 120 min using a Dionex™ Integrion™ HPIC™ System (Thermo Fisher, S1.2) to ensure that the tested low energy conditions were non-destructive for PFASs.

X-ray Photoelectron Spectroscopy (XPS) was performed on saturated GAC samples after exposure to ultrasound at 900 kHz and after stirring at 120 rpm for 2 h in order to assess the impact of ultrasound on the polyDADMAC coating as to justify the need to re-amend for regeneration.

The relative differences in nitrogen content between these samples could provide an indication of changes in the coating resulting from sloughing-off during ultrasound treatment. A sample of polyDADMAC-GAC with no treatment or saturation was also measured as a reference. Total nitrogen was measured on samples of the water where sonication of PFAS-saturated polyDADMAC-GAC was carried out to further understand the potential desorption of polyDADMAC induced by ultrasound, since polyDADMAC has a nitrogen-containing functional group per monomer. Hach Total Nitrogen (TN) Kits were used (Method 10072, Persulfate Digestion Method, detection limit 2 mg/L) to detect nitrogen. TN was measured on samples after ultrasound with 700 kHz, 900kHz or stirred at 120 rpm, as well as on a solution of polyDADMAC (0.00025%) and deionized water.

The toxicity of the solution after polyDADMAC-modified GAC was subjected to ultrasound was evaluated in terms of ATP content of *Escherichia coli* according to previously reported methods(Pica et al. 2021). *Escherichia coli* (clinical isolate) was grown in Luria Bertani (LB) broth (BD Difco, Sigma-Aldrich , St. Louis, MO) for 24 h at 37□C with 120 rpm constant shaking. Toxicity tests were carried out once the culture reached early stationary phase (Optical Density (OD) measured at 600 nm = 2)), using Adenosine Triphosphate (ATP) assay for cell viability as previously. 50 µL of bacterial culture were incubated with 50 µL of the solution where PFAS-saturated polyDADMAC-modified GAC was exposed to ultrasound at 700 kHz or 900 kHz for 4 h and 24 h in a 96-well plate with a clear, flat bottom surface

The adenosine triphosphate (ATP) concentration was measured using the BacTiter-Glo™ Microbial Cell Viability assay (Promega, Madison, WI). 100 µL of BacTiter-Glo reagent were then pipetted into the plate. Samples were incubated at room temperature for 5 minutes and analyzed for luminescence using a VICTOR 3 V plate reader (PerkinElmer, Waltham, MA) at 1

second intervals. Background luminescence was determined by following the same procedure as experimental samples but with sterile DI water and BacTiter-Glo reagent. Positive controls were measured following the same procedure as above except that 50 µL of bacterial culture were incubated with 50 µL of sterile deionized water. These studies were conducted to evaluate the possibility of generating toxic byproducts from polyDADMAC exposure to ultrasound.

3.2.5 PFAS Analytical Methods

Stock solutions of isotopically labeled internal PFAS standards were prepared using high-purity methanol in a 70:30 ratio of methanol to DI water at a concentration of 500 µg/L (**Table 3.3**). 0.5 mL of aqueous sample was pipetted into 1-mL polypropylene vials, and diluted with high-purity methanol until the final expected concentration of each PFAS in solution was 200 µg/L. The internal standard of each compound was added to a concentration of 50 µg/L to account for PFAS losses due to adsorption to the vial walls, sample processing, or analytical variability. The solution was mixed thoroughly and aliquoted into 200 µL polypropylene vials. Sample were analyzed using an Agilent 1290 Liquid Chromatograph paired with an Agilent 6460 Triple Quadrupole Mass Spectrometer (LC/QqQ-MS) equipped with a Poroshell 120 EC-C18, 2.1x100 mm, 2.7 µm column plus C18 guard and delay columns.

The instrument used in the analysis was an Agilent 1290 UPLC coupled to an Agilent 6460 triple quadrupole mass spectrometer, which was equipped with an electrospray ionization (ESI) source using Agilent Jet Stream Technology (Agilent, Santa Clara, CA). Analytes were separated on an Agilent Poroshell C18 column (2.1 mm x 100 mm, 2.7 µm particle size) at 40 °C. A sample volume of 15 µL was injected into a binary mixture of 5 mM ammonium acetate in water (A) and 5 mM ammonium acetate in methanol (B) at a flow rate of 0.4 mL/min. The gradient used was 20% B for 1 minute, increasing to 45% B at 2 min, and finally increased to 100% B at 5 min. The

ionization source conditions used were as follows: negative polarity, nebulizer of 15 psi, gas flow of 4 L/min at 230°C, sheath gas flow of 12 L/min at 350 °C, nozzle voltage of 500 V, and capillary voltage at 3500 V. Analytes were identified by comparison of retention times with analytical standards, individual MRM mass transitions, and with MS/MS ion ratios. Peaks matching retention within 5% and with ion ratios at 20% of the standard ratio were considered acceptable for identification. The data collection and processing were performed by using Agilent MassHunter Quantitative software (v B.07.01). Quantitation was performed with linear regression using calibration curves.

Several steps were taken to minimize system-related interferences or background. An Agilent Eclipse Plus C18 column (4.6 mm x 50 mm, 5 μm particle size) was installed immediately after the binary pump and prior to the injection port to perform as a delay column. The mobile phase degasser was bypassed allowing the mobile phase to enter the binary pump directly and avoiding contact with plastic filters. All plastic tubing in the LC-MS/MS system was replaced with PEEK tubing and plastic frits were replaced with stainless steel. All sample vials were polypropylene with polypropylene caps. Five injections of pure methanol were made prior to sample analysis to determine if any system background analyte levels were present. With these system changes, background levels for each analyte were not detected in blank samples.

Table 3. 3 PFAS Internal Standards

PFAS	**Internal Standard Used**
PFOA	Perfluoro-*n*-[$^{13}C_4$]octanoic acid
PFOS	Sodium perfluoro-1-[1,2,3,4- 13 C 4]octane sulfonate
PFBA	Perfluoro-*n*-[13 C 4]butanoic acid
PFBS	Sodium perfluoro-1-[2,3,4- 13 C 3]butane sulfonate
PFHxS	Sodium perfluoro-1-[1,2,3- 13 C 3]hexane sulfonate

3.2.6 Statistical analysis

Error bars for discrete values were calculated using standard deviation, while error bars for data reported as percentage change were calculated using the Delta Method based on Taylor's Formula. T-tests ($p<0.05$ significance level) were performed to determine the optimum modification dose, for evaluating the response to competitive ions, and to assess the effects of sonication and regeneration. Adsorption isotherm fits and regression coefficients for the fits were evaluated for the Langmuir and Freundlich models using Origin (Pro), Version 2021 (OriginLab Corporation, Northampton, MA, USA). To prevent drawbacks of the linearizing method for isotherm fitting, this study used iterative fitting to the non-linear isotherm equations to produce optimal goodness of fit to the experimental (Hossain et al. 2013).

3.3 Results and Discussion

3.3.1 Surface characterization of adsorbents

FTIR spectra for unmodified GAC and polyDADMAC-GAC (0.00025%) show differences indicating that the surface functionality of GAC is altered when modified with polyDADMAC, (**Figure 3.1**). The obtained polyDADMAC ATR FT-IR spectrum corresponded to what has been previously reported (Mwangi et al. 2012, Mwangi et al. 2013). The peak at 1396 cm^{-1} on the unmodified spectrum was attributed to carboxylic acid functional groups on the surface of GAC (Tessmer et al. 1997). The polyDADMAC-GAC spectrum shows a peak shift towards lower wavenumbers (1384 cm^{-1}). The N-H band for primary, secondary, and tertiary amines appears in this region, however quaternary ammonium salts do not typically have N-H stretching vibrations, therefore this peak was attributed to asymmetrical bending of –CH in polyDADMAC as a result of the positively charged environment created by the quaternary ammonium cation (Razali et al. 2012), (Mwangi et al. 2012), (Mwangi et al. 2013). The peak at 3397 cm^{-1} in the polyDADMAC-GAC spectrum is attributed to an –OH stretching vibration (Razali et al. 2012). This is the result

of DADMAC's hygroscopic nature, which causes it to readily absorb moisture from the environment (Dean and Dean 1995), (Razali et al. 2012). These two peaks are characteristic of polyDADMAC FTIR spectra (Razali et al. 2012), (Mwangi et al. 2012), (Mwangi et al. 2013), (Dean and Dean 1995) and thus confirm surface modification.

BET surface area measurements of modified GAC confirmed that addition of polyDADMAC up to a concentration of 0.5% did not significantly change GAC's surface area (**Figure 3.2**). BET surface area of unmodified GAC was measured at 732 ± 34 m^2/g compared to 707 ± 36 m^2/g with 0.5% polyDADMAC, indicating that N_2 was able to access GAC's pore openings at this concentration. This is in contrast to the decrease observed when 10% polyDADMAC was dosed, which resulted in a surface area of 536 ± 27 m^2/g, indicating that some of the pore openings may have been blocked by polyDADMAC when higher coating doses were used (Cho et al. 2011), (Leyva-Ramos et al. 2008), (Xu et al. 2011).

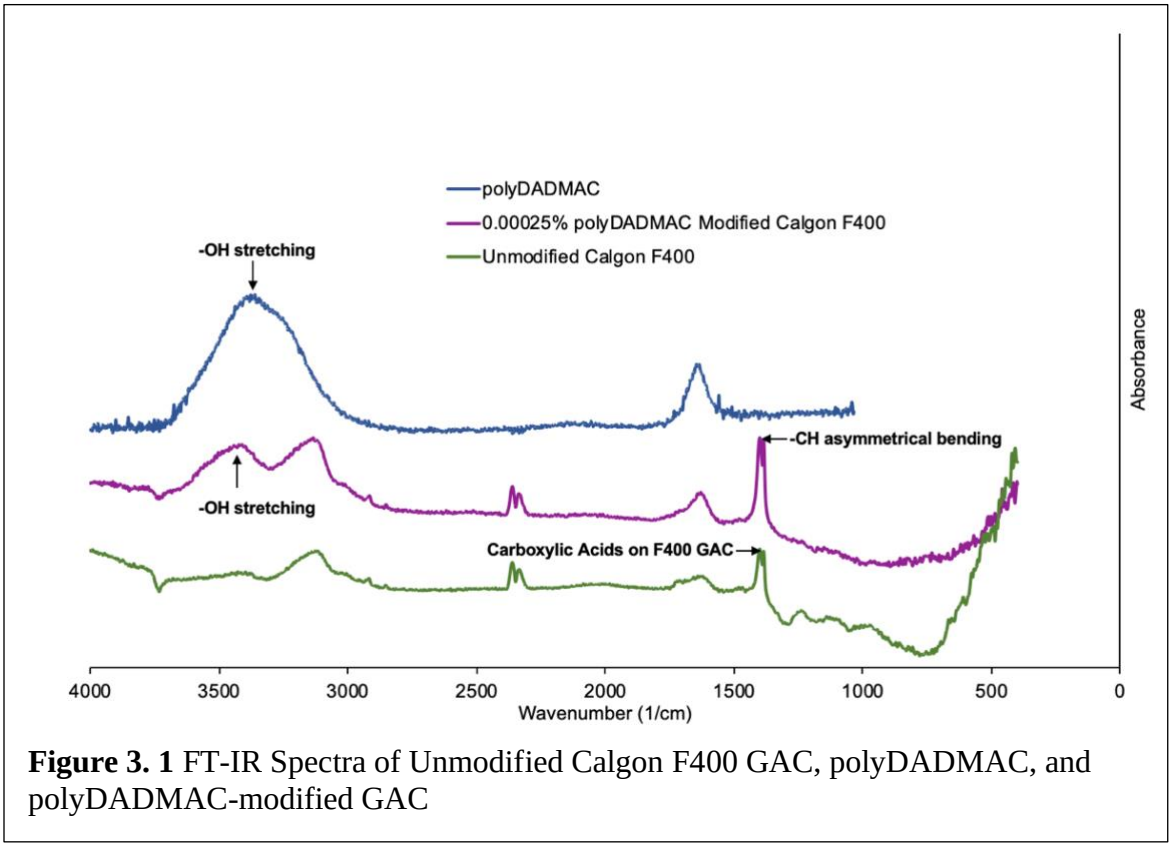

Figure 3. 1 FT-IR Spectra of Unmodified Calgon F400 GAC, polyDADMAC, and polyDADMAC-modified GAC

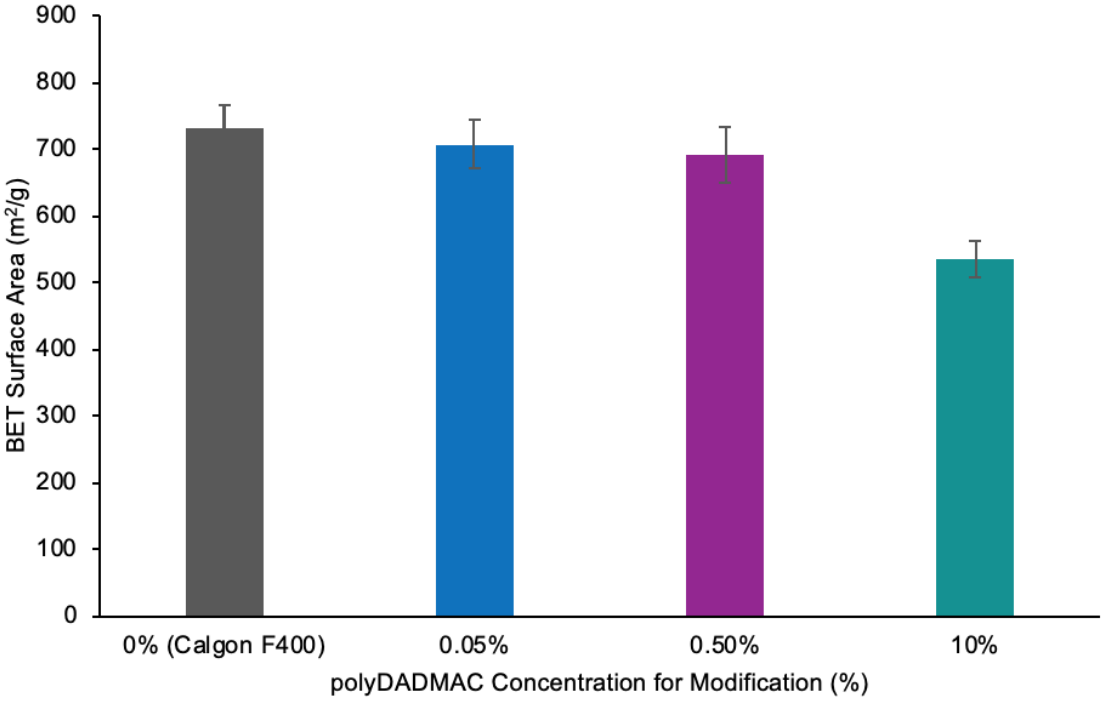

Figure 3. 2 BET Surface Area (m2/g) measurements of Calgon F400 GAC modified with different concentrations of polyDADMAC

3.3.2 Adsorption Isotherms

The adsorption of PFBA and PFOA followed a typical adsorption isotherm behavior showing increased adsorption when the equilibrium concentration increased (**Figure 3.3**). The models show correspondence with the Langmuir model as well as the Freundlich model for both PFOA (R^2 Langmuir = 0.99, R^2 Freundlich = 0.95) and PFBA (R^2 Langmuir = 0.97, R^2 Freundlich = 0.95) (**Table 3.4**). The Langmuir model assumes that adsorption occurs at homogenous sites, and has been used to fit isotherms for cationic polymer-modified sorbents (Cho et al. 2011), as well as for sorption of PFASs using GAC modified with cationic polymers (Aly et al. 2019), (Aly

et al. 2018). The Freundlich isotherm model assumes that adsorption processes occur on heterogeneous surfaces where active sites on the surface have different energies (Ayawei et al. 2017). Thus it could be expected from a theoretical perspective that the behavior of this modified sorbent could be accurately depicted by both models, since the coating of particles with cationic polymers does not occur homogenously but rather as a series of patches (Gregory 2006), thus introducing electrostatic interactions into a system where surface processes are dominated by hydrophobic interactions. This is likely mostly relevant at low ionic strength, based on the data shown below, since electrostatic interactions directly between polyDADMAC and PFASs are likely most relevant when there are no competing ions. Both adsorption isotherm models indicate that the adsorbent becomes saturated, which introduces the need for a strategy to encourage PFASs to become desorbed. Total nitrogen measurements following equilibration of the PFAS-containing solutions with polyDADMAC-modified GAC yielded non-detectable nitrogen indicating that no detectable amounts of polyDADMAC were leached from the modified GAC upon adsorption of PFAS.

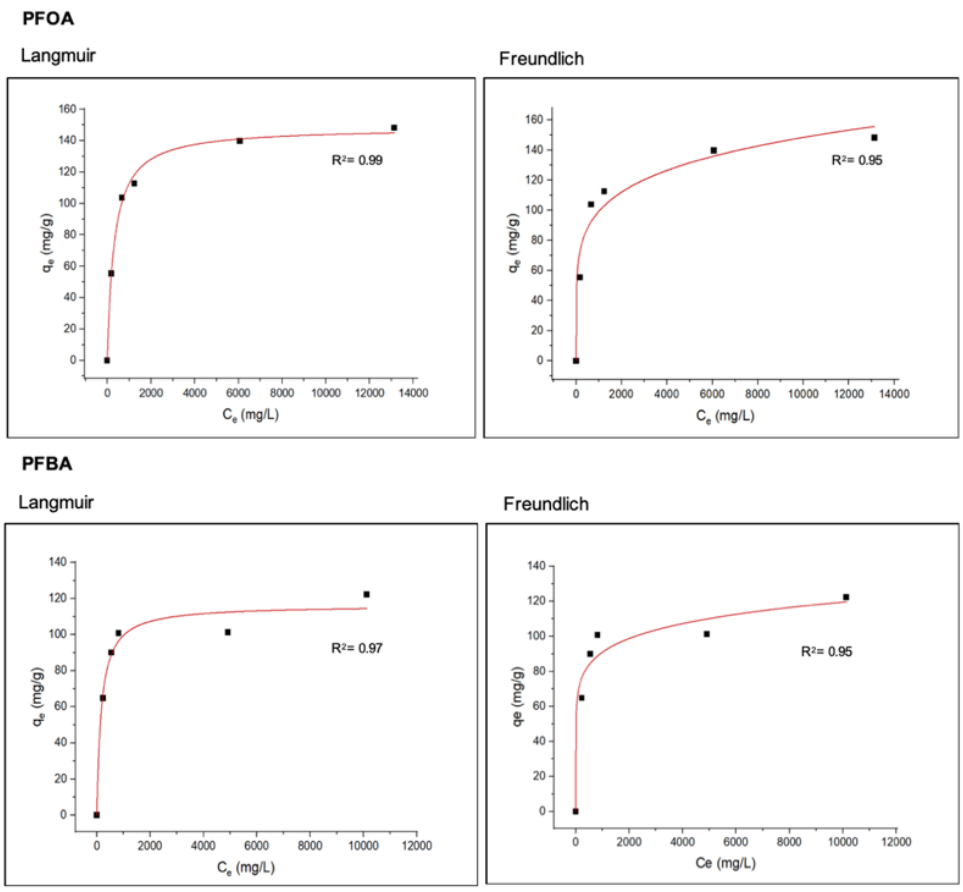

Figure 3. 3 Langmuir and Freundlich Isotherm Model Fits For Adsorption of PFOA and PFOS

PFAS Compound	K_L	Q_m	R^2 Langmuir	K_F	n	R^2 Freundlich
PFOA	0.47 ± 0.04	313.77	0.99	29.78 ± 8.61	5.73 ± 1.16	0.95
PFBA	0.70 ± 0.16	165. 68	0.97	40.12 ± 10.16	8.43 ± 2.32	0.95

Table 3. 4 Langmuir and Freundlich Isotherm constants and adsorption isotherm fits obtained by fitting the data to non-linear isotherm models

3.3.3 Effect of Competitive Ions

Results show a statistically significant increase in the adsorption capacity of polyDADMAC-GAC for PFBA and PFBS in all aqueous conditions when tested in a mixed PFAS system (**Figure 3.4**). This is ascribed to two factors, namely electrostatic interactions between PFBA and PFBS and polyDADMAC, as well as electrostatic interactions between polyDADMAC and competing ions. polyDADMAC is a high-molecular weight polymer with a high positive charge density, which means that its chains are able to extend beyond the electrical double layer associated with the anionic GAC surface (Liu et al. 2008) to which they are bound. This allows negative ions to bind electrostatically with polyDADMAC (Vajihinejad et al. 2018), (Gregory 2006). In addition, the ionic composition of the groundwater matrices (monovalent ions, divalent ions, humic acids) may facilitate aggregation of ions through divalent cation bridging effects and charge neutralization (Vajihinejad et al. 2018), (Gregory 2006). This allows some salinity ions or humic acid that would otherwise compete with PFASs for GAC's adsorption sites to be removed either by binding electrostatically with polyDADMAC's positive charge, or by forming aggregates with these bound ions, thus allowing more sites on the GAC to be free for PFAS adsorption. The difference in polyDADMAC-GAC's capacity to remove PFBA at 0.02 M compared to 0.2 M ionic strength was not statistically significant, which indicates that some PFAS removal at higher ionic strength was likely caused by ion bridging and ion aggregation and not exclusively by the mitigation effects of polyDADMAC.

PolyDADMAC-GAC performed significantly better at removing PFBA than unmodified GAC in the presence of HA ($p<0.01$) (**Figure 3.5**). This is because some HA molecules were likely able to bind electrostatically to the polyDADMAC. This is evidenced by zeta potential data presented in **Tables 3.5-3.9**. The positive zeta potential value obtained from a 1:1 mixture of

polyDADMAC and humic acid supports the stipulation that the cationic charge of the polyDADMAC is the dominant mechanism responsible for the observed mitigated effect of humic acid. This may prevent an increase in electrostatic repulsion between the surface and the PFASs when the humic acid binds to the surface of GAC (Vu and Wu 2020) as well as excessive blockage of GAC's pores by the large humic acid molecules. This allowed for more of the effective surface area of polyDADMAC-GAC to be used to adsorb PFBA as compared to that of unmodified GAC. The effects were most evident for PFBA since short-chained PFASs pose a greater challenge for removal by unmodified GAC because they are less hydrophobic and more mobile (Kothawala et al. 2017, Gobelius et al. 2018), (Vu and Wu 2020). This is particularly relevant in systems with competing molecules (Kothawala et al. 2017), (Vu and Wu 2020), since the short chain makes the hydrophobic interactions between the carbon-fluorine backbone and the GAC's surface weaker than those of their long-chained counterparts (Kothawala et al. 2017), (Vu and Wu 2020).

The effect observed in the remaining PFASs showed statistically significant improvement in the adsorption of PFBS and PFHxS by polyDADMAC-GAC only at a HA concentration of 45 mg/L (**Figure 3.6**), while no statistical significance was observed in any condition for PFOS. This could be caused by several factors. First, there is likely a strong competition between PFASs and HA for the same pore spaces and binding sites (Kothawala et al. 2017). Humic acid and PFASs can also potentially interact with each other through hydrophobic interactions which, at high enough HA concentrations, may allow for retention of PFASs to increasingly take place (Kothawala et al. 2017). This means that some of the removal at 45 mg/L may be attributed to associations with HA rather than with cationic polyDADMAC. . In general the charge effects become less important as PFAS chain length increases since long-chain PFASs adsorb more

favorably by hydrophobic interactions than short-chain compounds, which explains why the effects were most evident for shorter compounds (Gobelius et al. 2018), (Vu and Wu 2020).

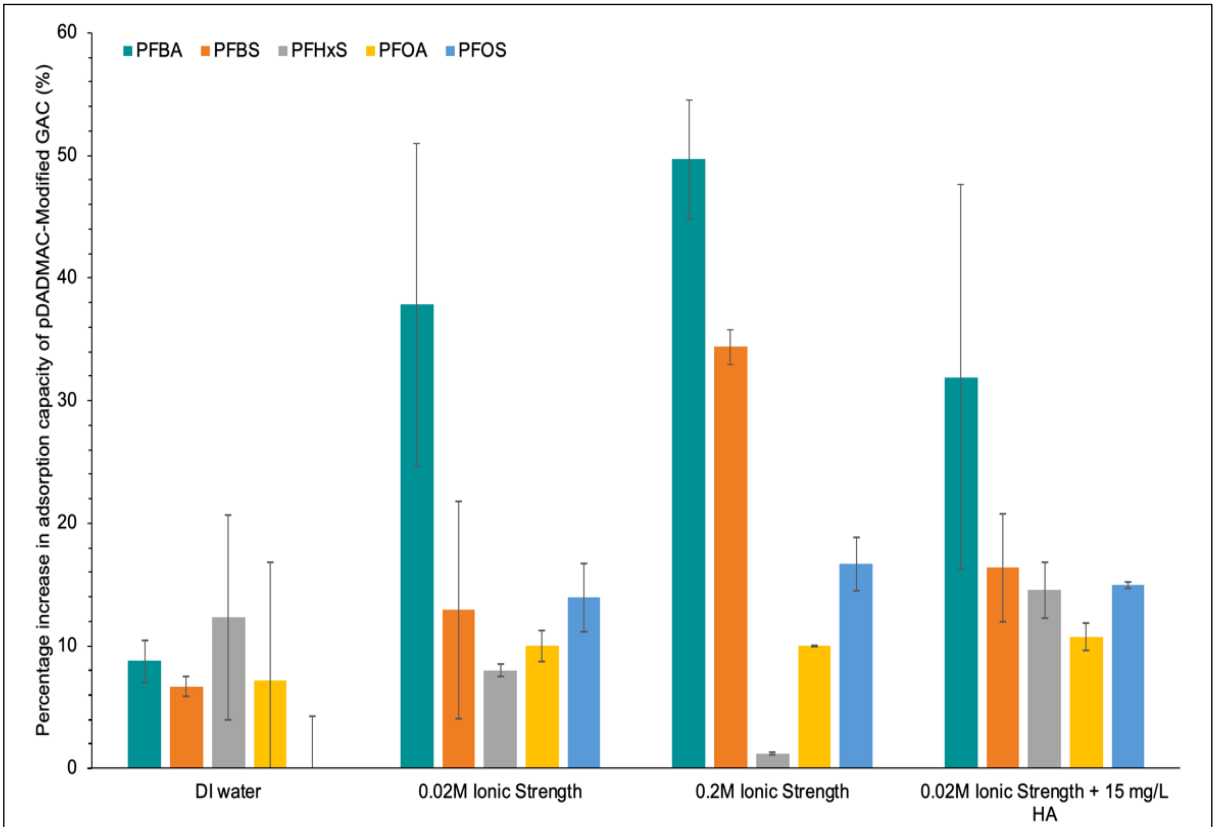

Figure 3. 4 Percentage Increase in Adsorption Capacity of polyDADMAC-Modified GAC

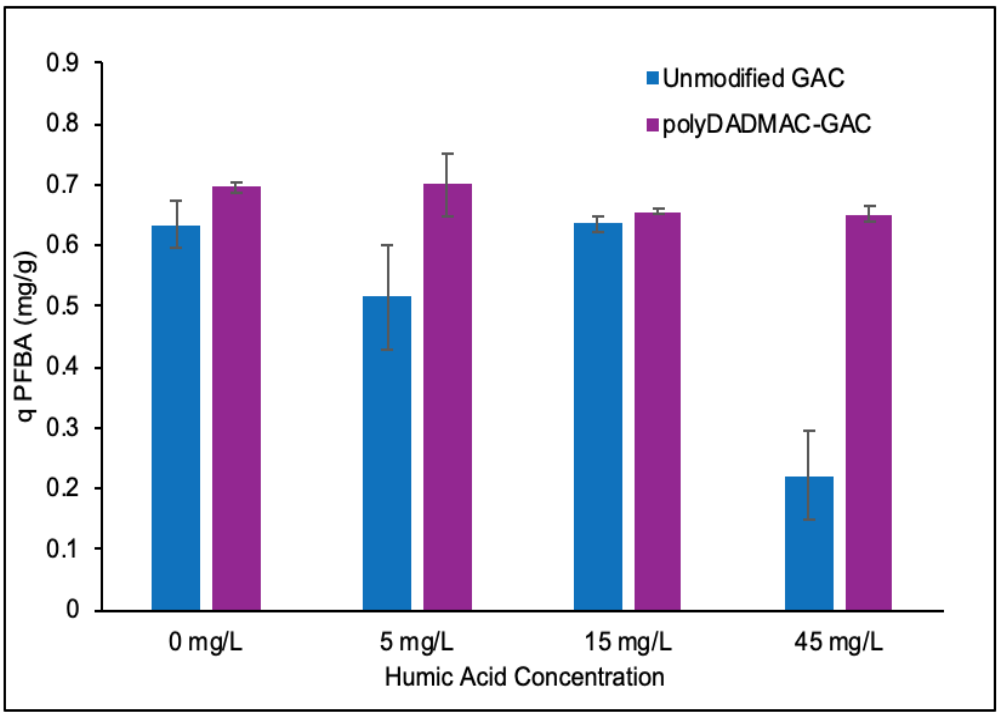

Figure 3. 5 Adsorption Capacity of polyDADMAC-GAC and Unmodified GAC for PFBA at Different Humic Acid Concentrations

Table 3. 5 polyDADMAC 0.00025%- pH 7.2

Measurement	Zeta Potential (mV)	Mobility
1	20.3	1.6
2	16.0	1.3
3	24.5	1.9
4	17.4	1.4
5	27.9	2.2
Mean	21.2	1.7
Standard Error	2.2	0.2

Table 3. 6 polyDADMAC + Humic Acid 5 mg/L pH 7.18

Measurement	Zeta Potential (mV)	Mobility
1	19.6	1.5
2	26.4	2.1
3	23.1	1.8
4	19.5	1.5
5	27.7	2.2
Mean	23.3	1.8
Standard Error	1.7	0.1

Table 3. 7 Humic Acid 5 mg/L pH 2.80

Measurement	Zeta Potential (mv)	Mobility
1	-12.2	-1.0
2	-14.0	-1.1
3	-5.4	-0.4
4	-14.6	-1.1
5	-19.8	-1.6
Mean	-13.2	-1.0
Standard Error	-2.3	0.2

Table 3. 8 Humic Acid 5 mg/L pH 5.90

Measurement	Zeta Potential (mv)	Mobility
1	-30.7	-2.4
2	-25.3	-2.0
3	-25.9	-2.0
4	-25.9	-2.0
5	-19.8	-2.7
Mean	-25.5	-2.2
Standard Error	3.5	0.3

Table 3. 9 Humic Acid 5 mg/L pH 8.70

Measurement	Zeta Potential (mv)	Mobility
1	-30.2	-2.3
2	-28.0	-2.2
3	-48.0	-3.8
4	-32.7	-2.6
5	-43.7	-3.4
Mean	-36.5	-2.9
Standard Error	3.9	0.3

3.3.4 Effect of cationic polymer dose

The greatest increase in adsorption capacity of all tested PFASs was observed for GAC modified with 0.00025% polyDADMAC (**Figure 3.7**) when different doses were tested in high salinity water. Additionally, it is possible to infer based on the data above that observed differences between modification doses would be augmented in less extreme salinity conditions. The increased adsorption capacity which occurs when modifying GAC with polyDADMAC is ascribed to the presence of quaternary ammonium functional groups on the surface (Cho et al. 2011), (Liu et al. 2020), (Aly et al. 2019). However, the role that this functional group plays presumably varies depending on the water chemistry conditions. When the matrix consists purely of DI water, the enhancement is solely due to electrostatic interactions between PFASs and the quaternary ammonium (Cho et al. 2011), (Liu et al. 2020), (Aly et al. 2019). However, as shown above, when the system includes competition, the increased capacity is also likely the result of interactions between the quaternary ammonium group and the competing ions, which allows more PFASs to interact with GAC directly through hydrophobic interactions.

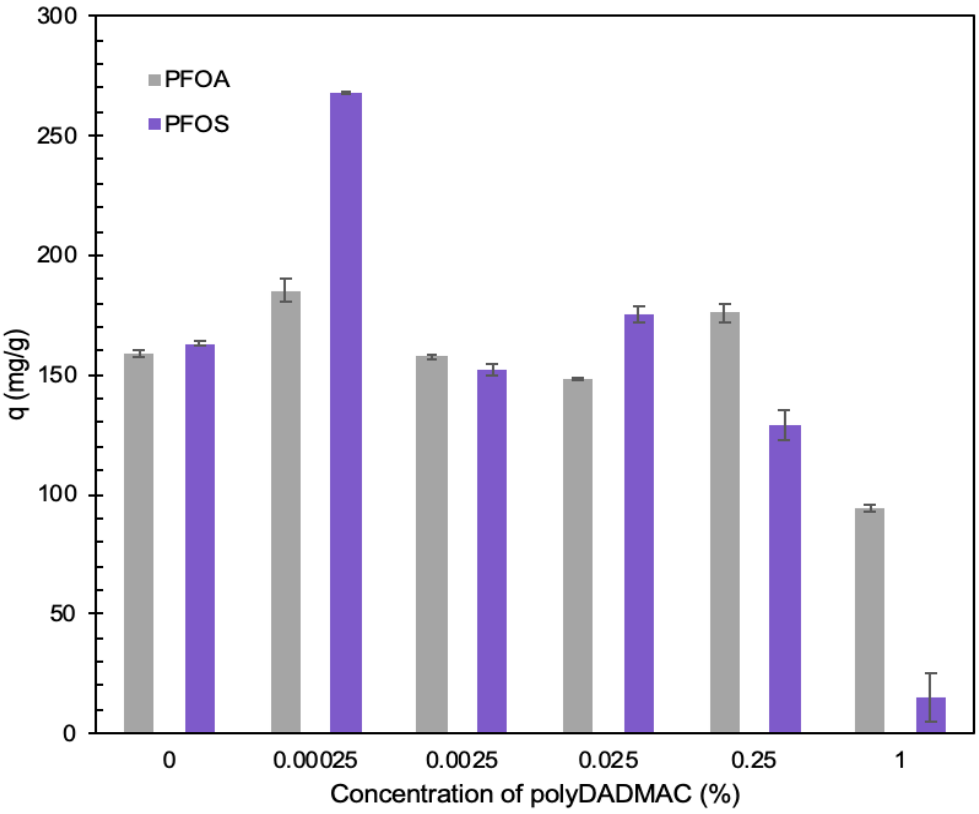

Figure 3. 6 Adsorption Capacity for PFOA and PFOS Upon Modification With Different Concentrations of polyDADMAC

The greatest improvement in capacity corresponds to the lowest tested polyDADMAC dose, pointing to the importance of optimizing the system when modifying GAC with cationic polymers to ensure that the modification is not being more detrimental than it is beneficial. The differences in capacity observed between the polymer concentrations are ascribed to two main factors. First, the relative ratio of polymer to GAC, which affects the extent to which the functional groups already present on GAC's surface are altered, since this can affect the interactions involved

in the adsorption process (Cho et al. 2011).The second factor is the effect of the addition of polymer on the ability of PFASs to access the sorbent's pores, which may be reduced when an excess of cationic polymer blocks pore openings, hindering access to essential sites inside GAC's pores (Cho et al. 2011), (Leyva-Ramos et al. 2008). The results observed from BET analysis support this hypothesis, since they showed a decrease in surface area as the polymer concentration used for modification was increased from 0% to 10% (**Figure 3.2**). This is especially important to consider when the material will be used in the presence of competing solutes. It is likely that when competing ions are present, the removal of PFASs is mainly the result of direct hydrophobic interactions with GAC rather than electrostatically with the quaternary ammonium, since the charge is employed to mitigate the effects of competitions. Thus, we assume that the presence of competing ions in these experiments is the reason why there was an observed decrease in capacity at 0.0025%, 0.025%, 0.25% and 1% polyDADMAC even though no significant changes in BET surface area were observed.

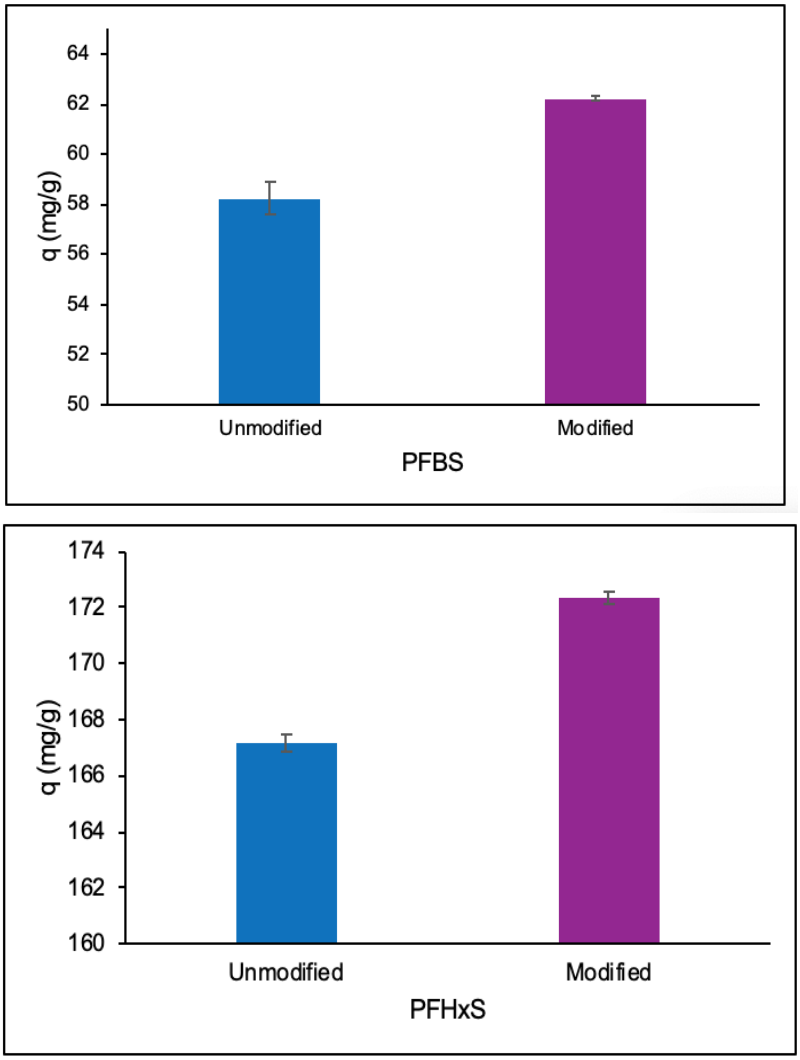

Figure 3. 7 Adsorption Capacity for PFBS and PFHxS for Unmodified and polyDADMAC-Modified GAC

3.3.5 Ultrasonic Desorption of PFAS and Regeneration Potential of polyDADMAC-GAC

As all other adsorbents, the lifespan of polyDADMAC-GAC is limited after becoming saturated with PFASs and a regeneration strategy is desirable in order to make the applications viable and more sustainable in the long-term (Lu and Wang 2010, Watanabe et al. 2018, Dai et al.

2019, Gagliano et al. 2020, Nuñes et al. 2020). Low power ultrasound was used for this purpose, with the greatest increase in the concentrations of both PFASs in solution observed when GAC was sonicated at 900kHz, while hardly any change was observed when stirred at 120 rpm (**Figure 3.8**). This means that the most desorption was achieved at 900 kHz, but also indicates a certain degree of stability in the interactions between polyDADMAC-GAC and PFASs since almost no desorption occurred after 2 h of mechanical stirring. The data also illustrate that the interactions between the polyDADMAC-GAC and longer-chain PFASs remained stronger than with the shorter-chain (as is the case of unmodified GAC) since the percentage increase in PFBA in solution after 2 h at both frequencies was more than one order of magnitude greater than the increase in PFOA (**Figure 3.8**), pointing to weaker surface interactions. Total fluoride measurements after 2 h showed no detectable fluoride indicating that no degradation of PFASs occurred under the tested conditions. This is expected based on the low power used in these experiments (Singh Kalra et al. 2021).

The adsorption capacity for PFBA of polyDADMAC-GAC treated only by stirring at 120 rpm decreased by about 34%, after one saturation cycle while the changes for the batches which underwent sonication were significantly less (7% when sonicated at 700 kHz, 6% for 900 kHz) with a similar trend was observed for PFOA (**Figure 3.9**). Overall, this indicates that treating saturated polyDADMAC-GAC with ultrasound is an effective means of desorbing PFASs while retaining adsorption capacity over two rounds of exposure to PFBA and PFOS. When the sorbent was regenerated by treating with low power ultrasound at 900 kHz and reamending with polyDADMAC, its capacity for PFBA over four rounds of adsorption decreased cumulatively by only 2-4% while the capacity decreased cumulatively by 59% for polyDADMAC-GAC that was not treated by ultrasound nor reamended (**Figure 3.9**). Similarly, the adsorption capacity of PFOA

over four rounds of adsorption decreased cumulatively by only 2-4% while the capacity decreased cumulatively by 63% for polyDADMAC-GAC that was not treated by ultrasound nor reamended.

Re-modification with polyDADMAC to regenerate the adsorbent was performed because the energy associated with sonication was strong enough to lead to the sloughing off of some polyDADMAC, since the adherence of the surface modification occurs through an aggregation of weak intermolecular forces rather than chemical bonds (Vajihinejad et al. 2018). XPS data (**Table 3.10, Figure 3.10**) supported this hypothesis since they revealed a notable difference between the samples. PolyDADMAC-GAC which underwent no PFAS saturation nor ultrasound treatment had a nitrogen content of approximately 1.87% (atomic), while samples after exposure to 900 kHz ultrasound had a nitrogen content approximately 0.38% (atomic) (**Table 3.10, Figure 3.10**). Since data indicated a considerable amount of desorption of PFASs at this frequency (**Figure 3.8**), it is possible to conclude that the change in nitrogen content was not an effect of PFAS saturation of the nitrogen-containing functional groups but rather due to sloughing off of polyDADMAC. TN samples further validate this hypothesis since water samples where polyDADMAC-GAC had been sonicated at 700 kHz and 900 kHz had detectable TN (4.3 ± 0.5 mg/L TN) while TN was not detected in control samples stirred at 120 rpm (**Table 3.11**).

It was expected that no toxic byproducts resulted from the exposure of polyDADMAC to ultrasound since the exposure of other polymers to ultrasound has been shown to result in homologous series of different molar masses of the same polymer, rather than altering the compounds' chemical structures (Schittenhelm and Kulicke 2000), (Goodwin et al. 2011), (Mohod and Gogate 2011). Toxicity tests performed by exposing *Escherichia coli* to the solution where the polyDADMAC-modified GAC was exposed to ultrasound showed no inhibitory effects after 4 h nor after 24 h (**Figure 3.11**) indicating no significant toxicity effects of concern. Overall, these

conclusions provide a possibility for an adsorbent that can be utilized multiple times with minimum decrease in capacity. Additionally, ultrasound has been proven effective at degrading PFASs without generating toxic intermediates or byproducts, and has also been shown to degrade a range of compounds without the generation of disinfection byproducts (Singh Kalra et al. 2021). As a result, this could give rise to a simple treatment train approach for managing the concentrated waste streams generated by the sorption process where the same unit could be used to desorb PFASs from the sorbent as well as to treat the small volume of concentrated waste by simply changing the ultrasound power used for each purpose.

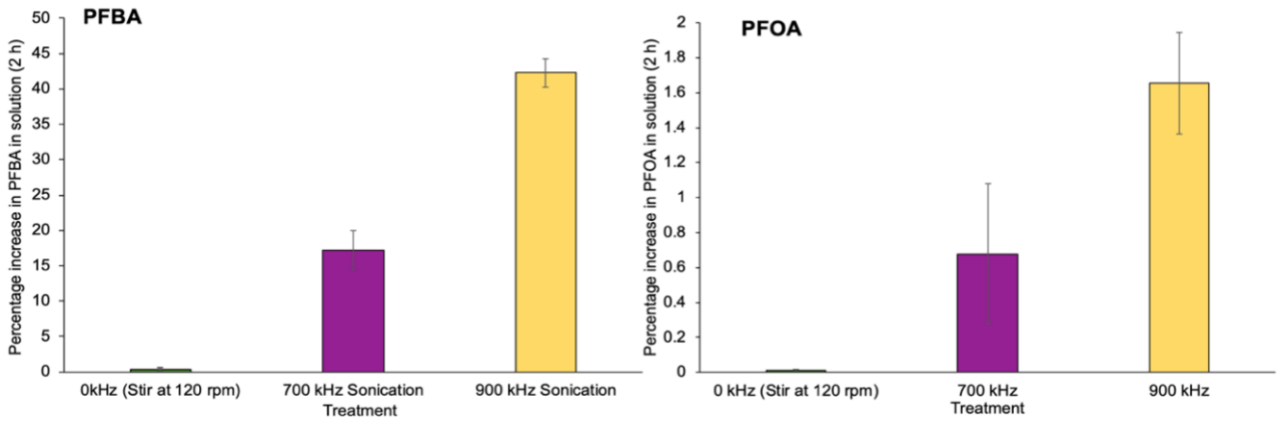

Figure 3. 8 Percentage Increase in PFBA and PFOA in Solution Upon Treatment with Ultrasound

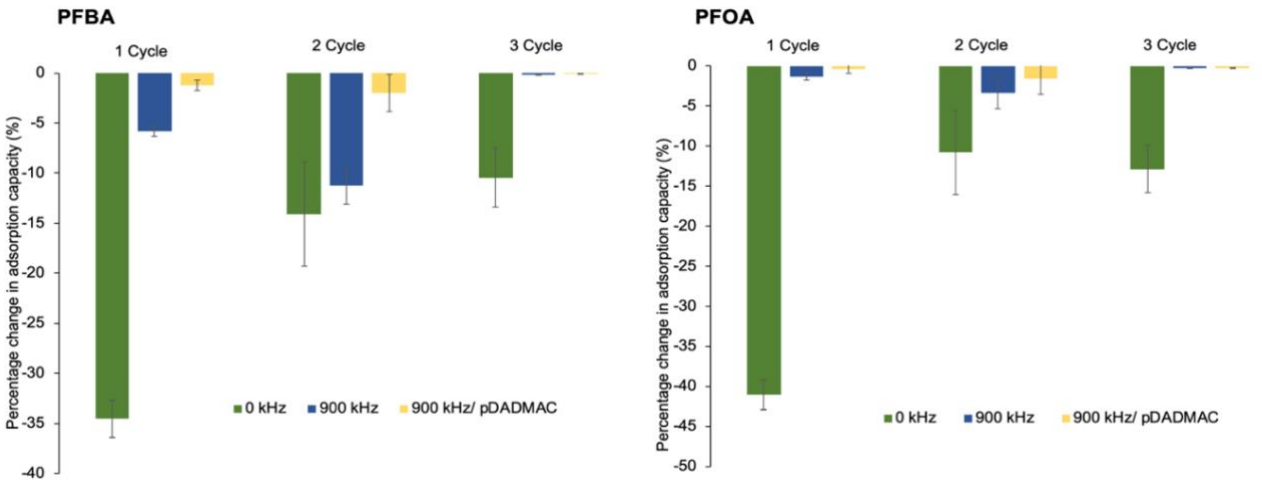

Figure 3. 9 Percentage change in adsorption capacity for PFBA and PFOA after Ultrasound Regeneration of polyDADMAC-GAC

Table 3. 10 Atomic Percentage of elements on the surface of granular activated carbon (polyDADMAC-modified) as determined by XPS

Element	**polyDADMAC-GAC (No PFAS, no ultrasound)**	**polyDADMAC-GAC (PFAS saturation followed by 900 kHz)**	**polyDADMAC-GAC (PFAS saturation followed by 120 rpm mixing-no ultrasound)**
Oxygen	9.92	6.51	6.69
Carbon	87.25	92.08	91.82
Nitrogen	1.87	0.38	0.46
Σ (Si, Al, S)	0.97	1.02	1.04

Table 3. 11 Total Dissolved Nitrogen in Sonicated polyDADMAC-GAC Samples (*Detection limit for Total Nitrogen (TN) (Method 10072, Persulfate Digestion Method is 2 mg/L)

Sample Name	Total Nitrogen (mg/L)
0.00025% polyDADMAC (Positive Control)	7.0 ± 0.71
polyDADMAC-GAC/ 900 kHz	4.3±0.47
polyDADMAC-GAC/700 kHz	4.3±0.22
polyDADMAC-GAC Stirred at 120 rpm- No ultrasound (Negative Control)	N.D.

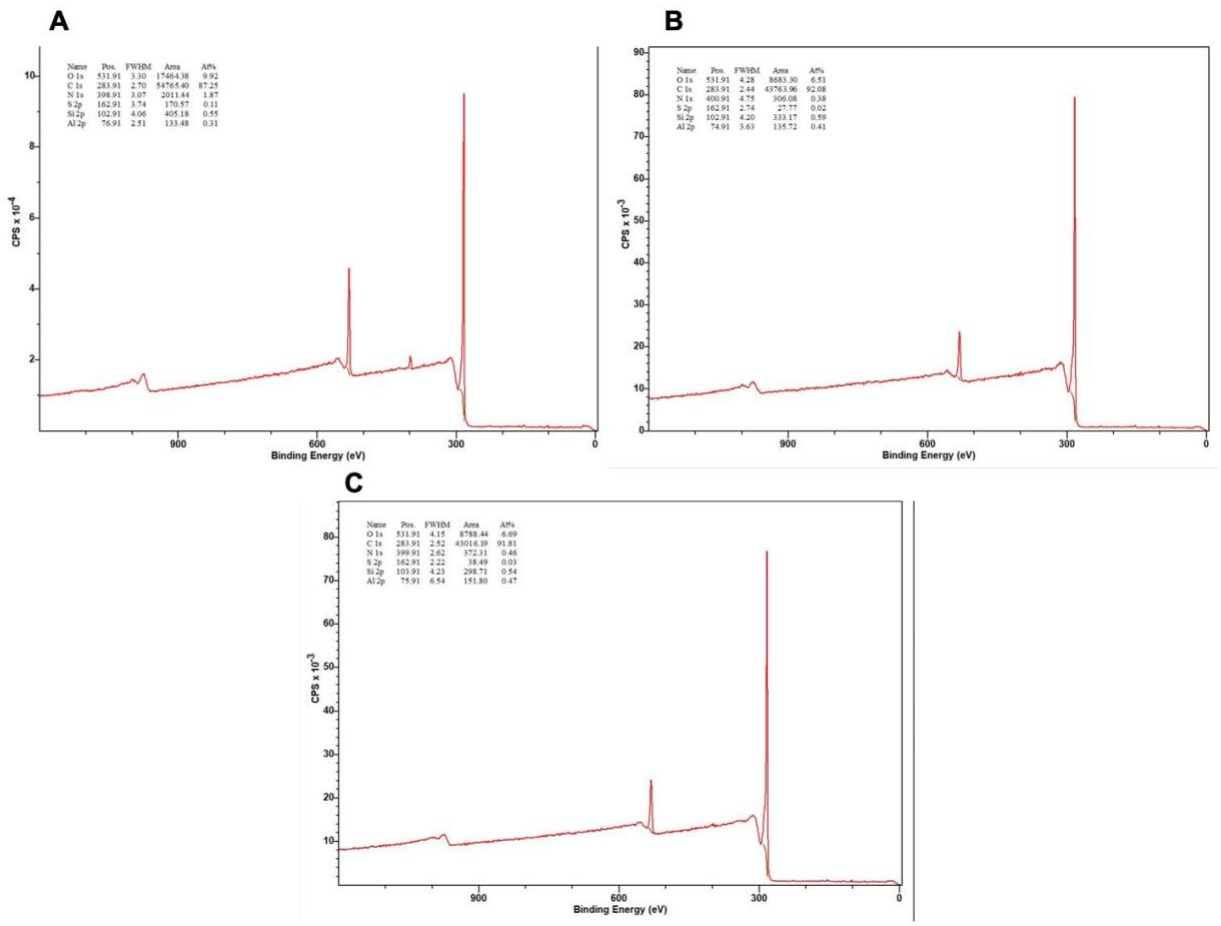

Figure 3. 10 XPS Spectra of polyDADMAC-GAC Surface After Ultrasound Treatment

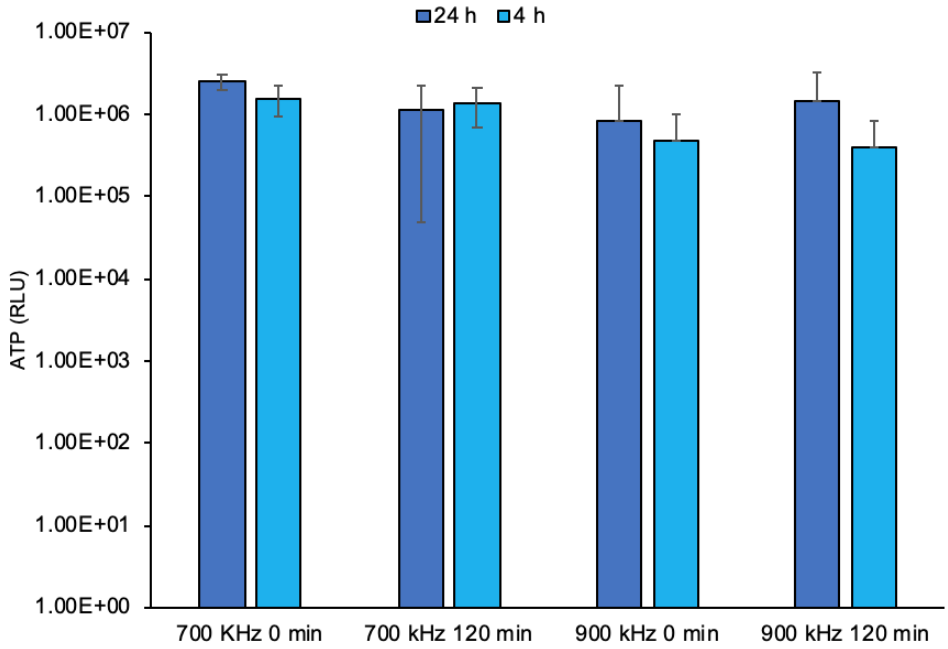

Figure 3. 11 ATP Assay on Microorganisms In Contact with Supernatant from polyDADMAC-GAC Ultrasound Treatment

3.4 Conclusion

This study found that modifying GAC's surface with polyDADMAC enhances the sorption of PFASs, particularly short-chain compounds, even in the presence of competing ions which are usually expected to rapidly exhaust GAC .PolyDADMAC-GAC's high removal capacity in the presence of humic acid and salinity ions suggests that electrostatic interactions with polyDADMAC's functional groups helped bind organic and inorganic ions as well as the headgroup of short-chain PFASs, allowing more overall removal by the GAC. Our results indicate that it is crucial to evaluate the effect of polymer dose on adsorption capacity in order to

prevent decreased removal resulting from masking of pore entrances. Low power ultrasound treatment of polyDADMAC-GAC after PFAS saturation restored GAC's adsorption capacity, indicating that polyDADMAC-modified GAC combined with ultrasound regeneration could provide a sustainable and effective treatment option for PFAS-impacted water. Collectively, A) the surprisingly low concentration of polyDADMAC required to increase sorption capacity, B) the effectiveness of the adsorbent in the presence of competing ions, and C) the possibility for regeneration allow this process to be cost effective and provide a simple and viable strategy for ex-situ field implementation.

Chapter 4: Effect of C/N influent ratios on biofilm characteristics in Pseudomonas aeruginosa, aerobic bacterial-based membrane bioreactors (MBRs), and combined bacterial-algal membrane bioreactors (CAMBRs)

4.1 Introduction

Biofilms are microbial communities that are metabolically and morphologically distinct from planktonic cells in ways that make microorganisms more resilient to environmental stressors (Flemming and Wingender 2010, Crouzet et al. 2014, Romling et al. 2014, Vasudevan 2014). In the water and wastewater treatment field biofilms can be both advantageous (Mpongwana 2022) as well as detrimental depending on the designated treatment process (Meng et al. 2017). Beneficial biofilms are those that are used for applications that benefit from the retention of high cell densities on surfaces or carrier media such as in trickling filters (Petrovich et al. 2017), membrane biofilm bioreactors, etc.(Saidulu et al. 2021), while they can be detrimental to effective treatment and may increase associated energy requirements in systems that rely on functional surfaces for the treatment process, such as in the case of membrane bioreactors (MBRs) (Hong et al. 2019) (Hong et al. 2018). Aside from the water treatment process, biofilms are relevant in distribution systems, where the biofouling of tanks or pipelines may expose the treated water to pathogenic microorganisms (Zuo et al. 2022).

Quorum sensing (QS) is a bacterial cell-to-cell signaling communication mechanism that allows the development of the distinct cooperative metabolic features that are present in biofilm communities(Mukherjee 2019) (Papenfort 2016). Understanding QS shifts in relation to water and wastewater treatment parameters is important because QS control has been shown to be an effective method for both biofouling prevention(Yeon et al. 2009) (Panchavinin et al. 2019, Hong et al. 2022) as well as for facilitation of successful biofilm growth for the degradation of

contaminants (Tripathi et al. 2022) , or for improving the retention of slower growing organisms that can aid in nutrient removal (Petrovich et al. 2017).

Composition of wastewater may vary greatly depending on geographic location, source, and season. The ratio of chemical oxygen demand (COD)/total nitrogen (TKN) or C/N ratio has been shown to be one of the most important parameters affecting characteristic of activated sludge microorganisms because of its effect on the overall composition of the extracellular polymeric substance matrix (EPS) (Xu et al. 2021) (Fan et al. 2015, Chen et al. 2021) (Miqueleto et al. 2010). EPS is mostly composed of polysaccharides that are excreted from cells as either soluble or insoluble polymers (Karygianni et al. 2020), with the specific composition, structure, and quantity of the substance being dependent on the specific microbial community present, as well as the nutrients and the operating parameters (Miqueleto et al. 2010). Influent C/N ratio is also known to affect the treatment efficacies of industrial and municipal wastewater treatment plants (WWTP), especially in the case when the systems are carbon limited (Erkhan and Engin 2019) (Xu et al. 2021).

Microbial communities in WWTP bioreactors are not static, but have been shown to include *Proteobacteria*, *Bacteroidetes*, *Firmicutes* and *Actinobacteria* as the most abundant phyla (de Celis et al. 2020) (Wu et al. 2019) . Studies have shown that communities shift to be dominated by the *Proteobacteria phylum when biofilms develop, notably containing orders such as Pseudomonadales, Rhizobiales, and Burkholderiales (Luo et al. 2017). Pseudomonas aeruginosa* is a common biofilm-forming Gram-negative bacteria that is an opportunistic human pathogen (Malesevic et al. 2019) and is also widespread in the environment, as well as in water distribution and storage systems (Chao et al. 2015) (Tanner et al. 2019) (Zuo et al. 2022). *P. aeruginosa* is also known to be an early colonizer of surfaces and facilitate subsequent

attachment of other organisms in reservoirs and distribution systems(Zuo et al. 2022) (Douterelo et al. 2014) (Liu et al. 2016) as well as in trickling filter communities(Petrovich et al. 2017). Due to its threat to human health, the biofilm formation mechanisms in *P. aeruginosa* are very well studied and therefore serves as a good model organism for biofilm-based studies (Abdelraheem et al. 2020).

This study evaluated the effect of the C/N ratio on the biofilm characteristics as well as the expression of QS and stress-related genes in a single-organism system. Due to the extensive literature on its QS pathways, *Pseudomonas aeruginosa* was used as a model organism to study the effects of the influent conditions on mechanisms of transcription regulation related to quorum sensing. The *Agrobacterium tumefaciens* bioassay was used for evaluating the effect of the feedwater conditions on QS signaling molecule (AHLs) production. The potential for chemical oxygen demand (COD) removal was also evaluated in the different conditions, and the removal potential achieved by both planktonic and biofilm-state bacteria were compared. Principal component analysis was performed on a vector of all the measured output variables to understand possible correlations between them as well as the relationship between the feedwater C/N conditions and the observed outputs. The development of a multispecies biofilm using a co-culture of *Pseudomonas aeruginosa* and *Nitrobacter winogradskyi* was explored to understand the effect of C/N on the retention of slower growing organisms due to the relevance in wastewater treatment applications such as biological nutrient removal.

4.2 Materials and Methods

4.2.1 Chemicals

Luria-Bertani Broth (LB Miller, DB Difco) was obtained from Sigma Aldrich. COD quantification kits were obtained from Hach Company (Loveland, CO). Dextran (dextran from

Leuconostocspp. Mr~40,000. 31389, Fluka) was obtained from Millipore Sigma (Burlington, MA). All other chemicals were ACS grade or higher.

4.2.2 Microbial Culture and Growth Conditions

Pseudomonas aeruginosa (clinical isolate) was grown in Luria-Bertani Broth (LB, Miller, Sigma Aldirch), at 37°C and 120 rpm. This culture was previously isolated from urine preserved in boric acid by UCLA Department of Pathology and Laboratory Medicine. Briefly, 1μL of the liquid urine was plated on blood agar and MacConkey agar, incubated at 35□C for 24-48 hours and then examined for specific colonies.

Nitrobacter winogradskyi (Winslow et al. ATCC 25391) was grown in DSMZ medium 756a at 30°C and 120 rpm. *Agrobacterium tumefaciens* NTL4 (pCF218) (pCF372) was generously provided by Dr. Clay Fuqua from Indiana University. Cultures of *Agrobacterium tumefaciens* NTL4 (pCF218) (pCF372) were grown in 500-mL containers at 30°C and 120 rpm, using AT minimal glucose medium at pH 7 (Tempe et al. 1997) with the antibiotic streptomycin (Kawaguchi et al. 2008).Killed controls of all experiments were performed using autoclaved organisms in the same conditions as the experimental settings described in the following sections.

4.2.3 Synthetic Feedwater Composition

Synthetic feedwaters of varying carbon-to-nitrogen (C/N) ratios were prepared according to the ratios and compositions proposed by Kim et al. (Kim et al. 2021). The carbon source was $CH_3COONa \cdot 3H_2O$, alkalinity was added as $NaHCO_3$, and the nitrogen source was $NaNO_3$ (Sigma Aldrich). $NaNO_3$ was selected as the nitrogen source so that the same feedwaters could be used in experiments using both *P. aeruginosa* and *N. winogradskyi.* The C/N ratio was varied

from 3-21 (3,6,9,12,15,18,21) according to several sources identifying this as a relevant ratio for wastewater influent (Kim et al. 2021) (Fan et al. 2015, Erkhan and Engin 2019).

4.2.4 Biofouling Tests

Pseudomonas aeruginosa was grown to early stationary phase (OD=2) as above before starting these experiments. 1- inch segments of silicone tubing (MasterFlex L/S ® 13) were used as a model inert surface to grow the biofilm. A 10% inoculation of active *P. aeruginosa* was added into sterile glass bottles containing sterilized feedwater of one of the defined C/N ratios. All bottles were filled to contain 1:5 headspace by volume and sealed. A sterile syringe needle with an attached filter was added to all bottles to further facilitate proper oxygenation, preventing the confounder of oxygen limitation-induced stress as a cause for biofilm formation. Cultures were allowed to grow in a shaking incubator for 24 h at 37°C and 120 rpm before extracting an analyzing the biofilm. All experimental conditions were carried out in triplicate.

4.2.5 Biofilm Extraction and Quantification Methods

Extraction was performed as previously described by Mandakhalikar et al. (Mandakhalikar et al. 2018). The 1-in tubing segments were lightly dried and placed in Falcon tubes containing sterile DI water according to the methodology proposed by Polasko and Ramos (Polasko et al. 2021). Falcon tubes were vortexed at full speed (10 speed) for 1 minute, then subjected to 50 seconds of probe sonication (QSonica, Newton, CT) at 20 kHz and an amplitude of 12 volts, and finally vortexed again for another minute at 10 speed. After this sequence of vortex-sonication-vortex was finalized, the tubing was removed, and the remaining suspension was used to carry out the following analyses.

Biofilm quantification and composition measurements were carried out according to the methodology proposed by Polasko and Ramos (Polasko et al. 2021). Briefly, a multiple lines of

evidence approach was used to quantify biofilm according to the key components of these structures which are carbohydrates, proteins, adenosine triphosphate (ATP), and DNA. Total carbohydrates were measured using the Periodic Acid-Schiff Assay Kit (Sigma Aldrich) with dextran as a standard, total proteins were measured using the Modified Lowry Protein Assay Kit (Sigma Aldrich) using Bovine Serum Albumin as a standard, total nucleic acids were measured using Quantitative Polymerase Chain Reaction (qPCR) with SYBR-green based detection of amplified genes, with a known concentration of DNA from a pure culture of *P. aeruginosa* or *N. winogradskyi* as standard. ATP concentrations were measured using the BacTiter-Glo™ Microbial Cell Viability assay (Promega, Madison, WI) with lyophilized luciferase (Sigma-Aldrich) as standard. Carbohydrate, protein, and ATP were measured on a VICTOR 3 V plate reader (PerkinElmer, Waltham, MA) at 1 s intervals in 96-well plates.

4.2.6 Total nucleic acids extraction, quantitative polymerase chain reaction, and cDNA synthesis

Isolation of total nucleic acids from experimental and killed-control samples was performed according to a previously described phenol-chloroform extraction method(Gedalanga et al. 2014). Quantitative polymerase chain reaction with SYBR-Green-based detection targets was then performed using an Applied Biosystems StepOnePlus (Life Technologies, Carlsbad, CA) to enumerate and quantify cell abundance and expression level for target genes. The specific biomarker targets used to determine cell abundance and gene expression were 16S rRNA(Polasko et al. 2021), *rpoD(Mahendra et al. 2007)*, *rpoS* (Whiteley et al. 2000), *lasI* (De Klevit et al. 2001), *lasR* (Lobo da Costa Lima et al. 2018), and *nwiI* (Shen et al. 2016) (primer sequences in **Table 4.1**). Melt curve analyses were performed during each run to ensure single product amplification. cDNA synthesis was performed using cDNA Synthesis EasyScript Plus ™. Gene expression was calculated by measuring the abundance of the target genes and

normalizing to the housekeeping gene RNA polymerase σ^D subunit (*rpoD*) (Mahendra et al. 2007) and subsequently to the equivalent values at the start of the experiment (time 0) or under the most standard conditions measured (C/N=12). The gene transcripts were quantified using the $2^{-\Delta\Delta CT}$ method (Rao et al. 2013). Positive values indicated upregulation of the gene, while negative values indicated downregulation.

Table 4. 1 Oligonucleotide Sequences for qPCR

Primer (Gene)	Sequence	Annealing Temp	Reference
Uni 16S For Uni16S Rev	5'-ATGGCTGTCGTCAGCT-3' 5'-ACGGGCGGTGTGTAC-3	55 °C	(Polasko et al. 2021)
lasI For *lasI* Rev	5'-GCGTGCTCAAGTGTTCAAGG-3' 5'-GGGCTTCAGGAGTATCTTCCTGG-3'	57.9°C	(De Klevit et al. 2001)
lasR For *lasR* Rev	5′-AAGTGGAAAATTGGAGTGGAG-3′ 5′-GTAGTTGCCGACGACGATGAAG-3′	52°C	(Lobo da Costa Lima et al. 2018)
rpoS For *rpoS* Rev	5'- CCA ACC TGC TGG AAA AAC CG-3' 5'-CAA CGA CTT CCC GCT GTT TG-3'	55°C	(Whiteley et al. 2000)
rpoD For *rpoD* Rev	5'-GGGCGAAGAAGGAAATGGTC-3' 5'-CAGGTGGCGTAGGTGGAGAA-3'	57 °C	(Mahendra and Alvarez-Cohen 2006)
nwiI For *nwiI* Rev	5′-CAGGATCCATGATTCACATCGTAACGGC-3′ 5′- CCGCTCGAGCTAGGCACGAAGCCGC-3′	50°C	(Shen et al. 2016)

4.2.7 N-acyl homoserine lactone (AHL) Quantification

A cell-free bioassay for the quantification of N-acyl homoserine lactone autoinducers (AHLs) involved in bacterial quorum sensing (QS) was performed according to the method proposed by Kawaguchi et al.(Kawaguchi et al. 2008). Briefly, a cell-free lysate of the reporter

strain *Agrobacterium tumefaciens* NTL4 (pCF218) (pCF372) was prepared as detailed by Kawaguchi et al. (Kawaguchi et al. 2008), and AHLs were measured by a luminescence-based assay. For the assay, 50 µl of sample of *P. aeruginosa* that had been allowed to grow in solutions of the different C/N for 24 h (10% inoculation, 37°C, 120 rpm) were added into a black-bottom 96-well plate. Following this, 50 µl of the prepared extract of *A. tumefaciens* were diluted in filter-sterilized 20 mM KH_2PO_4 buffer (pH 7.0), mixed, and incubated at 30°C for 2 h. 100 µl of Beta-Glo (Promega, Madison, WI) were then added to each well an incubated for 1 h at 30°C. Luminescence was measured on a VICTOR 3 V plate reader (PerkinElmer, Waltham, MA). Induction of β-galactosidase activity was calculated by dividing the sample luminescence by that of the control. An induction ratio greater than 3 was considered active for subsequent evaluations, according to previous works(Prakash Singh and Greenstein 2006).

4.2.8 Analysis of Rhamnolipid Biosurfactants

Rhamnolipid biosurfactants produced by *P. aeruginosa* cultures that had been allowed to grow in the varying C/N conditions (24 h, 37°C, 120 rpm) were measured according to the method proposed by Pinzon and Ju (Pinzon 2009). Briefly, the pH of each sample was adjusted to 2.3 with 1 N HCl. The sample was then extracted with five times volume of chloroform and 4 mL of the chloroform extract were then added to a methylene blue solution (freshly prepared, pH 8.6 adjusted with 50 mM borax buffer). All samples were mixed vigorously and left to stand for 15 minutes to allow separation of the aqueous phases. The chloroform phase was then transferred to a glass vial and absorbance was measured against a chloroform blank at 638 nm using a Hach UV/Vis spectrophotometer (Model DR 1900).

4.2.9 Chemical Oxygen Demand (COD) Removal

For determination of COD removal by planktonic bacteria, *P. aeruginosa* cultures that had been allowed to grow in the varying C/N conditions (37°C, 120 rpm) were sampled over time. For determination of COD removal by biofilm bacteria, *P. aeruginosa* biofilms were grown in the different C/N ratio waters by inoculating with 10% active culture, and 1- inch segments of silicone tubing (MasterFlex L/S ® 13) were added as above to allow biofilm formation. COD removal was monitored using the Hach Kit TNT 822 according to the manufacturer's instructions and measured using a Hach UV/Vis spectrophotometer (Model DR 1900).

4.2.10 Effect on Co-Culture Biofilm Formation

P. aeruginosa and *N. winogradskyi* were grown as a co-culture and allowed to develop biofilm on a surface to understand the effect of nutrient ratio on the development of multispecies biofilms involving a relatively fast-growing heterotroph (*P. aeruginosa*) and a relatively slow-growing facultative chemolithoautotrophy (*N. winogradskyi*) due to the relevance of this kind of biofilm development in biological nutrient removal systems such as trickling filters (Petrovich et al. 2017). *P. aeruginosa* and *N. winogradskyi* biofilms were grown on 1-in tubing pieces as above by performing a 10% inoculation of each pure culture in the different C/N feedwaters. The biofilm was allowed to develop for 5 days, which was longer than the single-organism systems to account for the slower growth of *N. winogradskyi*. After 5 days, the biofilm was extracted as above, and qPCR was performed to quantify the relative abundance of each organism by comparing the relative ratios of the abundances of specific indicative target genes (*lasI*, *nwiI*, and total 16s rRNA).

4.2.11 Statistical Analysis

Statistical significance was determined as $p < 0.05$ for all datasets. Principal component analysis (PCA) was computed using the "vegan" packages in RStudio (RStudio Team, 2022. Boston,

MA) to investigate the multivariate variation among the different characteristics measured in relation to the varying C/N ratios.

4.3. Results and Discussion

4.3.1 Effect of C/N on Biofilm Composition

C/N ratio was seen to affect all measured biofilm quantification parameters, with an overall notable effect at C/N= 9 as shown in **Figure 4.1**. Carbohydrates, proteins, ATP, and total nucleic acids in the biofilm were all influenced by C/N conditions. The effect of C/N on the development of EPS in activated sludge flocs has been widely studied due to the relevance of this property on COD removal and sludge settling properties in wastewater treatment systems (Ye et al. 2011), however the effect on surface-associated biofilm formation had not yet been investigated. Studies showed that floc size is greatly influenced by C/N ratio, with equivalent differences observed in terms of the composition of the EPS (proteins, carbohydrates). The differences observed in **Figure 4.1** are likely due to changes in the microbial physiology that affected the nature and contents of the polymers present in EPS. Normalization to the total attached biomass (as total 16S rRNA) was performed to gage at differences in biofilm properties independently of the number of attached cells. **Figure 4.2** shows the carbohydrate concentration as a function of C/N when normalization of the data is performed in terms of the initial carbohydrate concentration of the C/N waters, since these were evidently different at different C/N due to variations in carbon to achieve the variations in the ratios. As expected, the concentration of carbohydrates in the biofilm increases as the microorganisms are exposed to water of increasing carbohydrate concentrations, aligning with previous observations that as

more carbon is available organisms can use more carbon to incorporate into EPS in addition to their baseline physiologies (Ye et al. 2011).

The effects on carbohydrates and proteins, which have been previously described as the main components of activated sludge EPS (Ye et al. 2011), are notable ($p<0.05$) especially at C/N= 9. The limited effect of C/N on total bacterial 16S rRNA ($p>0.1$) indicates that these differences in carbohydrates and proteins are less the result of greater overall attachment of individual cells and more likely the result of differences in the biofilm composition induced by metabolic changes at different C/N. The initial ratio of COD/biomass at the different C/N is plotted on the same graphs in **Figure 4.1** because this can serve as an indicator of the F/M ratio, which is an important parameter in wastewater treatment that can be tunable by adjusting the operating conditions, thus contextualizing the findings reported herein. C/N=9 shows a relatively low COD/biomass ratio. It is known that when the F/M ratio is low bacteria develop thick EPS layers and denser flocs, which might align with the observations presented(Kim et al. 2021). Due to the known effects of F/M ratio on floc formation (denser flocs at lower ratios, better suspension at higher ratios)(Li et al. 2011, Kim et al. 2021) it is possible that at the lower and higher values studied here, the abundance of either carbon or nitrogen mitigates the effect of the limitation of the other, while at the middle values there is a more drastic effect on physiology. EPS properties are known to affect wastewater treatment and reclamation processes (Miqueleto et al. 2010, Kim et al. 2021) and are also differentially affected by various biofouling-removal

strategies(Chen et al. 2021), thus pointing to the need to understand the effects of these parameters on EPS and attached growth characteristics.

Figure 4.1

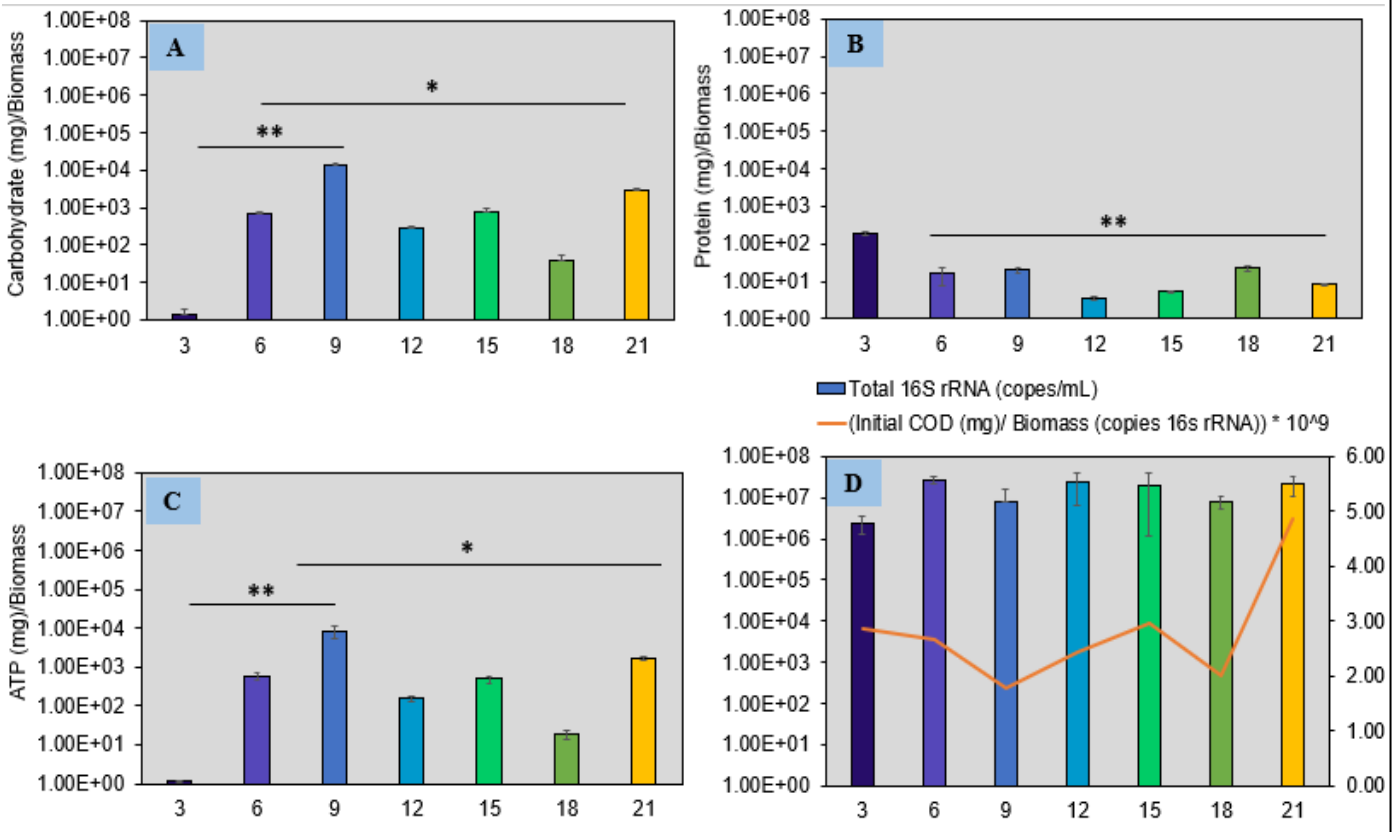

Figure 4. 1 Effect of C/N ratio on biofilm components (A) carbohydrates (mg), (B) total protein (mg), (C) ATP (mg) (D) total 16SrRNA (copies/mL). Carbohydrates, proteins, and ATP are normalized to the total biomass (16S rRNA copies/mL) in the biofilm.

Carbohydrates, proteins, and ATP are normalized to the total biomass (16S rRNA copies/mL) in the biofilm. Significant differences are observed in the composition of the biofilm in terms of carbohydrates, proteins, and ATP ($p<0.05$) as a function of C/N. The COD (mg)/ Biomass (copies 16S rRNA) in planktonic cells at the start of the experiment is plotted in orange as an surrogate for Food/Microorganism ratio at the start of the experiment since this parameter is known to influence biofilm characteristics.

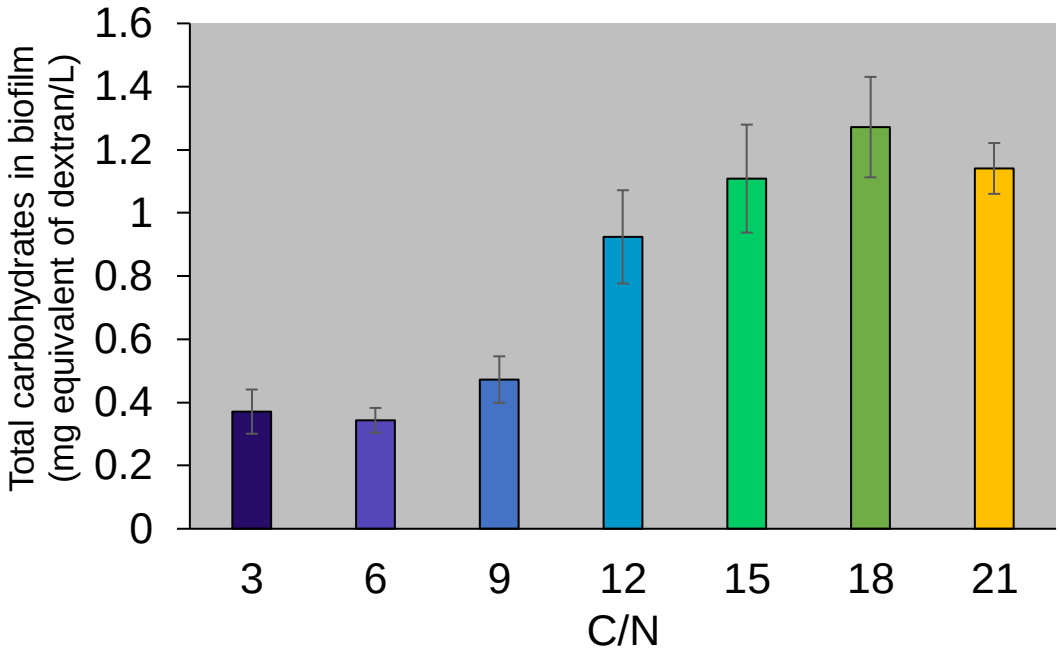

Figure 4. 2 Total carbohydrates in biofilm of P. aeruginosa normalized to carbohydrates in the feedwater

4.3.2 Effect of C/N on Quorum Sensing

Figure 4.3 shows the changes in gene abundance or expression for *Pseudomonas aeruginosa* genes involved in quorum sensing *(lasI, lasR*), and stress response (*rpoS)*. The *lasI* system has been shown to have a role in biofilm formation and maturation (Rasamiravaka et al. 2015) (Davies et al. 1998). Expression of *lasI* was seen to be affected by the C/N ratio in planktonic cells, with a significant upregulation of the gene observed at C/N=9 ($p<0.01$) but some upregulation observed in all ratios **(Figure 4.3A**). There is important downregulation of the *lasR* gene in planktonic cells at the tested conditions, with little-to-no difference at most of the tested ratios but a sharp change around C/N=12 and quick rebound back **(Figure 4.3B**). The transcription of the *lasI* gene is activated by the transcription factor LasR as well as other less

understood transcription factors, which in turn must first bind to the diffusible QS signaling molecule N-3-oxo-dodecanoyl homoserine lactone to induce transcription of several genes(De Klevit et al. 2001) (De Klevit et al. 2001, Rasamiravaka et al. 2015, Abdelraheem et al. 2020). N-acyl-L-homoserine lactones (AHLs) are the group of signaling molecules involved in QS for Gram-negative bacteria, which have been shown to be the most widespread organisms in relevant water and wastewater treatment environments such as the cake layer of fouled MBR membranes(Yeon et al. 2009) . The transcription of *lasI* is thus dependent on a positive feedback loop, the activation of which depends on the transcription of other genes such as *lasR.*

Evaluation of gene expression of *lasI* in the biofilm cells showed no significant differences between the different conditions, and most notably essentially no expression of the *lasI/lasR* genes (Cycle Threshold ≥ 34, which is the limit of quantification for the instrument used) meaning that contrary to what was observed in the planktonic cells (**Figure 4.3A**) the gene was neither upregulated nor downregulated in any of the conditions in attached cells. It has been observed that as the biofilm matures the expression of *lasI* decreases as other genes are activated to encourage biofilm differentiation at different strata, while quorum sensing genes for biofilm colonization are no longer required(De Klevit et al. 2001). Therefore, it is likely that at 24 hours the biofilm had reached a maturity point where any previous differences reflecting the trends in planktonic cells had become insignificant.

The *rpoS* gene has been shown to serve as a surrogate for stress response in *P. aeruginosa (Whiteley et al. 2000)*, as it corresponds to the bacterial σ^S factor which is considered a master stress response regulator (Whiteley et al. 2000). Differences in *rpoS* were statistically significant ($p<0.05$) between the C/N conditions. Lower expression of *rpoS* is seen in the conditions with higher concentration of carbohydrates and proteins, as well as higher expression

of *lasI* (**Figure 4.1**), indicating that in this case, C/N ratios= 9-12 resulted in the lowest stress, and these relatively low stress conditions resulted in higher biofilm production.

4.3.3 Effect of C/N on Biomolecules

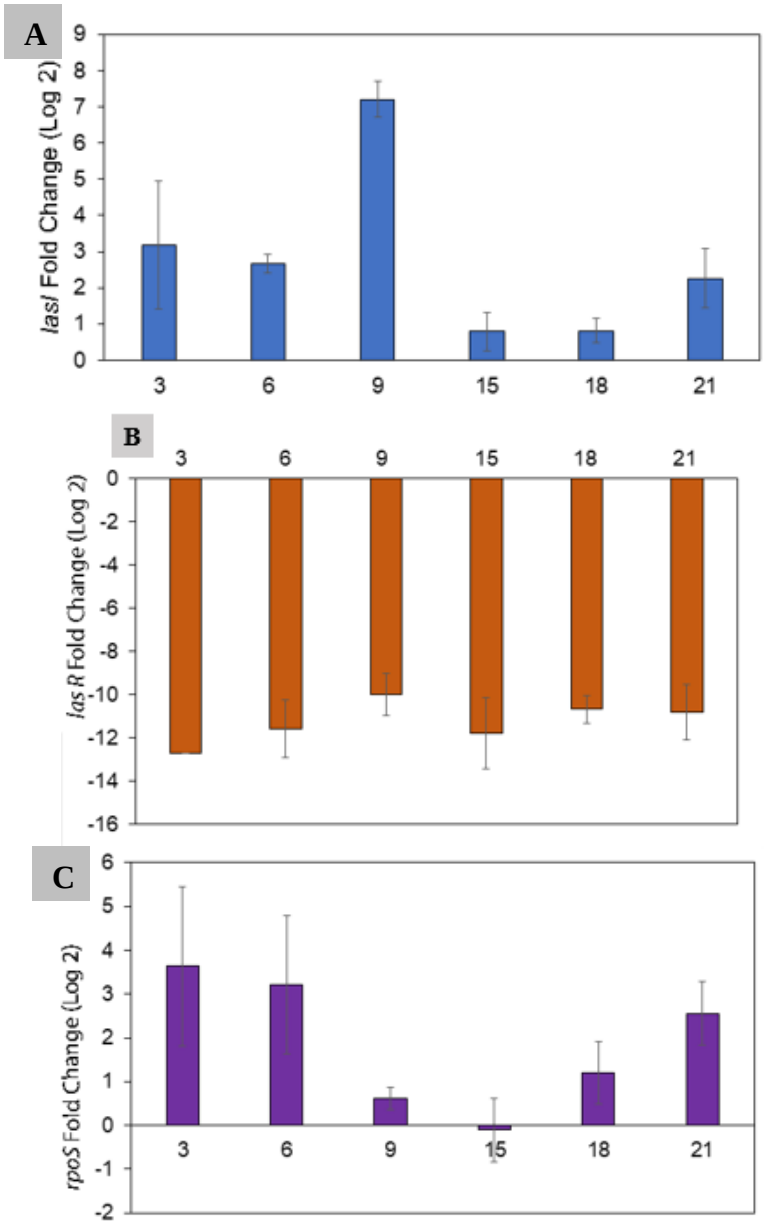

Figure 4. 3 Pseudomonas aeruginosa gene expression for (A) *lasI* (B) *lasR* and (C) *rpoS* shows differential expression for all genes at the different C/N conditions

In all cases, the range of C/N= 9-15 is important as an inflection point in the behavior of the genes where *lasI* is significantly ($p<0.01$) upregulated at C/N= 9, *lasR* has a sharp inflection around C/N=12, and *rpoS* is the least upregulated ($p<0.05$) at C/N=9-15. All values and error bars correspond to n=9.

Figure 4.4A shows the AHL induction ratio as determined by the *Agrobacterium tumefaciens* bioassay at the different C/N conditions in planktonic cells. High induction is observed once more at C/N=9, which corresponds with the higher expression of *lasI* genes in these conditions as well as the high concentrations of carbohydrates and proteins measured in the biofilms created at that ratio. This is because AHL concentration is proportional to cell density, and upon reaching a critical concentration these molecules activate transcription of genes involved in the induction of community-based behaviors such as biofilm formation (De Klevit et al. 2001, Rasamiravaka et al. 2015). Identifying that there is an effect of C/N on AHL concentration is relevant for applications purposes because AHLs have been identified as a biomolecule to target for biofilm development control (Yeon et al. 2009).

Biosurfactants in planktonic cells are shown in **Figure 4.4B** and show a similar trend as the rest of the parameters where C/N=9-12 show a higher absorbance, indicative of higher concentrations. Besides biofilm formation and virulence, AHLs in *P. aeruginosa* are also known to be responsible for the regulation of genes involved in the production of biosurfactants (Pamp and Tolker-Nielsen 2007), which in turn have roles in structural biofilm development (Pamp and Tolker-Nielsen 2007, Marchant and Banat 2012). Biosurfactants are known to influence bioremediation capabilities for example in the bioremediation of petroleum hydrocarbons (Karlapudi et al. 2018) , meaning that operational considerations of the observed effect of C/N ratio may be relevant in industrial wastewater treatment where processes would benefit from a more successful remediation of recalcitrant contaminants.

Figure 4.4

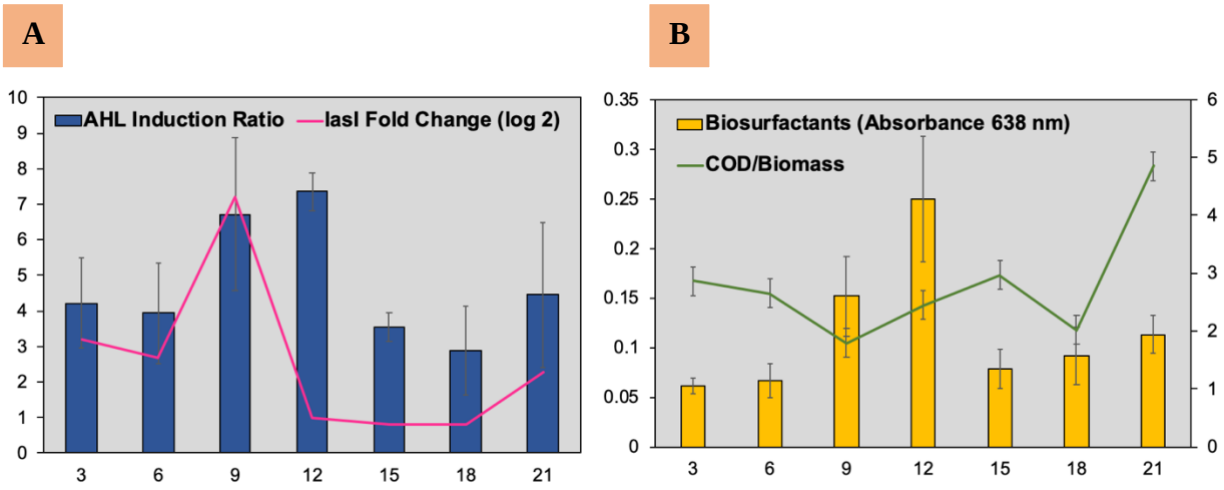

Figure 4. 4 C/N Affects Biomolecule Production (A) AHLs (B) Biosurfactants

Figure 4.4A: AHL Induction ratio as a function of C/N. Induction ratios greater than 3 were considered active. *lasI* (log 2 fold-change) is plotted in pink. High induction is observed at C/N=9, corresponding with the higher expression of *lasI* genes (pink).**Figure 4.4B:** Absorbance of biosurfactants at 638 nm as a function of C/N. Higher absorbance, corresponding with higher biosurfactant concentrations, occurs at C/N-9-12 . COD/biomass in planktonic cells at the start of the experiment is plotted in green. Values and error bars represent n=9.

4.3.4 Effect of C/N on Organic Compound Utilization

The effect of C/N on the utilization of organic compounds by both planktonic and biofilm bacteria shows improved removal by the organisms exposed to higher C/N ratios (**Figure 4.5(All)**). Additionally, removal rate by both planktonic and biofilm bacteria increased over time over the course of 6 days (**Figure 4.6**). The increased input of carbon source likely promoted the metabolic activity of the microorganisms, and even the highest concentrations used were not high enough to cause inhibition. The removal rate increase over time in both cases is likely the

result of a period of acclimation of the bacteria to the different conditions leading to an initial lag phase but subsequent recovery, which is a commonly observed phenomenon in microbial systems (Rittmann 2018) (Ly et al. 2019). Additionally, since there were no oxygen limitations due to the experimental setup there was no degradation inhibition caused by lack of available oxygen.

The COD removal rate was higher for planktonic bacteria compared to biofilm bacteria in all conditions, likely due to the higher relative ratio of biomass per mg of COD in the planktonic bacteria as compared to the biofilm (**Figure 4.6**). Despite these differences in rate the overall percentage removal after 6 days was higher in biofilm-treated systems compared to planktonic-treated systems (**Figure 4.5A**). It has been reported that biofilm bioreactors are often superior due to their ability to increase the bioavailability of the carbon and energy sources because of the unique biofilm architecture (Dasgupta et al. 2013) (Mangwani et al. 2015). It is important to acknowledge that the complexities of the microbial communities in wastewater treatment systems would change these observations due to redox cycling and its complex effects on the nitrogen and phosphorous cycles primarily, in addition to the organic matter degradation, however the results are valuable for understanding metabolic differences in *P. aeruginosa* induced by the different conditions. Results for killed-control conditions are shown in **4.7.**

Figure 4.5

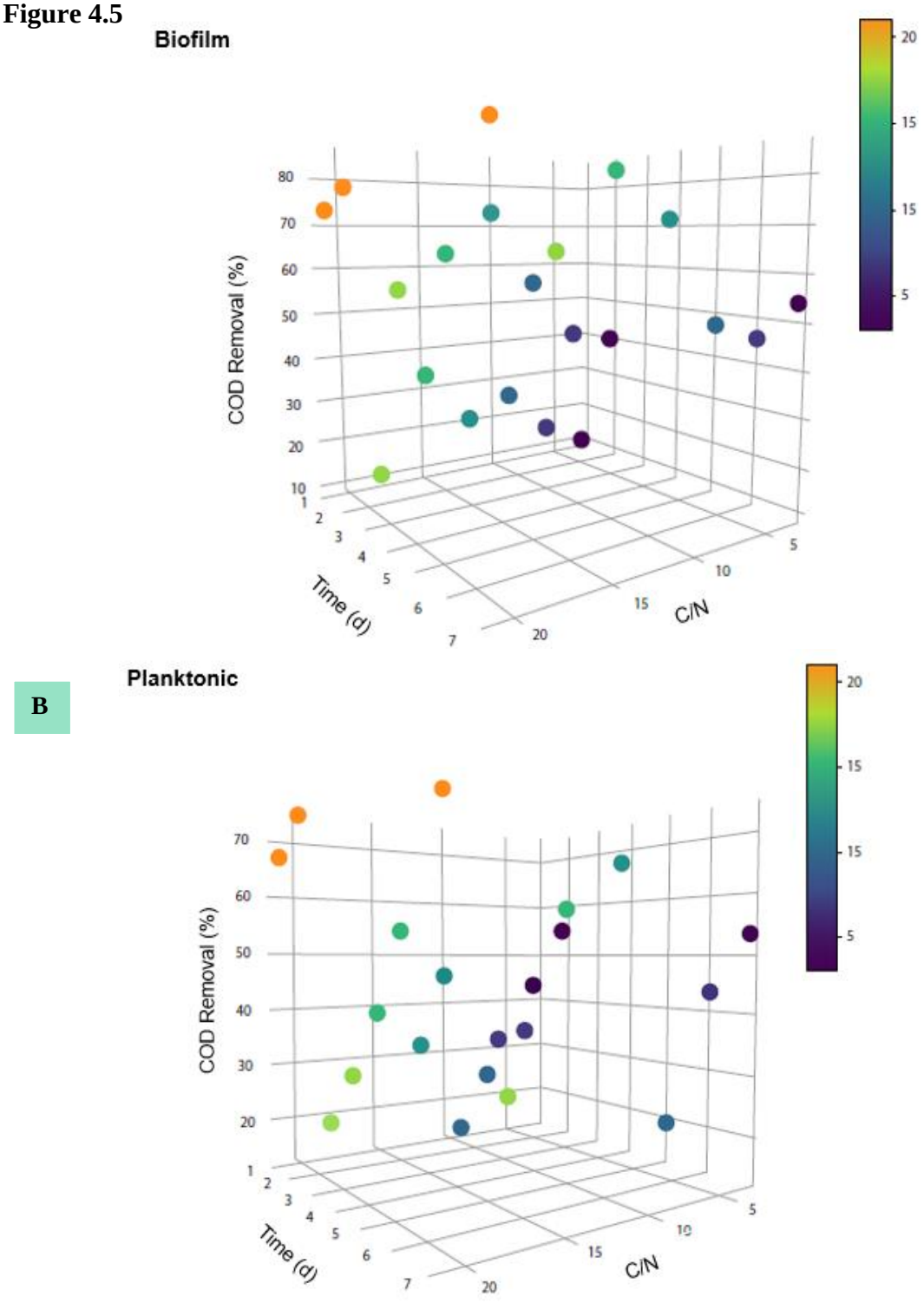

Figure 4. 5 Percentage removal of chemical oxygen demand (COD) as a function of C/N ratio and time by biofilm and planktonic bacteria

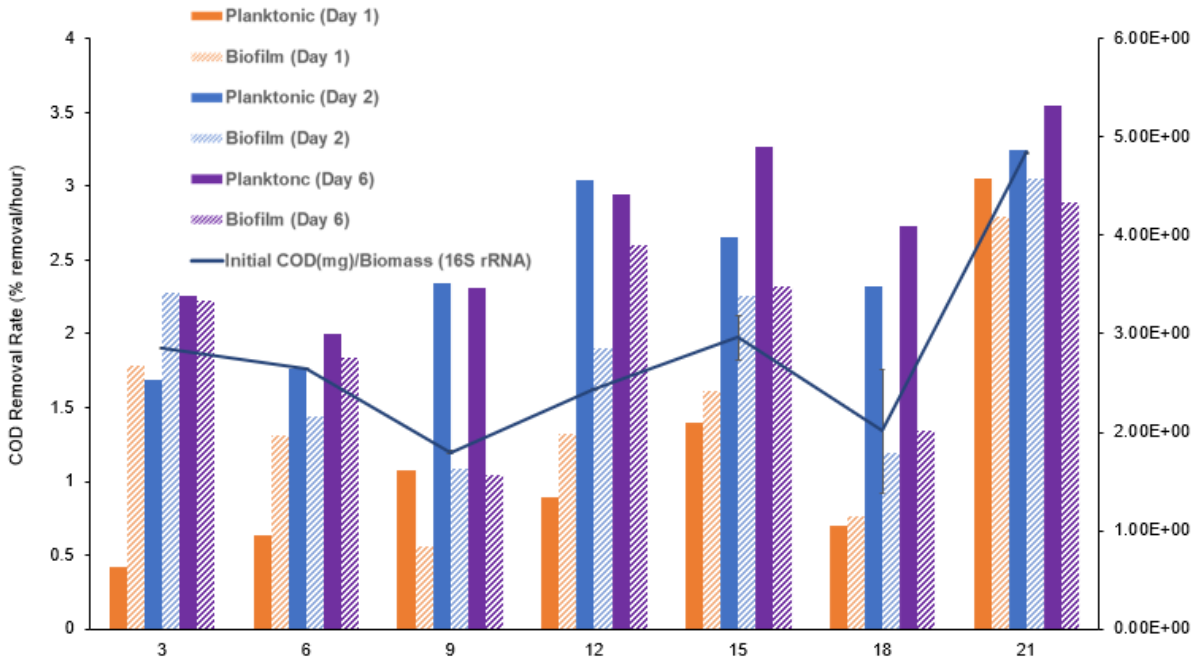

Figure 4. 6 COD removal rates for *P. aeruginosa* biofilms and planktonic cells as a function of C/N ratio

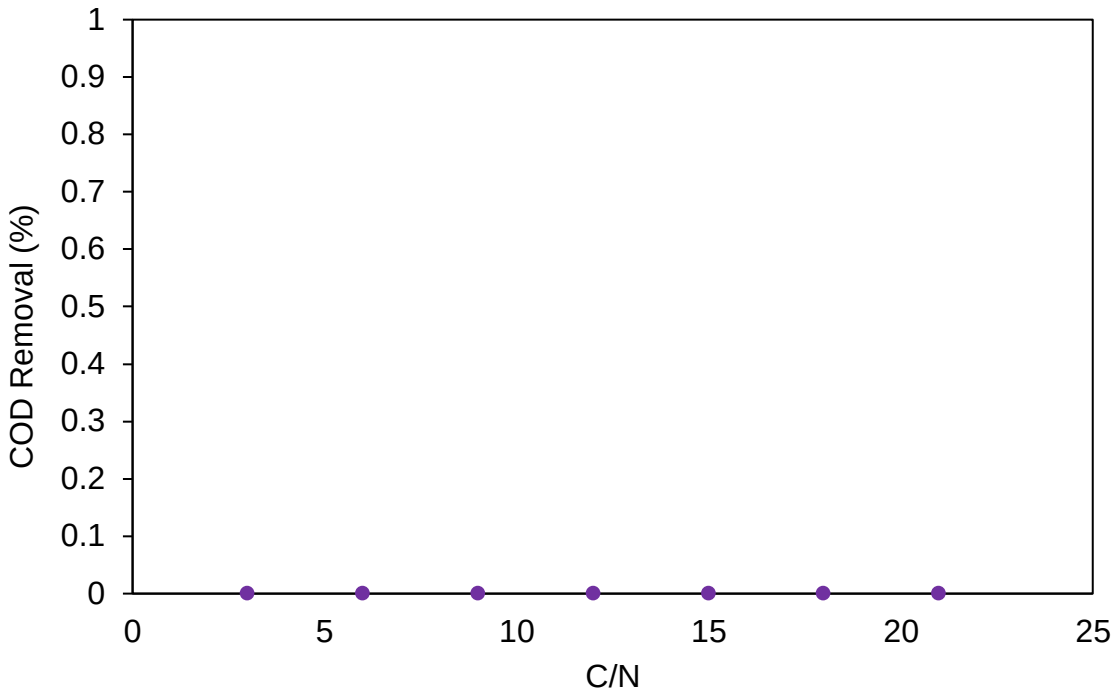

Figure 4. 7 COD Removal (%) by killed control samples as a function of C/N

4.3.5 Related Mechanistic Effects as Function of C/N

Multivariate principal component analysis (PCA) was applied to unravel the relationship among the different outcome variables measured for the different C/N conditions including expression and abundance of relevant genes (*lasI, lasR, rpoS*), concentration of biofilm biomolecules, biosurfactants, AHLs, and COD removal (**Figure 4.8**). Based on their presence in the different quadrants of the depicted plot, the C/N ratios, and especially C/N=9, had significantly differential effects. Carbohydrates and proteins have a high contribution to the overall variation in the dataset. Additionally, based on the proximity of these outcome variables

on the plot, there is a close correlation between COD removal by biofilms and the total carbohydrates in the biofilm. This is expected based on the data shown in **Figure 4.2** where the carbohydrate in the biofilm increases steadily as C/N ratio increases and in **Figure 4.5** where COD removal increases at higher C/N. AHL concentration and *lasI* expression are also closely correlated as expected since this is at the center of what is known about the P. aeruginosa QS pathway as explained above (De Klevit et al. 2001, Abdelraheem et al. 2020). Carbohydrates and proteins in biofilm normalized to total biomass are closely correlated as expected since the values are normalized to the same dataset on total 16S rRNA. The distance between carbohydrates in biofilm normalized to carbohydrates in the feedwater and total protein in the biofilm is also expected given what is known about activated sludge EPS, where the ratio of carbohydrates to proteins is greatly affected by the C/N ratio in an inverse manner (Tseng et al. 2015) meaning that the variables should have an inverse relationship. Considering a more complete picture of quorum sensing by *P. aeruginosa*, **Figure 4.9** includes consideration of the *rhlI* gene which is a quorum-sensing system that is hierarchically regulated with the *lasI/lasR* system. *rhlI* is responsible for the synthesis of a short chain AHL and shows a negative correlation with the *rpoS* master stress regulator as indicated by the relative positions of the corresponding vectors. This is noteworthy because it has been shown that *rpoS* influences the transcription of *rhlI* in an inverse manner, further emphasizing how the presented data aligns with the wider picture of what is known about the QS systems of this organism.

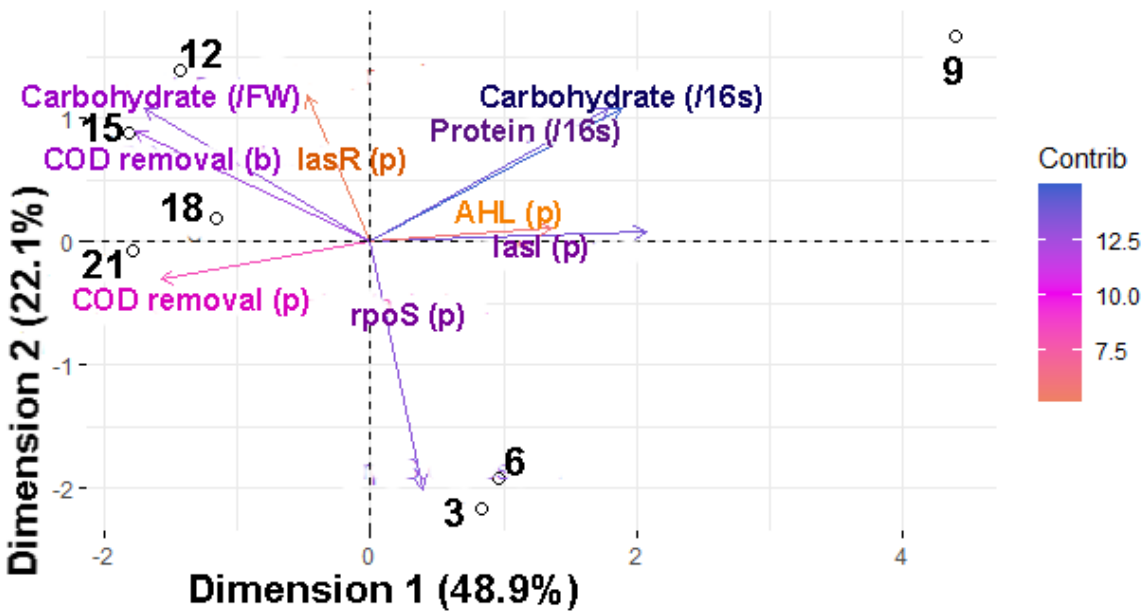

Figure 4. 8 Principal Component Analysis (PCA) for measured outputs as a function of C/N ratio**.**

Plotted outputs include ATP (biofilm), Protein (biofilm), Carbohydrate (biofilm), Total 16S rRNA (biofilm), *lasI* expression (planktonic), *lasR* expression (planktonic), *rpoS* expression (planktonic), AHL (planktonic), COD percent removal (planktonic), COD percent removal (biofilm). The contribution of the output variables to the observed variance in the dataset vector are plotted by color, with less contributing variables plotted in lighter pink colors, and greater contribution plotted in darker purples. C/N are plotted as points (3-21). A unique behavior is observed for C/N=9, indicated by its appearance in a different quadrant than the rest of the water chemistry conditions. Proximity of vectors relates to the correlation between the measured outputs, with closer proximity indicating higher positive correlations.

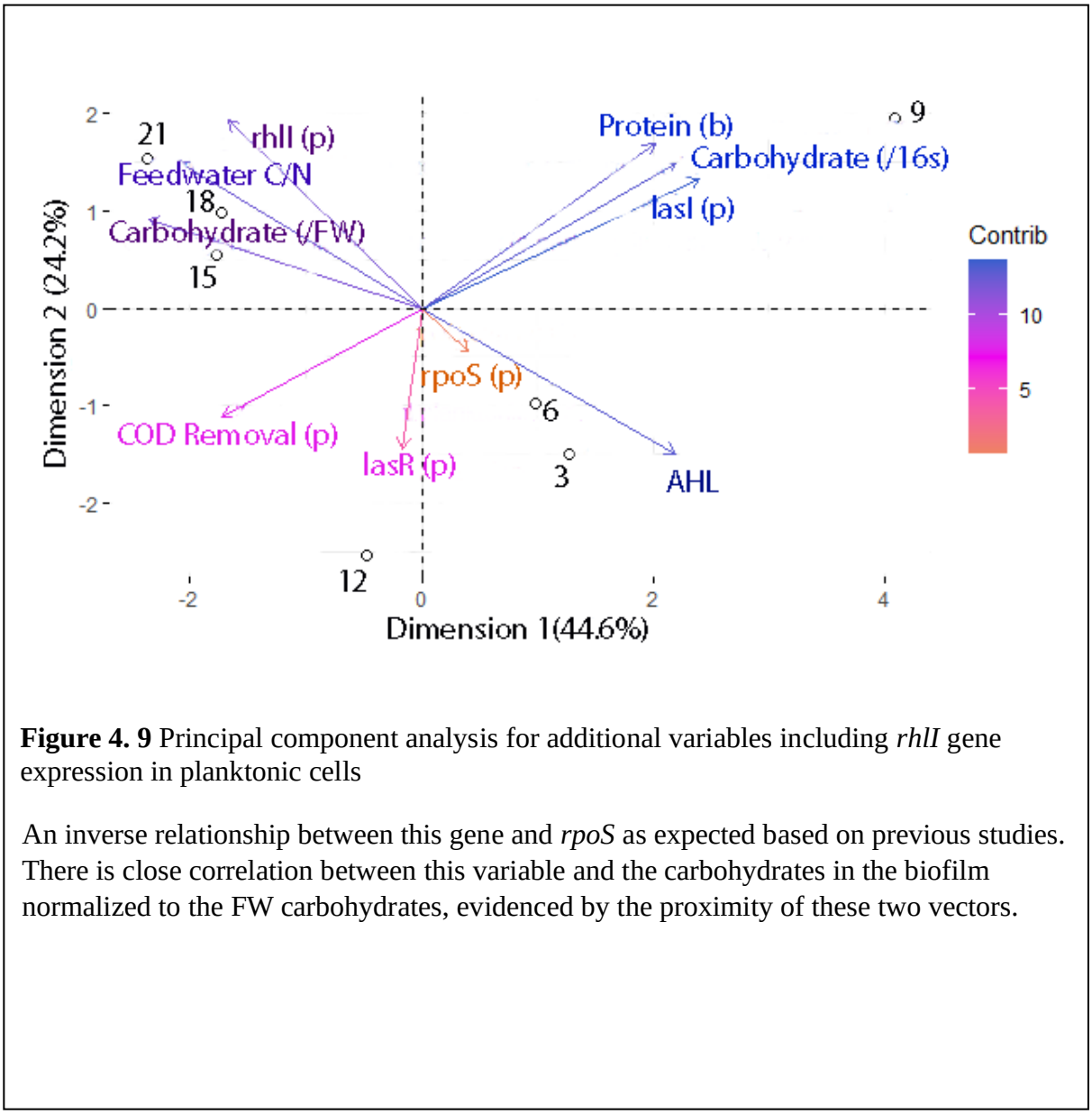

Figure 4. 9 Principal component analysis for additional variables including *rhlI* gene expression in planktonic cells

An inverse relationship between this gene and *rpoS* as expected based on previous studies. There is close correlation between this variable and the carbohydrates in the biofilm normalized to the FW carbohydrates, evidenced by the proximity of these two vectors.

4.3.6 Effect of C/N on Co-Culture Biofilm

The relative presence of *P. aeruginosa* and *N. winogradskyi* was significantly different in response to C/N ratio, notably with *N. winogradskyi*'s presence increasing beyond C/N=9 ($p<0.05$) (**Figure 4.10**). Retention of slow growing chemoorganotrophs such as *N. winogradskyi*

is important for biological nutrient removal by process systems such as trickling filters, tertiary treatment, or in advanced secondary treatment. These processes are often challenged by the slow growth and biofilm development of autotrophs, as well as the relative ease with which these organisms slough off due to their biofilm matrix characteristics (Xu et al. 2014) (Petrovich et al. 2017). Previous studies have shown that nitrogen-cycling bacteria are more successfully retained in biofilms with heterotrophs such as *P. aeruginosa* compared to single-species biofilms(Xu et al. 2014, Petrovich et al. 2017) due to favorable interactions with their EPS matrix, however the effect of the nutrient conditions in which these dual-species biofilms are grown had not been investigated.

The results depicted in **Figure 4.10** correspond with the less significant upregulation of the *lasI* gene (**Figure 4.3**) beyond C/N=9, which may help explain the high presence of *P. aeruginosa* (*lasI*) compared to *N. winogradskyi* (*nwiI)* at ratios below C/N=9. **Figure 4.1** shows a higher concentration of proteins and carbohydrates at C/N =12-21 compared to C/N= 3-6, which may partially explain the observed increase in *N. winogradskyi* in biofilms formed at C/N=12 and above. Petrovich et al. found that biofilms of the nitrogen-cycling bacterium *Nitrosomonas europea* were enhanced in the presence of *P. aeruginosa* biofilms by facilitating greater deposition and retention of cells because of increased surface roughness caused by the increased presence of biofilm (from the fast-growing biofilm forming heterotroph) (Petrovich et al. 2017). Greater cumulative concentrations of carbohydrates and proteins at C/N=12-21 compared to C/N=3-6 corresponds to greater overall biofilm, or more available surface for the deposition and retention of *N. winogradskyi* cells. The effect of nutrients on the relative presence of these two kinds of organisms is also relevant for wastewater treatment processes that perform advanced secondary treatment, where the retention and successful growth of slow-growing

nutrient-removing organisms. Lessons from this study point to a possibility for dosing with a carbon or nitrogen source as a valuable quick strategy for development of either of these organisms.

Figure 4.10

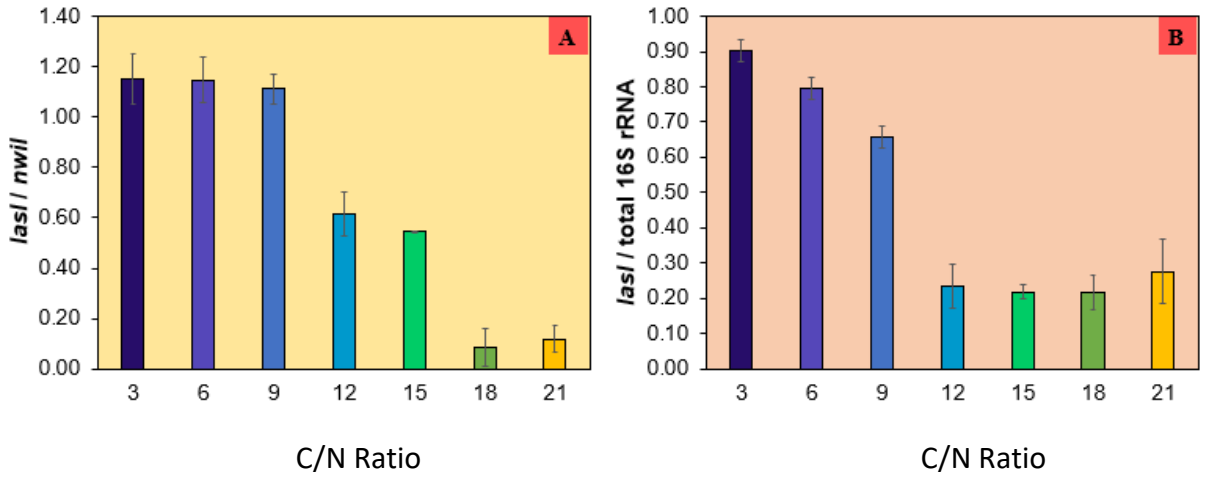

Figure 4. 10 Dual-species biofilm development of P. aeruginosa and N. winogradskyi as depicted by QS genes in each species (*lasI* for P. aeruginosa and *nwiI* for N. winogradskyi

Figure 4.10A *lasI/nwiI* as a function of C/N and **Figure 4.10B** *lasI*/total 16S rRNA. Both figures indicate that C/N ratio influences the relative dominance of each species in the biofilm, with *N. winogradskyi*'s presence increasing beyond C/N=9 ($p<0.05$). Data points and error bars represent to n=9.

4.4. Conclusion

The ratio of carbon/nitrogen content in the supernatant was shown to affect the biofilm composition, biomolecule production and quorum sensing activity of *Pseudomonas aeruginosa*. C/N=9 had a notable effect on biofilm composition as well as QS pathways, with higher concentrations of carbohydrates and proteins in the biofilm and a significant upregulation of the biofilm-forming QS gene *lasI* in planktonic cells at this ratio. C/N was also shown to influence

COD removal by both planktonic and sessile organisms, with a greater overall rate observed in planktonic cells but a greater percent removal by biofilm organisms after six days. The development of a dual-species biofilm of *P. aeruginosa* and *N. winogradskyi* was also influenced by C/N, with increase in the relative abundance of the slower-growing *N. winogradskyi* above C/N=9. It is crucial to understand effects of water chemistry on biofilm formation mechanisms because of their implications for preventing undesirable biofouling but also for engineering of novel biofilm-based wastewater treatment approaches.

4.5 Implications and Future Work

This work demonstrated the effect of C/N on not only the biofilm characteristics of *P. aeruginosa* but also the QS processes involved in these differences. Understanding a simple system such as what has been studied here is valuable as a first step for understanding more complex systems such as those present in wastewater treatment plants with complex microbial communities. Studies have sought to understand these complex microbial communities, specifically in terms of quorum sensing and AHL candidates (Panchavinin et al. 2019). Using the findings from those studies as a basis for candidates for molecular techniques, as well as the findings from the current chapter, future work may focus on trying to gage at the effects of nutrient conditions on EPS development and quorum sensing in wastewater treatment plants to get a sense of the implications this may have for membrane bioreactor-based treatment systems, or biofilm-based treatment processes such as moving biofilm bioreactors. More complex molecular tools such as microbial community analysis could also be used to understand the effects of nutrient ratios on microbial community development, or on regulation of a broader range of quorum sensing genes expressed by a wide range of organisms.

Moreover, expanding on the findings of the effect of C/N dual-biofilm development, ongoing and future work may be focused on determining the effect of different inoculation percentages in these co-cultures on the quorum sensing systems of heterotrophs such as *P. aeruginosa* and autotrophs such as *N. winogradskyi* or other nitrogen-cycling organisms. This work may also gage at the effects of influent nutrient conditions on nutrient cycling, since there is evidence that quorum sensing serves a role not only in biofilm formation but also in processes such as the nitrogen cycle (Shen et al. 2016). All these findings combined would be valuable for arriving at an improved understanding of operating parameters that may influence in the design of successful biological nutrient removal, as well as on biofilm-prevention in cases where this is undesirable such as in membrane bioreactors.

4.5.1 Effect of C/N on biofilm formation in Membrane Bioreactors

Following the basis established in this work, continuing and future work may focus on understanding whether the observed differences in the biofilm formed in a batch system translate into a flow-through membrane bioreactor considering the added complexities introduced by flow, flux, pressure, aeration, etc. which are relevant for real wastewater treatment systems. For this purpose, stir-cells or similar membrane bioreactor model systems may be used to understand the effect of C/N on the formation of biofilms in membranes. Studies have shown that changes in the composition of EPS influence the way that fouling happens on membranes (Ly et al. 2019, Chen et al. 2021). Considering this, experiments may focus on identifying whether there are any differences in the composition of the EPS in the tightly bound EPS of fouled membranes compared to the cake layers, as well as gaging at whether there are differences in the visible structure of the biofilm in these two layers, since some could be expected considering the effects of physical processes taking place such as aeration or flux. A pure culture may be used initially

as in the present work to be able to identify trends in gene expression in the different locations or conditions. Considering the interesting findings in terms of the quorum sensing genes and their abundance and expression responses to C/N, it may be valuable to identify whether there are different expression patterns in the different locations of the fouled membrane (cake layer, tightly bound EPS, outer surface, inner pores). The implications of these findings may be relevant since disruption of quorum sensing has been identified as a promising strategy for biofilm mitigation, through mechanisms such as quorum quenching (Yeon et al. 2009, Hong et al. 2022).

In terms of the development of multispecies biofilms, future works might investigate the effect of different inoculation percentages of *P. aeruginosa* to *N. winogradskyi* in a flow through system in terms of the effect this may have on successful dual-species biofilm formation as well as COD and nutrient removal for the implications that this could have in WWTP processes such as trickling filters or moving biofilm reactors. A more detailed understanding of the biofilm formation mechanisms in relation to more realistic industrially relevant setups might point to relevant considerations in terms of the biofilm configuration and stratification of species which can be valuable in the design of more successful treatment system.

4.5.2 Effect of C/N/P and Operating Parameters on Biofilm Formation by Algae in a Membrane Bioreactor

Current research on this project is related to the proposed development of a novel wastewater treatment solution focused on achieving energy-positive wastewater treatment by combining aerobic bacterial membrane bioreactors with algae-based membrane bioreactors. Previous works have shown that algae grown in biofilms accumulate a greater proportion of lipids in their cells (Shen et al. 2017), which is of interest if this biomass is to be used in the anaerobic digestion process in wastewater treatment since higher concentrations of methane in biogas are of interest in order to makes the produced gas closer to meeting standards for "pipeline readiness" (Ward et al. 2014, Zabed et al. 2019). This is important in order to realistically expect this to displace current fuel sources. Therefore, future work should also focus on optimizing algal-biofilm growth and understanding the impacts of influent nutrients as well as operating parameters such as lighting.

Growth of algal biofilms on inert surfaces, such as those used in the research in this section, can be evaluated in terms of the effect of carbon, nitrogen, and phosphorous on the development of algal biofilms that are able to remove significant nitrogen and phosphorous from the influent. The relevance of testing the impact of C/N/P in this case, as opposed to C/N only in the case of the prokaryotic biofilms in this section, is that algae growth depends on the assimilation of all three essential nutrients to an ideal proportion known as the Redfield Ratio. It is widely known that this is very relevant for mass-scale growth of planktonic-state or suspended algae based treatment systems (Kesaano and Sims 2014), however the way that this may translate into biofilm-based systems has not been widely studied. From the findings of the work presented in this section, it may also be interesting to evaluate the effect of this parameter on some nutrient-cycling genes in microalgae, in either single pure cultures by measuring gene

expression by qPCR or in more complex microalgal mixed cultures by microbial community analysis.

4.5.3. Effect of Influent Nutrients and Operating Parameters on Biofilm Formation by Algae and Bacteria in a Combined Algal-Bacterial Membrane Bioreactor (CAMBAR)

To reduce the footprint of the proposed WWTP system, it would be valuable to design a combined reactor which is able to treat the water for COD and nutrients at the same time by combining aerobic respiring bacteria membrane bioreactor and algal-based photobioreactor in the same reactor. Future research may focus on trying to achieve this by growing both organism groups in biofilm. Growing bacteria and algae in biofilm in the same system would have multiple benefits: (1) existing in biofilms as opposed to in suspended planktonic state would help both bacteria and microalgae to endure stressors induced by each other's cellular communication molecules, (2) having the biomass already purposefully growing in biofilms will lead to relatively lower biofouling of the submerged membranes used in the reactor as compared to if the system uses planktonic bacteria only, this is because there will be less suspended biomass since the bulk of the cells being used for treatment are attached, (3) growing in algae allows for greater accumulation of lipids, which would be beneficial for production of high-quality biogas.

Further research is required to understand if optimum reactor resign involves a single biofilm of both groups of organisms together or if encouraging growth in two separate biofilms is more desirable. A single biofilm system may be beneficial in terms of exchange of electron-donors and electron-acceptors between the two species, for instance with oxygen from algae photosynthesis becoming readily available to the bacteria thus facilitating and encouraging their growth and COD removal. However some studies have shown that when algae and bacteria are in close association, the bacteria may serve as a major sink for fatty acids and lipids produced by

the microalgae (Krohn-Molt et al. 2013), which would be a limitation for the purposes of energy-positive wastewater treatment since anaerobic digestion would benefit from using those lipids directly in order to produce methane-rich biogas. If a single biofilm system is decided on, future research may benefit from understanding how to grow this the most effectively (i.e., maximum COD removal, and maximum nutrient removal and accumulation of lipids by algae). Previous works have shown that multi-species biofilms in wastewater relevant systems such as trickling filters benefit from initial attachment of heterotrophs at the bottom with biofilm stratification encouraging the presence of slower growing autotrophs near the top (Petrovich et al. 2017). Future research is necessary to understand if algal-bacterial biofilm systems would benefit from a similar seeding and growth cycle.

Additionally, research into the design of a combined algal bacterial membrane bioreactor would benefit from studying the metagenomics of the interactions between the microalgal and aerobic heterotrophic bacterial species, as well as how they exist and which genes they express in the biofilms that they form. Previous studies such as that performed by Krohn-Molt et al (Krohn-Molt et al. 2013) have performed an evaluation of phylogenetic and metagenomic diversity in similar mixed biofilm systems however future research is needed to take their findings as first approximation and use them to evaluate the metagenomic and phylogenetic changes induced by different operating conditions such as C/N/P, lighting intensity and wavelength, hydraulic retention time, solids retention time, biofilm carrier media, among other variables. Additionally, it would be valuable to understand how changes in EPS induced by the different operating conditions may affect COD removal, nitrogen and phosphorous removal, algae lipid accumulation and methane yield from anaerobic digestion.

Chapter 5: Development of a Culture-Independent Protocol for Biofilm Quantification

5.1 Introduction

Chronic infections are associated with microbial growth in the form of adhered colonies surrounded by large exopolysaccharide matrices, which can lead to hazardous biofilms (Cucarella et al. 2004). Due to phenotypic changes or mutations, biofilms are less susceptible to host defenses such as macrophage phagocytosis and can become resistant or tolerant to antibiotics, resulting in reduced treatability (Bjarnsholt 2013). Medical tubing is susceptible to biofilm formation and is often the cause of severe infections, especially because it serves as a hiding place for microbes where the immune system is less effective (Trevisani et al. 2005, Stickler 2014). For example, urinary catheter tubing is associated with over 75% of urinary tract infections, which are the most common health care-associated infections (HCAIs) (CDC 2015).

The current 'gold standard' used to evaluate the presence of infections on medical tubing is culturing from urine. However, because catheter-associated urinary tract infections are often preceded by biofilm formation, it would be advantageous to make an earlier, faster, and more direct measurement of adhered microorganisms to assist in the diagnosis and prevention of clinical infections (Percival et al. 2015). Current standard methods target: 1) Viable cells via plate counting or flow cytometry, 2) Total biomass via optical density, 3) Extracellular polymeric substances (EPS) via resazurin dye, crystal violet dye, or live/dead staining, or 4) Cellular activity via ATP quantification (Stepanović et al. 2000, Stepanović et al. 2007, Doll et al. 2016, Singh et al. 2017). Reliable detection by these assays is limited by factors such as small-colony variants, non-culturable microorganisms, and false positives resulting from the inability to distinguish live from dead cells. Additionally many current methods evaluate planktonic cells rather than biofilm even though the data are not directly transferrable (López

Pérez et al. 2017), while they also lack in QA-QC methodologies. These limitations, along with the fact that the methods are rarely performed together, prevent accurate quantification or identification of problematic biofilms. Single pronged approaches, such as those listed above, are not generalizable for all strains since the composition of biofilm is not universal among all microorganisms (Stepanović et al. 2000, Stepanović et al. 2007, Doll et al. 2016, López Pérez et al. 2017, Singh et al. 2017).

Due to the widespread occurrence of biofilms and their negative effects on patient outcomes (Gomila et al. 2019), catheters were used as model surfaces to test our approach of quantifying biofilms. The goals of this study were to: (1) optimize the extraction protocol of biofilms from catheter segments; (2) formulate a protocol for biofilm quantification that provides data on both the cellular constituents and the extracellular matrix; and (3) develop a multipronged approach that is reproducible, sensitive, culture independent, and suitable for clinical settings.

5.2 Materials and Methods

5.2.1 Pure Strain Clinical Isolates and Catheter Conditions

In vitro experiments were carried out using common microbial pathogens encountered in catheter-associated urinary tract infection patients (Gad et al. 2009, Mittal et al. 2009, Behzadi et al. 2015). Clinical isolates of *Staphylococcus aureus*, methicillin resistant-*Staphylococcus aureus* (*MRSA*), *Pseudomonas aeruginosa*, and *Candida albicans* were previously isolated from urine preserved in boric acid by UCLA Department of Pathology and Laboratory Medicine. Ten catheter samples, which had resided in male patients from 2-30 days, were obtained in collaboration with Cedars-Sinai Urology Department. Once removed, the catheters were placed on ice and transported to UCLA for further analysis.

5.2.2 Design of In Vitro Experiments and Detachment of Adhered Biofilms

Catheter Preparation and Incubation

In vitro experiments were performed by cutting the catheter tubing into 1-inch segments (16 Fr diameter, 5.3 mm, Type: Foley) and placing each segment into a sterile, 20 mL glass scintillation vial. Silicone catheters and silicone catheters modified with a hydrophilic coating were selected due to their widespread clinical use (Feneley et al. 2015) and reduced biofilm formation susceptibility (Lin et al. 2019, Yan et al. 2020). After each 1-inch coated or uncoated catheter segment was placed into a scintillation vial, it was submerged in 10 mL of tryptic soy broth with an OD of 0.1 and allowed to incubate at 37°C with 120 rpm shaking. After the initial 24 hours, 9 mL of culture were removed and replenished with 9 mL of LB broth to ensure sufficient nutrient content. The samples were then allowed to incubate for an additional 24 hours. After the total 48-hour incubation period, the catheters were removed and dried by rolling the full segment's perimeter on sterile absorbent paper and gently tapping each edge of the tube to remove any excess liquid, loosely bound cells, and liquid adhered to the inner lumens. Each catheter segment was then transferred into 5 mL of sterile deionized (DI) water in 15 mL Falcon tubes.

Biofilm Extraction

The extraction of tightly bound cells and EPS components was carried out as previously described by Mandakhalikar *et al.* (Mandakhalikar et al. 2018).Validation of successful extraction of EPS and QA-QC are provided in the publication by Mandakhalikar *et al.* (Mandakhalikar et al. 2018) including visualization with electron microscopy and mixed model statistics. Falcon tubes containing sterile DI water and the dried catheter segments were vortexed continuously at full speed (10 speed) for 1 minute. The samples were then subjected to 50

seconds of probe sonication (QSonica, Newtown, CT) at 20 kHz and 12 volts amplitude. Finally, samples were vortexed for another minute (10 speed). After the vortex-sonication-vortex sequence was completed, the catheter pieces were removed from the tube and the remaining suspension was used to carry out subsequent analyses. Optimization parameters of this method included the use of 16 Fr diameters instead of 3-14 Fr diameters, 1 inch vs 1 cm segments, and probe sonication duration.

5.2.3 Analytical Methods

Total Nucleic Acids Extraction and Quantitative Polymerase Chain Reaction

Extraction of nucleic acids was carried out using a phenol-chloroform extraction method as previously described (Gedalanga et al. 2014). For cell density measurements, 500 μL liquid samples were collected after incubation, with cells harvested via centrifugation (21,000 x *g*, 10 min at 4°C) and the supernatant was discarded. Additional details are presented in the SI. The number cells were determined by amplification of the 16S rRNA or 18S rRNA taxonomic genes. Primer sequences are listed in **Table 5.1**.

Table 5. 1 Sequences of Oligonucleotide Primers Used in This Study

Primers	Sequence	Reference
Universal 16S for	5'-ATGGCTGTCGTCAGCT-3'	(Amann et al. 1995)
Universal 16S rev	5'-ACGGGCGGTGTGTAC-3'	
18S for	5'-ACTTCTTAGAGGGACTATTGGCG-3'	(Fu et al. 2017)
18S rev	5'-CCTTGTTACGACTTCTCCTTCCT-3'	

For cell density measurements, 500 μL liquid samples were collected during incubation, with cells harvested via centrifugation (21,000 x g, 10 min at 4 °C) and the supernatant was discarded. Cells were lysed by adding 250 μL of lysis buffer (50 mM sodium acetate, 10 mM EDTA [pH 5.1]), 100 μL 10% sodium dodecyl sulfate, 1.0 mL pH 8.0 buffer-equilibrated phenol, and 1 g of 100 μm-diameter zirconia−silica beads (Biospec Products, Bartlesville, OK), followed by heating at 65°C for 2 min, bead beating for 2 min with a Mini-Beadbeater (Biospec Products, Bartlesville, OK), incubating for 8 min at 65°C, and bead beating again for 2 minutes. The lysate was collected by centrifugation at 13000 g for 5 min, followed by phenol−chloroform−isoamyl alcohol purification (1 volume) and chloroform−isoamyl alcohol purification (1 volume). Precipitation of total nucleic acids was performed by the addition of 3 M sodium acetate (0.1 volume) and isopropanol (1 volume) followed by incubation at −20°C overnight. Nucleic acid pellets were collected by centrifugation at 4°C for 30 min at 20000 g. The precipitate was washed with 70% ethanol and resuspended in 100 μL DNase- and RNase-free water. The purity of DNA and RNA were determined by a Nanodrop 2000C spectrophotometer (Thermo Scientific, Wilmington, DE). All reactions were run on a StepOnePlus thermocycler (Life Technologies, Carlsbad, CA) using a total volume of 20 μL containing 1× Luminaris Color HiGreen−HiROX qPCR Master Mix (Thermo Scientific, Waltham, MA), 0.3 μM primers, and 2.5 μL of DNA (1−10 ng/μL) template. The cycling parameters to amplify the 16S rRNA gene fragment included sample holds at 95°C for 10 min, followed by 40 cycles of 95°C for 15 s and 60°C for 60 s. The cycling parameters to amplify the 18S rRNA gene fragment included sample holds at 95°C for 5 min, followed by 45 cycles of 95°C for 10 s and 56°C for 30 s and 72°C for 15 s. All reactions were accompanied by a melt curve analysis to confirm the specificity of qPCR products. Melt-curve analyses that were within

the ranges of 81.7°C (16S rRNA) and 84.3°C (18S rRNA) were considered specific to each target gene. C_T values of 45 or higher were labeled as undetermined.

Modified Lowry Assay for Protein Quantification

Tightly bound protein measurements were accomplished with the Pierce Modified Lowry Protein assay (Fisher Scientific, Pittsburgh, PA), using bovine serum albumin as the standard (1 mg/L - 1,500 mg/L). 40 µL of sample or standard was combined with 200 µL of Modified Lowry Reagent and incubated for 10 minutes. Subsequently, 20 µL of 1X Folin-Ciocalteau Reagent was amended and the plate was re-incubated for 30 minutes. Absorbance was measured at 750 nm using VICTOR 3 V plate reader (PerkinElmer, Waltham, MA) at 1 second intervals in a 96-well clear bottom, opaque-walled plate.

Adenosine Triphosphate (ATP) Assay for Cell Viability

The adenosine triphosphate (ATP) concentration was measured using the BacTiter-Glo™ Microbial Cell Viability assay (Promega, Madison, WI). A calibration curve was prepared from lyophilized luciferase (Sigma-Aldrich) ranging from 0.0057 mg/L to 5.7 mg/L. 100 µL of cell sample and 100 µL of BacTiter-Glo reagent were pipetted into a 96-well opaque flat bottom and opaque-walled plate. Samples were incubated at room temperature for 5 minutes and analyzed for luminescence using the spectrophotometer plate reader mentioned above. Background luminescence was determined by following the same procedure as experimental samples but with sterile deionized water and BacTiter-Glo reagent. In order to account for variations in clinical isolate samples, bound ATP was normalized to the amount of ATP in the corresponding supernatant as shown below in **Equation 5.1**.

$$\frac{Bound\ ATP_{catheter\ segment} - Background\ ATP_{deionized\ water}}{Supernatant\ ATP_{catheter\ segement} - Background\ ATP_{deionized\ water}}$$

Periodic-Schiff Assay for Carbohydrate Quantification

The polysaccharide fraction, as calibrated by dextran, was extracted from samples using a modified carbohydrate extraction method as described previously (Kilcoyne et al. 2011, Randrianjatovo-Gbalou et al. 2016). For this assay, 25 µL sample or standard were pipetted into a 96-well plate with 120 µL of freshly prepared solution containing 0.06% periodic acid in 7% acetic acid with gentle pipette mixing. Then a cover was secured to the multi-well plate, paraffined and incubated for 30 minutes at 37°C with 60 rpm shaking. After incubation, 100 µL of room temperature Schiff reagent was pipetted into each well, mixed via tapping the well plate, and incubated again at 37°C for 20 hours to allow for color development. Absorbance was read in a 96-well clear bottom, opaque-walled plate at 550 nm using the spectrophotometer plate reader mentioned above. Dextran, a homopolymer of glucose, had a standard solution range from 210 mg/L to 50,000 mg/L.

5.2.4 Statistical Analyses

Statistical differences between the coated and uncoated catheters were determined by a two-tailed, two-sample *t*-test that assumes equal variance. All experiments were performed in triplicate with analytical duplicates or triplicates. The results are presented as the mean $\pm$ the standard deviations (SD). The values were deemed statistically significant at p-values < 0.05.

5.3 Results and Discussion

The enumeration of DNA in extracellular polymeric matrices attached to catheters is a critical parameter that facilitates microbial growth, adhesion, and overall biofilm integrity. Extracellular DNA (eDNA) typically originates from cell lysis and/or active or passive extrusion

mechanisms (Pietramellara et al. 2009, Nagler et al. 2018). eDNA has been shown to be a universal adhesive substance and aids in biofilm formation (Okshevsky and Meyer 2015, Okshevsky et al. 2015), which is why this parameter is of great importance when trying to quantify biofilm presence and growth. qPCR is a rapid and targeted quantification method that can accurately detect various nucleic acid biomarkers (Kralik and Ricchi 2017).

qPCR and universal gene targets effectively identify and enumerate nucleic acids, yet this technique remains largely absent from methods striving to quantify adhered biofilms on medical surfaces. By targeting highly conserved and reliable sites within the genome via the 16S or 18S primers, gene abundance inside the biofilm was quantified on catheter segments. Cycle threshold (C_T), which is proportional to the -log of the nucleic acid concentration, is reported because of its use in clinical settings to diagnose patient infections (Wellinghausen et al. 2009, Stenehjem et al. 2012, Héry-Arnaud et al. 2017). Results demonstrated that within the adhered biofilm, bacterial or fungal DNA was successfully detected across all undiluted catheter segment samples, but that the ability to accurately quantify the DNA decreased when samples were diluted 10-fold and 100-fold to represent clinically-ambiguous copy numbers (**Figure 5.1A, Figure 5.2AA, Figure 5.3, Table 5.2**). *MRSA* and *P. aeruginosa* clinical isolates showed the greatest overall surface attachment to uncoated catheters both with an average C_T value of 15.1 (**Figure 5.4**). EPS contains nucleic acids in the form of RNA and eDNA (Yin et al. 2019). Studies have shown that several species including *S. aureus* and *P. aeruginosa*, can utilize eDNA to promote or modulate the development of biofilms (Allesen-Holm et al. 2006, Okshevsky and Meyer 2015). Microbial cells have also been shown to prefer hydrophobic surfaces when developing a biofilm (Doyle 2000). Our results showed that bound DNA was significantly greater on the uncoated silicone segments compared to coated hydrophilic segments across all clinical isolates tested. This could

be attributed to the fact that eDNA enhances adhesion to hydrophobic surfaces due to the amphiphilic nature of DNA (Das et al. 2011b). Correspondingly, *P. aeruginosa* showed the most significant difference between coated and uncoated catheters (p-value < 0.01).

Quantifying proteins in the biofilm of pathogenic microorganisms is an important metric because it provides indicators of components contributing to adhesion, as well as to an infection's virulence (Cramton et al. 1999, Bhowmick et al. 2008, Gad et al. 2009, Patel et al. 2012, Stauder et al. 2012, Wong et al. 2012, Fong and Yildiz 2015). Protein components of biofilm include secreted extracellular proteins, protein subunits of pili or flagella, proteins of outer membrane vesicles, and cell surface adhesins (Fong and Yildiz 2015).

The modified Lowry method was selected because it has been shown to be the optimal protein quantification method for natural biofilms when compared to others such as the Bicinchoninic acid (BCA) or Bradford Coomassie protein assays. For example, the Lowry assay has a lower detection limit than both the BCA and Coomassie assays. Additionally, the Coomassie assay has been shown to underestimate the concentration of glycoproteins, and the BCA assay shows interference with saccharides and lipids (10 mM-100 mM) (Fountoulakis et al. 1992, Richards et al. 2020). Contrary to these methods, the modified Lowry method's major interfering factors are not major components of biofilms but are instead anthropogenic compounds such as detergents, chaotropes, and reducing agents, which are unlikely to appear in biofilms(Noble and Bailey 2009). Furthermore, all reagents used in the Lowry assay are stable at room temperature, granting it a relatively low susceptibility to experimental error or reagent degradation.

Total protein content measured by the modified Lowry assay showed greater protein association to uncoated catheter segments compared to coated segments (**Figure 5.1B & Figure**

5.2B). The greatest amount of protein on unmodified catheters corresponded to *S. aureus* with values of 176 ± 19.6 mg/L, while the least amount of protein was measured for *MRSA* (98 ± 6.8 mg /L) on coated catheters. Differences between amounts of protein measured among strains may indicate differences in their ability to colonize surfaces, but also result from the fact that the composition of extracellular matrix varies between species, as well as among strains of the same species (e.g., *MRSA* vs. *S. aureus*) (Floyd et al. 2017). The greatest difference between uncoated/coated catheters occurred with *P. aeruginosa* (*p*-value < 0.01). *P. aeruginosa* proteomics have shown that the EPS of this species contains mostly outer membrane proteins, but also includes cytoplasmic, secreted, and periplasmic proteins, which are directly linked to adhesion and biofilm stability (Fong and Yildiz 2015).

ATP plays an essential role in cellular respiration, metabolism, and energy storage (Mempin et al. 2013). The ATP concentration within a biofilm matrix can provide insight into the performance of the biofilm and overall cellular virility (Heffernan et al. 2009). Viable microbial load within the biofilm was quantified via the BacTiter-Glo cell viability assay (Sánchez et al. 2013). Previous studies have shown that there is a linear relationship between intracellular ATP and the number of viable cells (Kapoor and Yadav 2010, Herten et al. 2017), which is why this assay was selected to characterize and quantify biofilm production. This luminescence-based assay enables the detection of ATP in catheter-associated biofilms.

ATP concentrations were successfully quantified across all samples and showed that greater ATP was associated with the uncoated catheters than the coated catheters (**Figure 5.1C & Figure 5.2C**). Coated catheter segments had significantly less ATP than uncoated segments across all clinical isolates. *P. aeruginosa* showed the greatest difference between the coated (6.88 $\pm$ 2.44 mg/L) and uncoated (2.87 $\pm$ 1.22 mg/L) catheters. This could be linked to the fact that the

phosphate kinase gene (PPK), which encodes for the inorganic phosphate in ATP in *P. aeruginosa*, is responsible for thick and differentiated biofilm formation (Rashid and Kornberg 2000). Contrastingly, *C. albicans* had the lowest overall concentrations of ATP on the catheters, but still showed significantly more ATP on uncoated catheter segments (1.77 $\pm$ 0.45 mg/L) than coated catheter segments (0.81 $\pm$ 0.13 mg/L). These results are consistent with Haghighi *et al.*, (Haghighi et al. 2012) in which the ATP assay was used to measure the ability of TiO_2-coated catheters to resist *C. albicans* adhesion.

Quantifying total carbohydrates is essential in evaluating the presence of biofilm because EPS is the most abundant component of the extracellular matrix of many biofilm-forming pathogens (Floyd et al. 2017). Additionally, polysaccharides are integral constituents in determining biofilm structure and integrity (Colvin et al. 2013). For instance, one of the prevalent carbohydrates in *P. aeruginosa* facilitates cell-to-cell adhesion within the biofilm by crosslinking eDNA within the extracellular matrix (Floyd et al. 2017). Carbohydrate quantification is thus considered a crucial component in the evaluation of biofilms due to their significance for biofilm stability.

Detection and analysis of complex carbohydrates is typically performed via colorimetric assays, including phenol-sulfuric acid (Masuko et al. 2005), Monsigny resorcinol (Monsigny et al. 1988), resazurin (Peeters et al. 2008) and crystal violet (O'Toole 2011). The Periodic Acid-Schiff reagent (PAS) is widely used to visualize tissues by staining glycogen and other polysaccharides (Speranza et al. 1997, Bock et al. 2007, Kilcoyne et al. 2011). In contrast to other methods, the PAS assay does not face interference from proteins or sugars, has the ability to capture neutral and charged carbohydrates, and is not specific to any kind of glycosidic linkage (Kilcoyne et al. 2011, Randrianjatovo-Gbalou et al. 2016). This is important when

concerned with quantifying carbohydrates in real biofilms because there are many carbohydrates present in EPS, even within the EPS of a single species (Floyd et al. 2017). For instance, studies on the extracellular matrix of *P. aeruginosa* have shown that different strains secrete as much as three types of matrix exopolysaccharides (Hatch and Schiller 1998, Jackson et al. 2004, Yang et al. 2007, Zhao et al. 2013, Floyd et al. 2017). Ensuring the universality of the assay is critical for its widespread clinical applicability. Kilcoyne *et al.*, (Kilcoyne et al. 2011) developed a method to use the PAS assay in a microtiter plate format for the *in vitro* quantification of dissolved carbohydrates (Kilcoyne et al. 2011), introducing the possibility to use it as a high-throughput method. However, this method had yet to be explored as a strategy for quantifying biofilms extracted from indwelling medical tubing.

Results from the PAS assay showed that the concentration of bound carbohydrates was significantly greater in uncoated catheter segments compared to coated ones (**Figure 5.1D & Figure 5.2D**. *P. aeruginosa* had the greatest amount of bound carbohydrate on coated catheters (3,411 ± 505 mg equivalent dextran/L), while *MRSA* had the lowest concentration (411 ± 126 mg equivalent dextran/L) on coated catheters. *S. aureus* showed the greatest difference between uncoated/coated segments (p-value < 0.001). The linearity of the response of a number of polysaccharides to the assay indicates (Kilcoyne et al. 2011) that it can be reliably used for different strains regardless of the dominant carbohydrate in their EPS. Thus, in contrast to other methods, the selected assay is not only useful for a large range of microorganisms but can also be confidently used with microbial communities, such as those present in clinical settings. Additionally, the PAS assay requires low sample volume and generates small amounts of non-hazardous waste, so it has the potential to be used as a high-throughput assay for biofilm quantification in clinical settings.

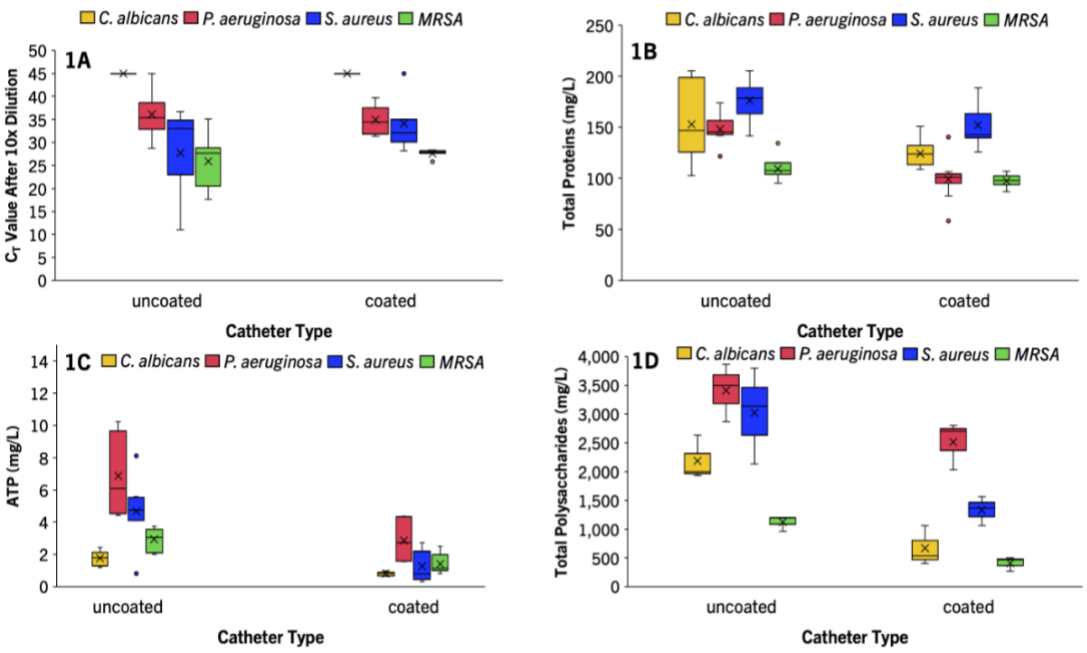

Figure 5. 1 Gene abundance, polysaccharide, ATP, and total protein concentrations from adhered biofilms on coated and uncoated catheter segments

A). Gene abundance represented by C_T values. B). Total protein concentration as estimated via a bovine serum albumin standard. C). ATP concentration. D). Carbohydrate concentration as µg equivalents of dextran. Each value represents average and quartiles of experimental triplicates, each measured thrice (n = 9).

Figure 5.2 shows that all four assays were successful at detecting and quantifying polymicrobial biofilms extracted from catheters that were previously implanted in patients. ATP and gene abundance were evaluated for the same set of patient samples because both have a presence in clinical contexts. Gene abundance has been used to diagnose *S. aureus*, *C. albicans*, and *P. aeruginosa* infections via C_T value (Wellinghausen et al. 2009, Stenehjem et al. 2012, Héry-Arnaud et al. 2017) and ATP has been used to estimate antimicrobial effects (Schwarz et

al. 2005, Sánchez et al. 2013). Based upon existing infection guidelines, patients 6 and 8 could be diagnosed relatively easily with only qPCR since the distance from the infection positive threshold was consistent for most of the replicates (**Figure 5.2A, Table 5.2**). Correspondingly, the average ATP concentrations in patient 8 was high (likely infection) (0.66 mg/L) and low in the case of patient 6 (0.20 mg/L). However, for patients 2, 4, and 7 the distribution of points for gene abundance was considered inconclusive in the diagnosis of an infection since the replicate analyses straddle the threshold (**Figure 5.2C**). In these instances, additional data would be needed. For example, the ATP measurements indicate that patient 2 had a high average amount of ATP (1.9 mg/L), while patients 4 and 7 had average ATP concentrations that were similar to a patient with a no infection qPCR result, (0.75 mg/L and 0.29 mg/L). Polysaccharides and total proteins were measured for patients 21-25 because these two methods are currently not widely used in clinical settings to diagnose infections and have no established threshold for presence or absence of infection. **Figures 5.2B** and **Figure 5.2D** show similar trends in the variation and distribution for proteins and polysaccharides in different patients, indicating the value of these multiple lines of evidence in accurate identification of infections caused by biofilms. The ability of the four methods to provide accurate quantification of proteins, nucleic acids, carbohydrates and ATP regardless of the specific chemical composition of the biofilm makes the approach valuable in the quantification of real clinical biofilms which are made up of a variety of microorganisms since the non-specificity of the reactions involved in each assay prevents detrimental biases.

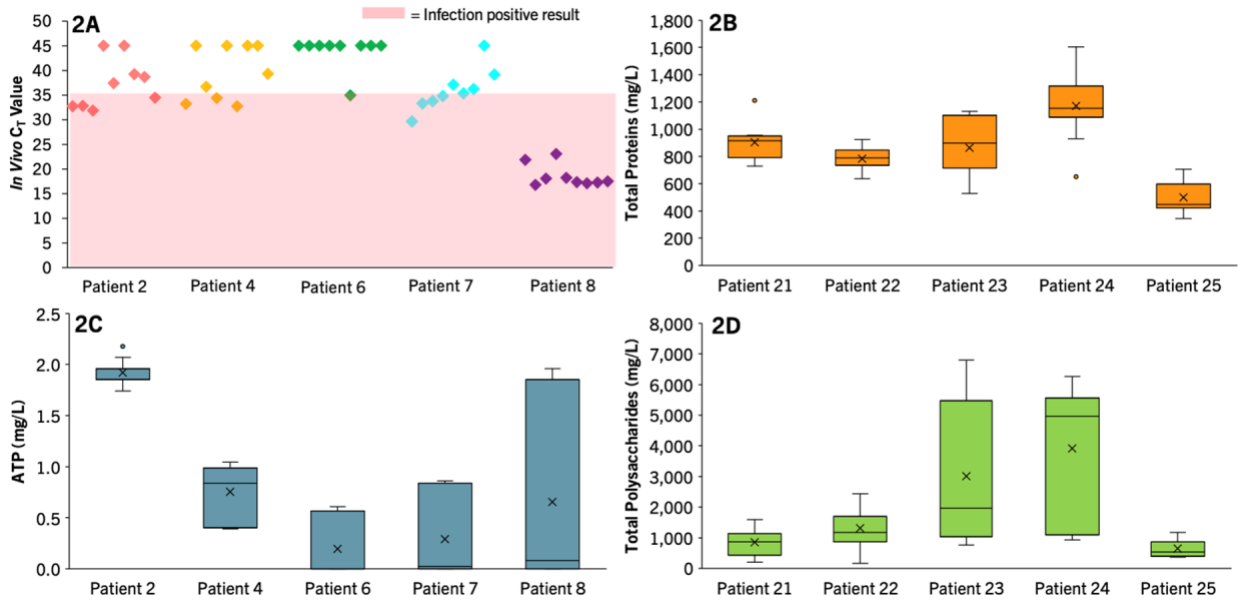

Figure 5. 2 Total biomass, proteins, ATP, and polysaccharides in biofilms extracted from indwelling catheters

In order to test whether qPCR would be sufficient for samples with lower quantities of nucleic acids, samples were diluted 10-fold and 100-fold and measured via qPCR in addition to the undiluted samples. The C_T results are shown in **Figure 5.3**

In this study, four methods based on different biological and chemical parameters were evaluated in regard to their ability to quantify bacterial biofilm bound to catheter surfaces. Each method was able to detect and quantify bacterial/fungal cells, biofilm matrices and differences in catheter performance. Additionally, cost and time for each assay were taken into account as this can be a limiting factor for many research and clinical institutions. Cost was estimated using the list prices from Thermo Fisher Scientific (Periodic Acid-Schiff, Modified Lowry Protein, qPCR) and Promega (BacTiter-Glo). Average time was based on the reaction time of the reagents for each method and did not take into account the time of labor due to the fact that this may vary depending upon experience and access to multichannel pipettors. These features are summarized in **Table 5.2**.

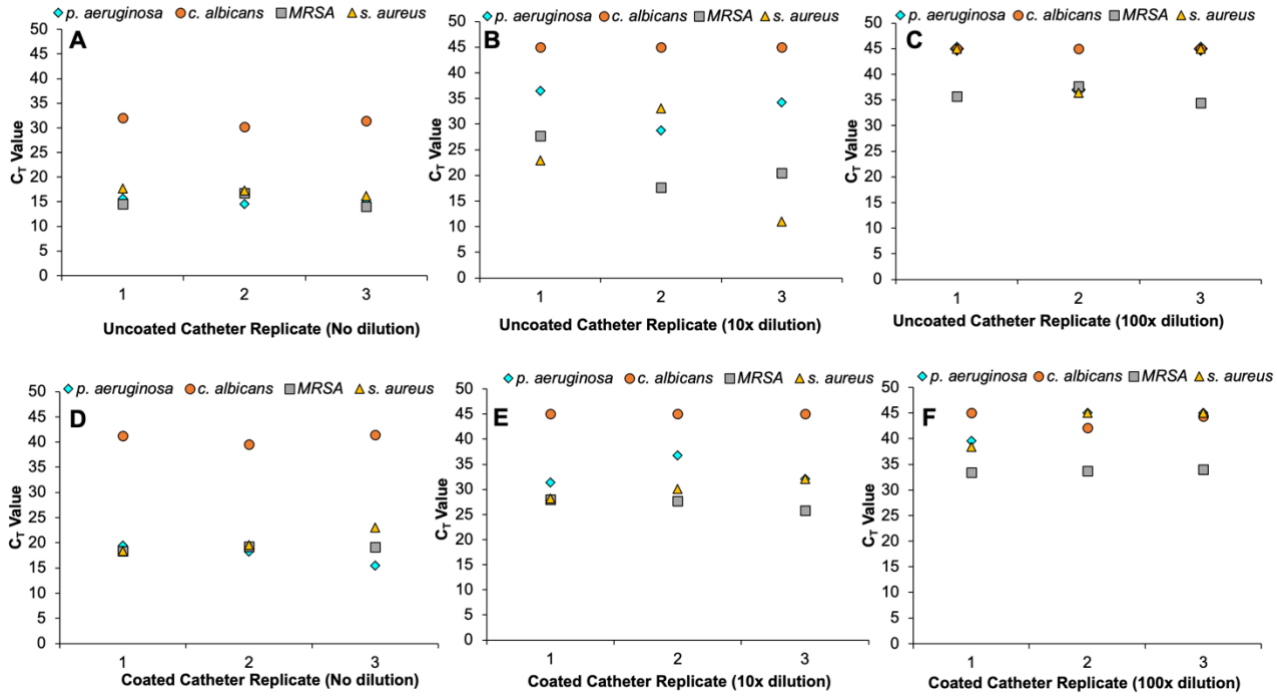

Figure 5. 3 Bacterial or fungal gene abundance adhered to catheters and represented as CT values.

A). Uncoated catheter with no sample dilution B). Uncoated catheter with 10x sample dilution C). Uncoated catheter with 100x sample dilution D). Coated catheter with no sample dilution E). Coated catheter with 10x sample dilution F). Coated catheter with 100x sample dilution

Table 5.2. Summary of Biofilm Quantification Methods

Method	Measurement of		Information on			Considered		
	Cells	Biofilm	Ability to grow	Metabolic activity	Membrane integrity	Time (hrs) *	Costs **	Assay Target
Modified Lowry Protein Assay	✓	✓	No	No	No	0.7	$0.08	Protein
BacTiter-Glo™	✓		Yes	Yes	No	0.1	$0.36	ATP
Periodic-Schiff Assay		✓	No	No	No	24	$0.33	Poly-sacchrides
qPCR	✓	✓	No	No	No	2	$0.81	Nucleic Acids
Notes:	*Time calculated based on reaction time for reagents until results are obtained. Time for instrumental analysis also included for 96-well plate. **Material cost based on list price from vendor for reagents and are calculated as cost per well.							

5.4 Conclusion

This study emphasizes a multiple lines of evidence approach for characterizing and quantifying catheter-associated biofilms *in vitro*. When implemented in a clinical setting, these assays collectively aid the accurate enumeration of infections and inform costs and patient care decisions.

Chapter 6: Design of Antimicrobial Hydrogels: Physical and Antimicrobial Properties of Chitosan/ Silver Nanoparticle Composite Hydrogels -Role of Crosslinker

6.1 Introduction

Biofouling gives rise to problems in a wide range of industrial processes such as water treatment, electricity production, and the health sector (Gule et al. 2015). The microbial community structure of biofilms provides bacteria with important advantages because it helps them better endure stressors and harsh conditions (Flemming 2020). This makes the presence of biofilms on industrially or medically relevant surfaces problematic because it makes the microorganisms more resistant, in turn making them difficult and expensive to remove (Flemming and Wingender 2010). The U.S. National Institutes of Health estimate that 65% of all microbial infections are associated with biofilm (Jamal et al. 2018). In the water treatment sector biofilms generate costly problems because they can induce corrosion, clogged piping and membranes, unexpected equipment failure and reduced efficiency (Maan et al. 2020). Effective methods to combat biofouling using materials with low toxicity are therefore needed for medical and environmental applications.

It has long been shown that it is possible to design surfaces with the ability to prevent attachment of microorganisms by modifying their surface chemistry (Chen et al. 2010, Magin et al. 2010, Thérien-Aubin et al. 2011, Maan et al. 2020). Specifically, introducing hydrophilic character is a common surface modification for antifouling purposes (Chen et al. 2010, Yeh et al. 2014). The antifouling ability of hydrophilic surfaces is the result of the formation of a layer of high hydration, which presents both a physical and an energetic barrier to attachment. (Yeh et al. 2014, Maan et al. 2020). Additionally if antimicrobial moieties are incorporated inside the antifouling coatings, microbes can be killed upon settlement (Maan et al. 2020).

Chitosan is a natural polysaccharide derived from the widespread biomolecule chitin (Zou et al. 2015), (Elieh-Ali-Komi and Hamblin 2016). It is one of most prevalent natural polymers, second only to cellulose (Zou et al. 2015, Elieh-Ali-Komi and Hamblin 2016). It is a material of great interest because of its biodegradability, biocompatibility, nontoxicity, and antimicrobial abilities(Elieh-Ali-Komi and Hamblin 2016). Its antimicrobial properties are due to its overall positive charge under acidic conditions, since the presence of its polycation can have detrimental interactions with microbial cell walls (Elieh-Ali-Komi and Hamblin 2016). Recent studies have shown it's possible to synthesize chitosan hydrogels using the non-cytotoxic crosslinker glyceraldehyde in addition to more widespread methods using crosslinkers like glutaraldehyde and genipin (Carmona et al. 2021), however this activity is limited to acidic conditions since its water solubility is limited to conditions where the cationic charge is present as a result of low pH. It is possible to modify chitosan's structure to overcome this limitation (Roberts and Taylor 1989, Lim and Hudson 2004, Zou et al. 2015, Elieh-Ali-Komi and Hamblin 2016). Many studies have reported a simple modification of chitosan enabling its conversion into the derivative N-(2-hydroxy-3-trimethylammonium)propyl] chitosan chloride (HTCC). HTCC is a quaternary ammonium compound, and therefore has a permanent positive charge at neutral pH, making it water soluble and antimicrobial under a wider range of conditions (Roberts and Taylor 1989, Lim and Hudson 2004, Zou et al. 2015, Xie et al. 2018).

Silver has long been used as an antimicrobial agent, and silver nanoparticles have been shown to have even greater bactericidal effects due to their size (Li et al. 2012, Abd El-Hady and Saeed 2020, Zakia et al. 2020). Silver nanoparticles (Ag-NPs) have been incorporated into hydrogels as well as hydrogels of chitosan, a combination which has proven beneficial for the antimicrobial as well as the mechanical properties of the materials(Xie et al. 2018). It has been

shown that Ag-NPs inside chitosan hydrogels served as secondary reinforcement agents, yielding hydrogels with ultrahigh mechanical strength (Xie et al. 2018). Chitosan hydrogels also help to stabilize the nanoparticles because the functional groups on chitosan serves as a stabilizing ligands, a beneficial mechanism that may mitigate the human toxicity of the silver metal while still allowing it to aid in infection mitigation (Zakia et al. 2020).

This study aimed to provide a comparison of the effects of three crosslinking agents (glutaraldehyde, sodium tripolyphosphate, citric acid) on the physical and antimicrobial/antifouling properties of HTCC hydrogels incorporating Ag-NPs. Crosslinkers of different know cytotoxicity were selected as each could be considered for different applications (citric acid and sodium tripolyphosphate are non-toxic, while glutaraldehyde is). The effect of crosslinking agents on physical properties such as swelling, pH sensitivity, mechanical properties, and hydrophilicity were evaluated. The effects of the crosslinking agent on physical properties following silver incorporation were compared. The antimicrobial and antifouling properties of the hydrogels containing Ag-NPs were evaluated, while the potential mechanisms for these properties were investigated. Investigating the range of physical properties, together with the observed antimicrobial and antifouling potentials of the three synthesize materials provides a basis for assessing the possibility of producing a material that can be altered depending on the desired properties for different applications.

6.2 Materials and Methods

6.2.1 Synthesis of cationic chitosan (HTCC)

N-(2-hydroxy-3-trimethylammonium)propyl] chitosan chloride (HTCC) was synthesized using the method proposed by Lim et al. (Lim and Hudson 2004). Briefly, a 5% (w/v) solution

of N-(2-hydroxy-3-trimethylammonium)propyl] chitosan chloride (HTCC) was prepared by dispersing deacetylated chitosan as purchased in deionized (DI) water which had been allowed to reach 85°C. Glycidyl trimethyl ammonium chloride (GTMAC) was added in three portions at 2-hour intervals each. The ratio of chitosan/GTMAC was set at 1:5 in order to attain the highest degree of substitution based on results from Zou et al. (Zou et al. 2015) . The reaction was allowed to proceed for 10 total hours, after which the resulting clear yellowish solution was poured into cold acetone while stirring, and left under refrigeration overnight (Zou et al. 2015). Acetone was decanted and the product was further purified by washing with methanol and acetone three times each. The degree of deacetylation of the purchased chitosan was estimated based on H-NMR spectrum of the material (**Figure 6.1**). The average yield from all syntheses performed was 85%. The degree of substitution estimated based on the product's H-NMR and C-NMR spectra (**Figure 6.1**) was calculated as 58%. H-NMR and C-NMR spectra were recorded with a Bruker 500 MHz NMR Instrument.

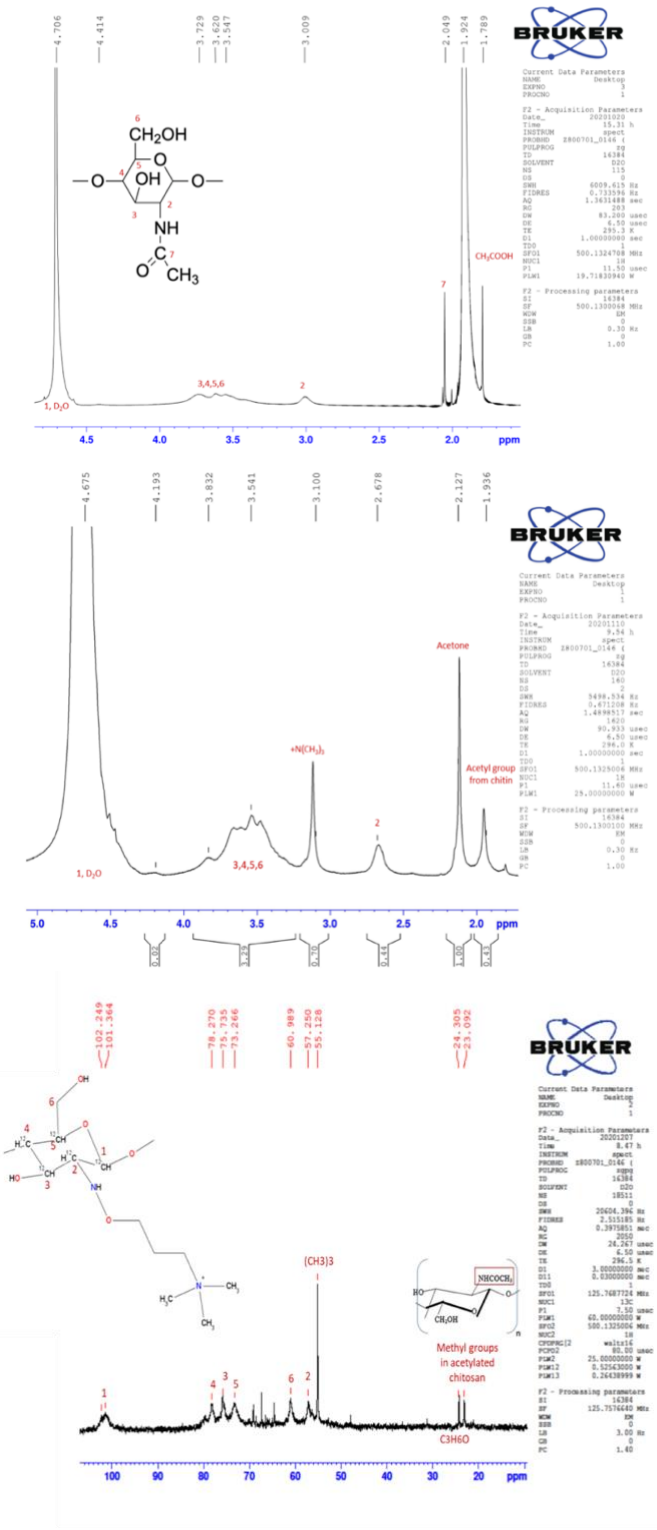

Figure 6. 1 NMR Spectra of chitosan (Sigma-Aldrich), and HTCC modified chitosan (H-NMR and C-NMR)

6.2.2 Preparation of HTCC hydrogels

Hydrogels of the synthesized HTCC were prepared by crosslinking with sodium tripolyphosphate (TPP), glutaraldehyde (GA), and citric acid (CA). Crosslinking mechanisms are different for each of the compounds used and are further explained in the following sections. All gels were prepared to the same theoretical degree of crosslinking of 90 moles of monomer of HTCC per mole of crosslinker, according to the equation presented below (**Equation 6.1**). A solution of 1% (w/v) TPP was prepared in DI water for crosslinking based on previous works (Bhumkar and Pokharkar 2006). GA aqueous solution was used as purchased. CA was used as a 30% (w/v) solution. HTCC was dissolved in DI water to a concentration of 5% w/v with mechanical stirring and the calculated amounts of crosslinker based on the equation were added. The reaction was allowed to proceed for two hours with mechanical stirring. Hydrogels prepared with TPP, and GA were placed in an oven at 37°C overnight in order to remove excess water. Hydrogels prepared with CA were placed in an oven at 90°C to dry for 4 hours based on the study by Khouri et al (Khouri et al. 2019) which stipulated that heating chitosan hydrogels crosslinked by CA may induce covalent crosslinking.

Equation 6.1 Calculation for theoretical degree of crosslinking

$$\boldsymbol{m_{HTCC} + m_{water} = m_{total}}$$

$$\boldsymbol{m_{HTCC} = X_{wt,HTCC} * m_{total}}$$

$$n_{HTCC} = \frac{m_{HTCC}}{MW_{Monomer\ HTCC}} = \frac{X_{wt,HTCC} * m_{total}}{MW_{monomer\ HTCC}}$$

$$\frac{n_{monomer\ HTCC}}{n_{crosslinker}} = A \rightarrow n_{crosslinker} = \frac{n_{monomer\ HTCC}}{A}$$

$$V_{crosslinker}\ (\mu L) = 2 * MW_{crosslinker} * \left(\frac{X_{wt,HTCC} * m_{total}}{\rho_{crosslinker,sol} * A * MW_{monomer\ HTCC}}\right) * 1000$$

Where:

m_{HTCC}= Mass of HTCC

m_{water}= Mass of water

m_{total}= Total mass

$X_{wt,HTCC}$= Weight of HTCC added

$MW_{crosslinker}$= Molecular weight of crosslinking agent

A= theoretical degree of crosslinking

ρ = crosslinking agent density

$V_{crosslinker}$= volume of crosslinking agent added

The multiplication factor (2) varies depending on the percentage concentration of each crosslinker in solution

6.2.3 Incorporation of silver nanoparticles

In-situ synthesis of silver nanoparticles (Ag-NPs) by reduction of 0.1M $AgNO_3$ with trisodium citrate was carried out following a modification of the methodology by Xie et al.(Xie et al. 2018). The previously prepared dried hydrogels were placed in DI water and allowed to

swell for 24 h. Swollen hydrogels crosslinked with sodium tripolyphosphate, glutaraldehyde, and citric acid were submerged in a 0.1 M solution of $AgNO_3$. This concentration was determined based on a trial an error sequence whereby different concentrations of $AgNO_3$ were used in this initial step. The selected concentration of silver nitrate was based on SEM imaging of the hydrogels resulting from the different trials and was selected based on the observation that this concentration was low enough to prevent a complete coating of the surface of the hydrogel with silver. The hydrogels were left in $AgNO_3$ for 24 h to allow for equilibration of silver ions inside and outside the hydrogel. After 24 h, the hydrogels were removed, washed in DI water, and blotted dry to prevent excessive silver nanoparticles to form on the surface. The hydrogels were then submerged in a solution of 1% (w/v) trisodium citrate for 24 h in order to reduce the silver ions to silver nanoparticles, after which they were removed and placed in DI water for 2 h in order to remove any excess unreacted trisodium citrate from their interior (Xie et al. 2018). Confirmation of the synthesis of Ag NPs was achieved by using Fourier-Transform Infrared Spectrometer (FT-IR) (Nicolet iS10 spectrometer, Thermo Fisher) and High-Resolution Scanning Electron Microscope (Verios 460L HRSEM, Thermo Fisher) with Energy-Dispersive X-ray Spectrometer (EDS, Oxford Instruments). A reference solution of silver nanoparticles was synthesized according to the method by Yerragopu et al (Yerragopu et al. 2020) as a positive control for UV-Visible spectrophotometry measurements. Briefly, 100 mL of 0.1M $AgNO_3$ solution was heated to 90°C for 5 minutes using a water bath. 12.5 mL of 1% (w/v) trisodium citrate were added dropwise with continuous stirring for 20 minutes.

6.2.4 Analysis of silver nanoparticles

Swollen hydrogel/Ag NP composites were sliced at a cross-section and imaged using SEM from different positions as to achieve a view not only of the surface but also of the interior NP

distribution. Size distribution and area coverage of Ag-NPs on and inside the hydrogels were determined by measuring the nanoparticles visible in the SEM images using ImageJ 1.x. (Bethesda, Maryland). Size distribution was determined using R statistical programming language (Vienna, Austria).

6.2.5 Evaluation of Swelling Ratio and Hydrophobicity

Swelling ratio for the hydrogels was determined according to the equation:

$$\text{Swelling Ratio} = \frac{\text{Wt} - \text{Wd}}{\text{Wd}} \qquad (\boldsymbol{Equation\ 6.2})$$

Where W_t is the weight of the swollen hydrogel at equilibrium (48 h) and W_d is the weight of the dry hydrogel. Hydrophobicity was determined according to the method proposed by Muñoz-Pinto et al (Munoz-Pinto et al. 2012). Hydrophobicity index was defined as the ratio of the equilibrium mass swelling (q = Wt./Wd) of the hydrogels in a solvent of low polarity (70% aq. isopropanol) to the swelling in a solvent of high polarity (deionized (DI) water) according to the equation:

$$\text{Hydrophobicity Index} = \frac{\text{q Isopropanol}}{\text{q DI Water}} \qquad (\boldsymbol{Equation\ 6.3})$$

6.2.6 pH Effect

Previous studies on chitosan hydrogels showed pH effect on the swelling properties when certain crosslinkers are used, thus we compared the effect of pH on the swelling of HTCC hydrogels crosslinked with GA, CA, and TPP. PBS at pH 5.0, 6.8, 7.2 and 9.0 was prepared by titrating with HCl or NaOH (Sigma-Aldrich). Hydrogels were submerged in each of these solutions for 48 h and the weight of the hydrogels before and after swelling was compared. Swelling ratio was calculated according to **Equation 6.2** above.

6.2.7 Evaluation of Rheology Properties

Low amplitude oscillatory shear experiments were used to evaluate the mechanical properties of the HTCC hydrogels crosslinked with CA, GA, and TPP. The samples were placed between two parallel plates (diameter 8 mm) mounted on ARES (TA Instruments) strain-controlled rheometer equipped with a Peltier system for temperature control. A water saturated enclosure was mounted on the geometry to prevent water evaporation when testing water swollen hydrogels. The temperature was kept at 298K. A strain amplitude sweep was performed at oscillation frequency of 1 rad/s to determine upper limit of the linear strain range. Subsequently, increasing followed by decreasing frequency sweep was performed in the range of 1-10 rad/s at .1%-0.3% strains well within the linear regime.

6.2.8 Evaluation of nano-physical properties by Atomic Force Microscopy

Atomic Force Microscopy (AFM) was used to evaluate differences in the micro-scale mechanical properties of hydrogels at equilibrium swelling. Nano-indentation measurements were performed on a Luigs & Neurann LTD AFM apparatus and processed and analyzed with Igor Pro

6.37 (Wavematrics) custom written software. The measurements were carried out in PBS buffer (20 mM PBS, 150 mM NaCl, pH 7.24) at room temperature. Force–distance (FD) curves were collected by approaching a silicon nitride triangular cantilever (V-shape MLCT, Bruker, with measured normal spring constant of 0.03 N/m) towards the sample until engaging full contact and indenting into it. The FD curves were collected by at a constant velocity of 400 nm/s. Upon contact, the cantilever deflects proportionally to the compliance of the sample, and elastically deforms. The deformation region in the FD curve is fitted with the Sneddon model (for an elastic contact between pyramid or conical probe with a flat surface) to extract the local Young modulus. 100 FD curves were analyzed for each sample.

6.2.9 Evaluation of silver nanoparticle leaching and silver ion release

The potential leaching of silver nanoparticles from HTCC hydrogels crosslinked with CA, GA, and TPP was evaluated to understand whether the antimicrobial and antifouling mechanisms of the hydrogels were due to leaching of Ag-NPs. A solution of 0.1 M Ag-NPs was prepared as a positive control according to previous studies (Sodha et al. 2015, Yerragopu et al. 2020). Hydrogels were completely submerged in DI and vortexed lightly for 1 minute. Hydrogels remained submerged for one week, and the wash solution were then measured using a Carry 500 UV-VIS-NIR Spectrophotometer. Release of silver ions from HTCC hydrogels crosslinked with CA, GA, and TPP was evaluated and compared to understand whether antimicrobial and antifouling mechanisms of the hydrogels were due to the release of silver ions. Hydrogels were submerged in DI and vortexed lightly for 1 minute. Hydrogels remained submerged for one week, and the wash solution were then measured using an Avio 200 ICP-OES (Perkin Elmer).

6.2.10 Evaluation of hydrogel antimicrobial properties on planktonic cells by disk diffusion method

Acinetobacter baumannii, Escherichia coli and Pseudomonas aeruginosa PAO1 were cultivated for 24 h in LB Broth (Miller) (Sigma-Aldrich). *Bacillus subtilis* was cultivated in LB medium (Difco Luria-Bertani medium, Lennox) for 24 h. All the cultures were incubated at a constant temperature of 37 °C with shaking (120 rpm). All microorganisms were supplied by Prof. Ariel Kushmaro from the Department of Biotechnology Engineering at Ben-Gurion University.

100 μL of freshly grown cultures were prepared and seeded on a Petri dish containing the appropriate nutrient agar for each species. The hydrogels were sterilized using a Stratalinker® UV Crosslinker for 20 min and were then placed on the agar plates and incubated at 37 °C for 24 h. 10 μL chitosan and 50 μL AgNP solutions were used. Antimicrobial activity was reflected in a clear zone around the hydrogel. The clear zone ratios were calculated by the following equation, d_s is the diameter of the sample and d_i is the diameter of the clear zone after 24 h:

$$Clear\ Ratio\ (\%) = \frac{di - ds}{di} * 100 \qquad (\boldsymbol{Equation\ 6.4})$$

Antibacterial activity of the hydrogels was evaluated by the agar diffusion method (Shnit-Orland and Kushmaro 2009). HTCC hydrogels crosslinked with TPP, GA, or CA containing Ag-NPs were compared, 50% ethanol was used as a positive control and a hydrogel of carrageenan crosslinked with GA was used as a negative control since this material has no antimicrobial properties. HTCC crosslinked with TPP was compared with HTCC, chitosan, and Ag-NPs on a range of Gram-positive and Gram-negative microorganisms.

6.2.11 Biofilm Visualization using SEM

After 24 h of incubation as above, the samples were prepared for SEM studies as follows: After fixation in 2.5% buffered glutaraldehyde, the samples were dehydrated via an increasing serial ethanol gradient and immersed in a hexamethyldisilazane (HMDS)/ethanol gradient solution (25%, 50%, 75%, 90%, 95% and 100%). The treated specimens were air dried for 24 h, and in preparation for SEM scanning (JSM-7400F, JEOL) they were sputter coated with a 15 nm layer of gold using an EMITECH K575x sputtering device (Emitech Ltd, UK).

The potential for the materials to prevent biofilm formation was assessed using HR-SEM. Hydrogels of TPP-crosslinked HTCC with Ag-NPs were compared with TPP-crosslinked HTCC without Ag-NPs as control. A section of each hydrogel was placed on a glass microscope slide and incubated by submerging in culture of *Bacillus subtilis* or *Acinetobacter baumannii* for 24 h. Biofilm shape factor was determined using SEM images according to the methods proposed by Kwok et al.(Kwok et al. 1998) who showed a linear relationship between shape factor and biofilm production(Kwok et al. 1998). Average shape factor was calculated as the ratio between the perimeter of an equivalent circle and the measured perimeter of a biofilm particle. Image analysis was performed using ImageJ 1.x (Bethesda, Maryland).

6.2.12 Evaluation of hydrogel antimicrobial and antifouling properties by Quantitative Polymerase Chain Reaction (qPCR) and Adenosine Triphosphate (ATP) Assay

Pseudomonas aeruginosa (clinical isolate) was used as the model organism for these studies because it is known to be a successful biofilm forming pathogen with identified genes involved in biofilm formation, virulence, and quorum sensing such as *lasI* (Malesevic et al. 2019). Understanding whether interactions with hydrogels affect the abundance and expression

of this gene may provide insight into the mechanism responsible for conferring antimicrobial traits.

A clinical isolate of *Pseudomonas aeruginosa* was previously isolated from urine preserved in boric acid by UCLA Department of Pathology and Laboratory Medicine. 1µL of the liquid urine sample was plated onto blood or MacConkey agar, incubated at 35°C for 24-48 hours and then examined for specific colonies. The culture was sub-cultured with a 1% (v/v) transfer into LB broth at 37°C with 120 rpm shaking. Once the cultures reached early stationary phase (Approximate Optical Density (OD) measured at 600 nm = 2)), it was diluted to an OD_{600} = 0.1 and transferred to experimental vials. *In vitro* experiments were performed in triplicate in sterile 20 mL glass scintillation vials. Hydrogels of HTCC crosslinked with GA, TPP, and CA were compared while a hydrogel of alginate crosslinked with $CaCl_2$ according to previously described methods (Haldar and Chakraborty 2019) was used as a negative control. Hydrogel segments 6mm*5mm*2mm were cut under sterile conditions. Sterilization of hydrogels was achieved by submerging in 70% ethanol for 25 minutes followed by 1 hour in sterile deionized water according to the method proposed by Stoppel et al(Stoppel et al. 2014).

Each hydrogel piece was placed into a scintillation vial and completely submerged under 10 mL of *Pseudomonas aeruginosa* culture with OD of 0.1. The culture was incubated at 37°C with 120 rpm shaking for 24 hours. After the incubation period, the hydrogels were removed and dried using a sterile absorbent paper in order to remove excess liquid or loosely bound cells. Each hydrogel was then transferred into 5 mL of sterile deionized (DI) water in 15 mL Falcon tubes. Tightly bound EPS was dislodged following a vortex-sonication-vortex sequence as previously described (Mandakhalikar et al. 2018, Polasko et al. 2021)

Incubation suspensions as well as extracted biofilm samples were analyzed by qPCR and ATP assay to assess the presence and activity of planktonic or attached microorganisms (Polasko et al. 2021). ATP was used as a measure for metabolically active cells (Pica et al. 2021),(Kapoor and Yadav 2010, Mempin et al. 2013, Herten et al. 2017). The adenosine triphosphate (ATP) concentration was measured using the BacTiter-Glo™ Microbial Cell Viability assay (Promega, Madison, WI). A calibration curve was prepared from lyophilized luciferase (Sigma-Aldrich) ranging from 0.0057 mg/L to 5.7 mg/L. 100 µL of cell sample and 100 µL of BacTiter-Glo reagent were pipetted into a 96-well opaque flat bottom and opaque-walled plate. Samples were incubated at room temperature for 5 minutes and analyzed for luminescence using the spectrophotometer plate reader mentioned above. Background luminescence was determined by following the same procedure as experimental samples but with sterile deionized water and BacTiter-Glo reagent.

Bacterial Universal 16S rRNA gene targets were used as a biomarker for total abundance of microorganisms in each sample, while the *lasI* gene was used as a biomarker for biofilm formation and quorum sensing(Malesevic et al. 2019). Extraction of nucleic acids was carried out using a phenol-chloroform extraction method as previously described(Gedalanga et al. 2014). Briefly, To measure cell density, 500 µL liquid samples were collected during incubation, harvesting cells by centrifugation (21,000 x g, 10 min at 4 °C) and the supernatant was discarded. Cells were lysed by adding 250 µL of lysis buffer (50 mM sodium acetate, 10 mM EDTA [pH 5.1]), 100 µL 10% sodium dodecyl sulfate, 1.0 mL pH 8.0 buffer-equilibrated phenol, and 1 g of 100 µm-diameter zirconia−silica beads (Biospec Products, Bartlesville, OK). Samples were then heated at 65°C for 2 min followed by bead beating for 2 min with a Mini-Beadbeater (Biospec Products, Bartlesville, OK), incubated for 8 min at 65°C, and bead beat

again for 2 minutes. The lysate was collected by centrifugation at 13000 x g for 5 min, followed by phenol−chloroform−isoamyl alcohol purification (1 volume) and chloroform−isoamyl alcohol purification (1 volume). Precipitation of total nucleic acids was performed by the addition of 3 M sodium acetate (0.1 volume) and isopropanol (1 volume) followed by incubation at −20°C overnight. Nucleic acid pellets were collected by centrifugation at 4°C for 30 min at 20000 x g. The precipitate was washed with 70% ethanol and resuspended in 100 μL DNase- and RNase-free water. The purity of DNA and RNA were determined by a Nanodrop 2000C spectrophotometer (Thermo Scientific, Wilmington, DE).

To separate DNA and RNA, genomic DNA was digested using RapidOUT DNA Removal Kit, and the resulting RNA was reverse transcribed into complementary DNA (cDNA) according to the manufacturer's instructions (Thermo Fisher Scientific, Waltham, MA). All reactions were run on a StepOnePlus thermocycler (Life Technologies, Carlsbad, CA) using a total volume of 20 μL containing 1× Luminaris Color HiGreen−HiROX qPCR Master Mix (Thermo Scientific, Waltham, MA), 0.3 μM primers, and 2.5 μL of DNA (1−10 ng/μL) template. The cycling parameters to amplify the 16S rRNA gene fragment included sample holds at 95°C for 10 min, followed by 40 cycles of 95°C for 15 s and 60°C for 60 s. All reactions were accompanied by a melt curve analysis to confirm the specificity of qPCR products. Melt-curve analyses that were within the ranges of 81.5°C-83.6°C (16S rRNA) were considered specific to each target gene. The cycling parameters to amplify the *lasI* gene fragment included sample holds at 95°C for 3 min followed by 40 cycles at 95°C for 15 s and 57.9°C for 1 minute. All reactions were accompanied by a melt curve analysis to confirm the specificity of qPCR products. C_T values of 45 or higher were labeled as undetermined. Primer sequences are listed below in **Table 6.1 below.**

Quantitative Polymerase Chain Reaction (qPCR) with SYBR-green-based detection reagents were utilized to quantify gene copy numbers in each isolate. The calibration curve consisted of 16S or *lasI* and a no template control and was run on each plate. Melt curve analyses were performed after each run to ensure single product amplification.

Table 6. 1 Oligonucleotide sequences for qPCR

Primers	**Sequence**	**Reference**
Universal 16S for	5'-ATGGCTGTCGTCAGCT-3'	(Gedalanga et al. 2014)
Universal 16S rev	5'-ACGGGCGGTGTGTAC-3'	
lasI for	5'-GCGTGCTCAAGTGTTCAAGG-3'	(De Klevit et al. 2001, Malesevic et al. 2019)
lasI rev	5'-GGGCTTCAGGAGTATCTTCCTGG-3'	

6.2.13 Statistical Analyses

Analyses for calculating p-values for hypothesis testing were performed in Microsoft Excel. Nanoparticle analyses were done in R statistical programming language (Vienna, Austria).

6.3 Results and Discussion

6.3.1 Crosslinking Mechanisms and Swelling:

The hydrophilicity of HTCC allowed the formation of hydrogels with all crosslinking methods, however the hydrophobicity of the resultant hydrogels was influenced by the crosslinking agent used, likely as a result of the distinct reaction mechanisms taking place, and functional groups involved in these in each case. Swelling capacity and hydrophilicity of

hydrogels with antimicrobial properties plays an important role in antibacterial activity and other parameters relevant for industrial applications such as wound healing(Xie et al. 2018).

Important differences in swelling were observed between hydrogels crosslinked by the three methods, which may be explained by the different crosslinking mechanisms involved in each case. Potential differences in the efficiencies of the three crosslinking reactions may have led divergence between the presumed theoretical degree of crosslinking and the achieved actual degrees, further affecting the swelling potentials achieved. Additionally, differences in the crosslinking mechanisms themselves may also explain the swelling differences, since they involved differences in the relative presence of polyelectrolyte ions as well as in the consumption of the hydrophilicity-imparting HTCC functional group(Arens et al. 2017).

In the case of TPP, crosslinking is based on electrostatic interactions between the positively charged functional quaternary ammonium groups in the substituted chitosan and the negatively charged hydroxyl and phosphate ions from sodium tripolyphosphate. Studies showed that crosslinking chitosan with TPP at pH 9 results in a network with relatively large mesh size attributed to a relatively low crosslinking density(Bhumkar and Pokharkar 2006). Crosslinking with CA is assumed to be the results of covalent bonds between a carbon in the carboxylate ion in CA and nitrogen in the side group of HTCC (Khouri et al. 2019), the characteristics of these hydrogels may indicate that the amount of crosslinks actually formed are relatively few in comparison, giving rise to larger mesh size than the one obtained by glutaraldehyde crosslinking. The case of crosslinking with GA is not as well understood since several mechanisms are possible for its reaction with amines(Roberts and Taylor 1989, Meonteiro Jr. and Airoldi 1999, Kildeeva et al. 2009, Ramachandran et al. 2011, Hu et al. 2020). However, based on visual observations of color change we hypothesized that the crosslinking mechanism in this case

followed the formation of a Schiff base (Meonteiro Jr. and Airoldi 1999, Hu et al. 2020). This crosslinking thus involves the formation of covalent bonds and results in tight structures, which are the tightest of the three. Swelling differences are therefore also likely the result of a difference in consumption of the quaternary ammonium groups by the different crosslinkers, resulting in differences in the resulting solubility. These differences in crosslinking mechanism gave rise to differences in swelling and hydrophobicity as depicted in **Figure 6.2**.

Hydrogels of HTCC crosslinked with TPP had the highest swelling, approximately 2350% on average and those crosslinked with GA had the lowest swelling, approximately 350% on average, while CA yielded hydrogels with intermediate properties with swelling at approximately 1100% on average. The opposite trend was observed with regards to hydrophobicity, with the most hydrophobic being those crosslinked by GA while those crosslinked with TPP or CA had lower hydrophobicity. Further, hydrogels crosslinked with TPP showed a pH-response to their swelling as depicted in **Figure 6.3**, this behavior was not observed in the other two systems**.** Higher swelling at lower pH and lower swelling at higher pH occurred due to an increase in electrostatic repulsions at lower pH as the chains of the unsubstituted chitosan monomers became positively charged in acidic environments (Xie et al.

2018). This behavior provides the possibility to use for applications such as drug delivery by adapting to different pH environments(Xie et al. 2018) (Abd El-Hady and Saeed 2020).

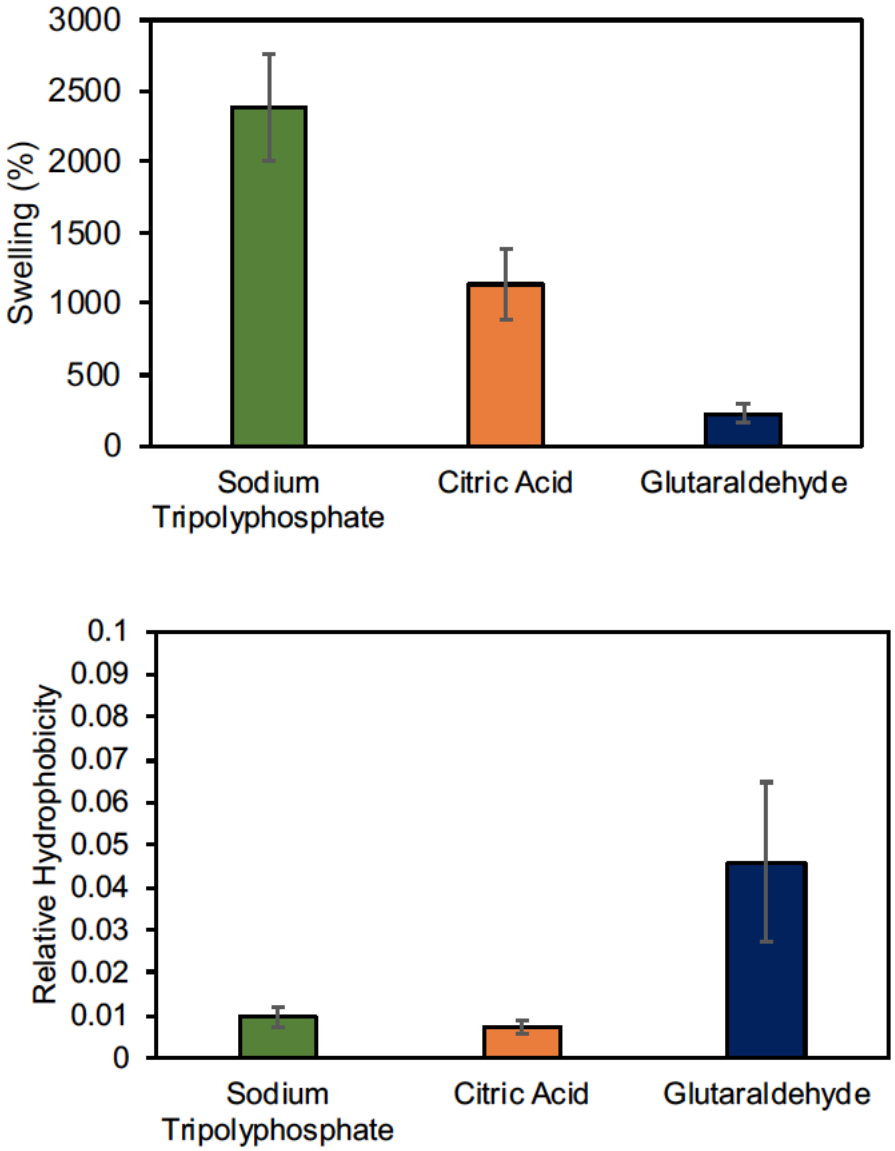

Figure 6. 2 Percentage swelling and hydrophobicity index for hydrogels crosslinked by TPP, GA, and CA

Highest swelling when crosslinked with TPP and lowest swelling when crosslinked with GA. Error bars represent standard deviations (n=3), $p<0.05$ for GA vs. TPP and GA vs CA for both percentage swelling and relative hydrophobicity, $p<0.05$ for TPP vs. CA for percentage swelling but the difference in relative hydrophobicity for TPP vs. CA is not statistically significant.

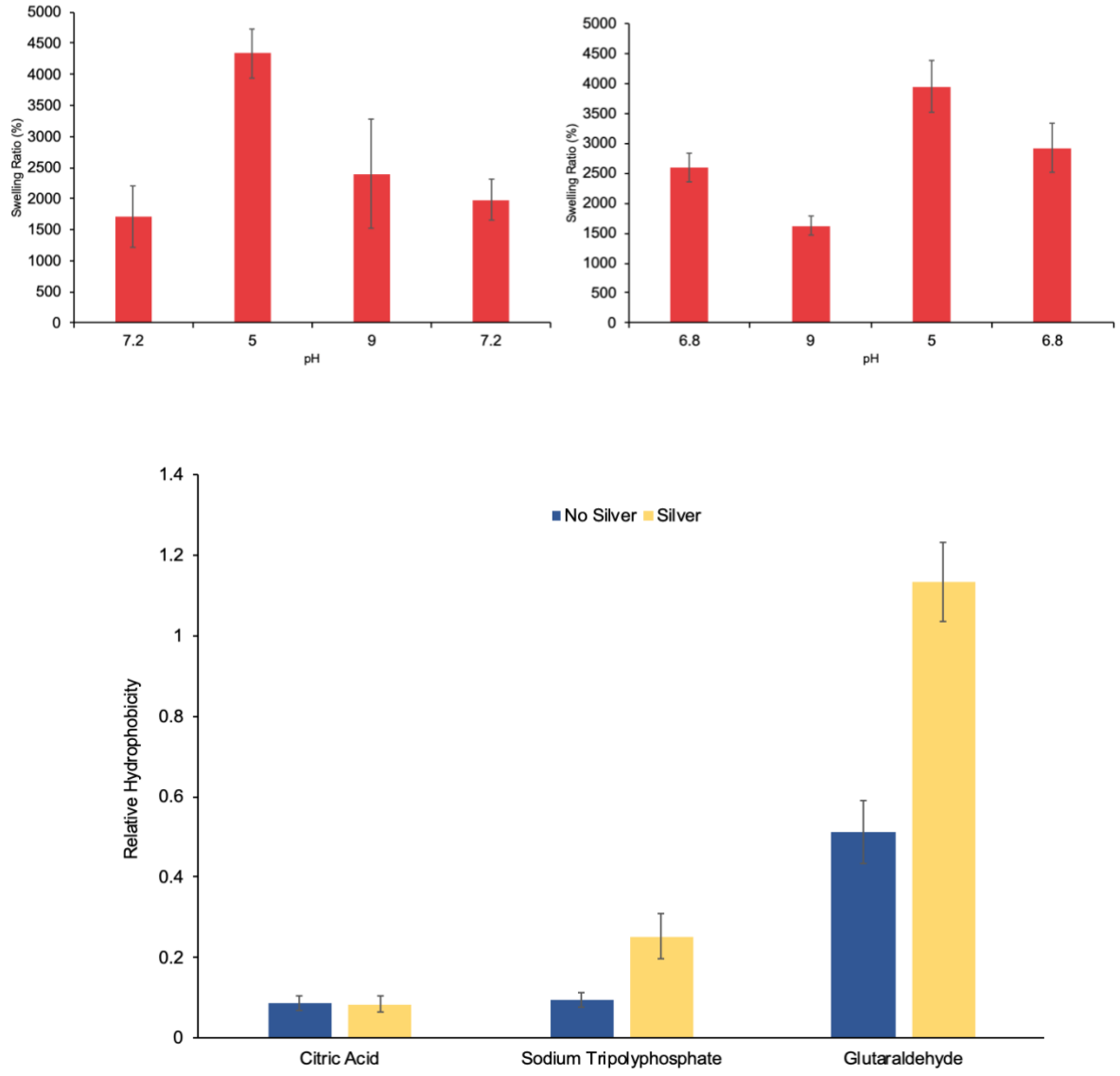

Figure 6. 3 pH Effect and Relative Hydrophobicity Upon Ag NP Incorporation

Figure 6.3 (Top) HTCC hydrogels crosslinked with sodium tripolyphosphate (TPP) showed a pH responsive behavior to their swelling, with higher swelling achieved at lower pH (pH=5) and lower swelling achieved at higher pH (pH=9). This behavior occurred irrespective of whether the initial conditions were slightly acidic or slightly basic. Error bars represent standard deviations from triplicate experiments **Figure 6 (Bottom)** HTCC hydrogels crosslinked with different crosslinkers showed greater hydrophobicity upon the incorporation of silver nanoparticles, with the greatest increase observed when the crosslinker used was glutaraldehyde. Error bars represent standard deviations from triplicate experiments.

6.3.2 Synthesis and Visualization of HTCC-Ag nanoparticle hydrogels

The concentration of silver nitrate used in this process followed a careful optimization which relied on a visualization of the system using HR-SEM and was determined as 0.1 M (**Figure 6.4**). Excess concentrations were determined as those which caused a complete coating of the hydrogel surface with silver, while the desired concentrations were those which allowed the visualization of individual nanoparticles. This concentration also allowed a distribution of nanoparticles in the interior of the hydrogels (**Figure 6.5**). The optimum concentration used for synthesis was determined to be 0.1M.

Incorporation of Ag-NPs resulted in the increase of hydrophobicity for all three hydrogel types as depicted in **Figure 6.3 (Bottom).** This is expected since incorporating Ag-NPs increases the overall degree of crosslinking in the system, which impacts the ability of water to be incorporated. Additionally, it introduces metallic character into the system, increasing hydrophobicity. The greatest difference in hydrophobicity after addition of Ag-NPs was observed for hydrogels crosslinked with GA, while the smallest difference was observed for CA. An explanation for this can be found in SEM images (**Figure 6.5, Figure 6.6**), showing that crosslinking with CA resulted in well-dispersed nanoparticles on the inside of the hydrogel, while the GA-crosslinked system had most of the particles form agglomerates on the surface, thus having a significant impact on the solvent's access into the gel's interior.

Figure 6.6A depicts a SEM-EDX spectra of the nanoparticles, confirming that the overarching component of the nanoparticles was silver. Visualization of the silver nanoparticles is shown in **Figures 6.6 (All)** shows that different crosslinking agents used in the preparation of the hydrogels resulted in differences in the distribution of the nanoparticles inside and outside the hydrogel surfaces, and **Figure 6.6C** depicts differences in the area coverage by nanoparticles

depending on crosslinker. This may be due to several factors, primarily the relative differences in the swelling potentials between the hydrogels formed by the different methods(Casolaro et al. 2018, Mekkawy et al. 2018, Xie et al. 2018, Abd El-Hady and Saeed 2020, Alcântara et al. 2020). In the case of hydrogels crosslinked with GA, the majority of nanoparticles were found on the outside of the surface, while in the case of crosslinking with CA the majority were found on the inside. Crosslinking with TPP resulted in a distribution about equal inside and outside. This can be explained by the rigidity of the networks formed in each case, since the hydrogels crosslinked with GA were likely the tightest (Ou and Bo 2017, Mekkawy et al. 2018, Xie et al. 2018), seen also in the stiffness of the materials formed. As explained above, the crosslinking mechanism of GA involves covalent bond formation, while CA works by formation of weak covalent bonds and TPP crosslinks via ionic electrostatic interactions. Additionally, there is a correspondence between the hydrophobicity of the hydrogels (**Figure 6.2**) and the presence of the nanoparticles inside and outside the surface. This could explain the distribution of nanoparticles because since the formation of the nanoparticles was *in situ*, it depended on the diffusion of silver ions dissolved in water into the hydrogel. If the material is less hydrophilic, as in the case of hydrogels crosslinked by GA, less ions may enter the network and will therefore become concentrated on the surface. The opposite is true for the more hydrophilic CA and TPP-crosslinked hydrogels.

Figure 6.6 (All), show that there are differences in the nanoparticle shape, size, and size distribution depending on the crosslinking agent used to make the hydrogels, while **Figure 6.7** shows the nanoparticle coverage area fraction in relation to crosslinking agent used. This is likely also related to the rigidity of the networks formed in each case. Hydrogels crosslinked with GA formed more spherical particles, while CA formed cubic-shaped particles and TPP formed

cubic and starred-shaped nanoparticles. Additionally, particles crosslinked with TPP show a size distribution towards predominantly lower sizes (**Figure 6.6C**). This may also be related to the crosslinking density since networks that are more tightly crosslinked will form smaller particles(Ou and Bo 2017, Xie et al. 2018). Similarly when the majority of the particles form on the surface rather than inside the network, as when crosslinked with glutaraldehyde, it is more likely that the nanoparticles will form in less of a controlled manner or form aggregates since the hydrogel pore sizes are not able to serve as scaffolds as they are in the interior of the structure. (Xie et al. 2018).

Figure 6.4

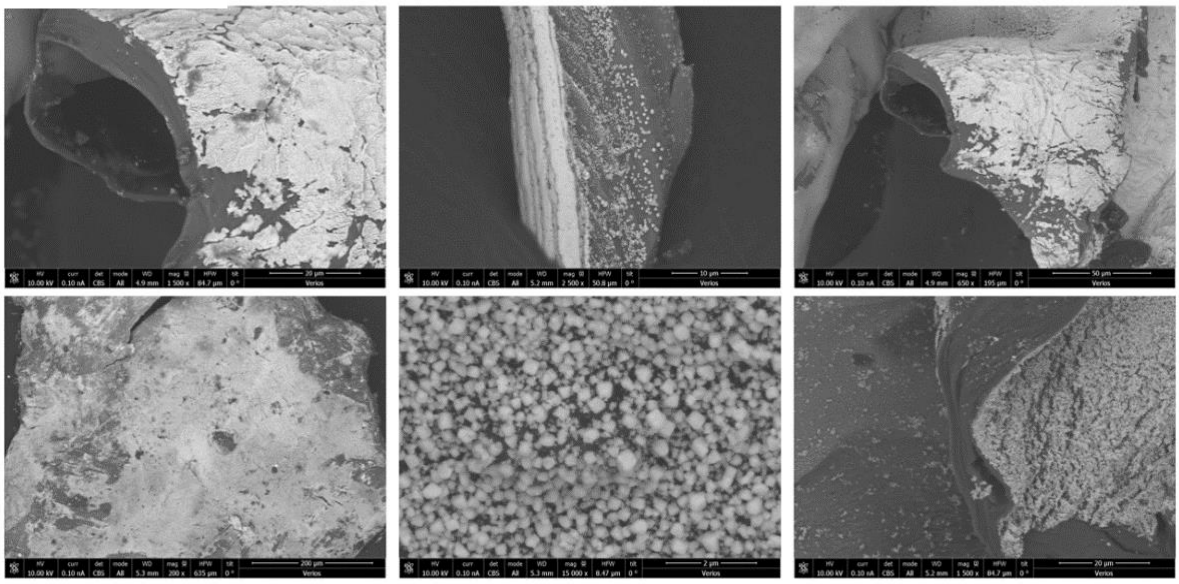

Figure 6. 4 Trial-And-Error Optimization of Ag NP Concentration

Optimization of $AgNO_3$ solution by trial-and-error sequence showed excess concentration in initial phases as hydrogel surface became coated by silver an no nanoparticles were incorporated inside the surface

Figure 6.5

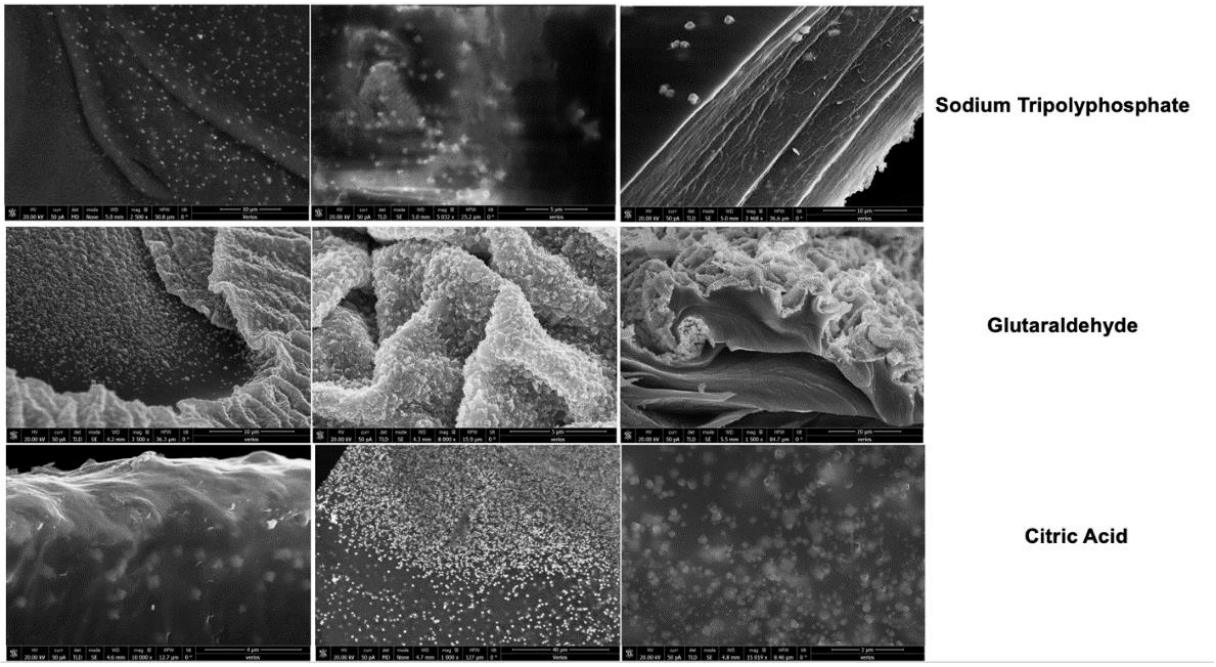

Figure 6. 5 Optimization of Ag NP in the three hydrogel systems

Optimization of $AgNO_3$ solution by trial-and-error sequence showed appropriate concentration of silver nanoparticles for hydrogels crosslinked by sodium tripolyphosphate (top), glutaraldehyde (middle), and citric acid (bottom) as seen by the presence of individual silver nanoparticles inside and outside the hydrogel surface with differences in distribution depending on crosslinking agent.

Figure 6.6A

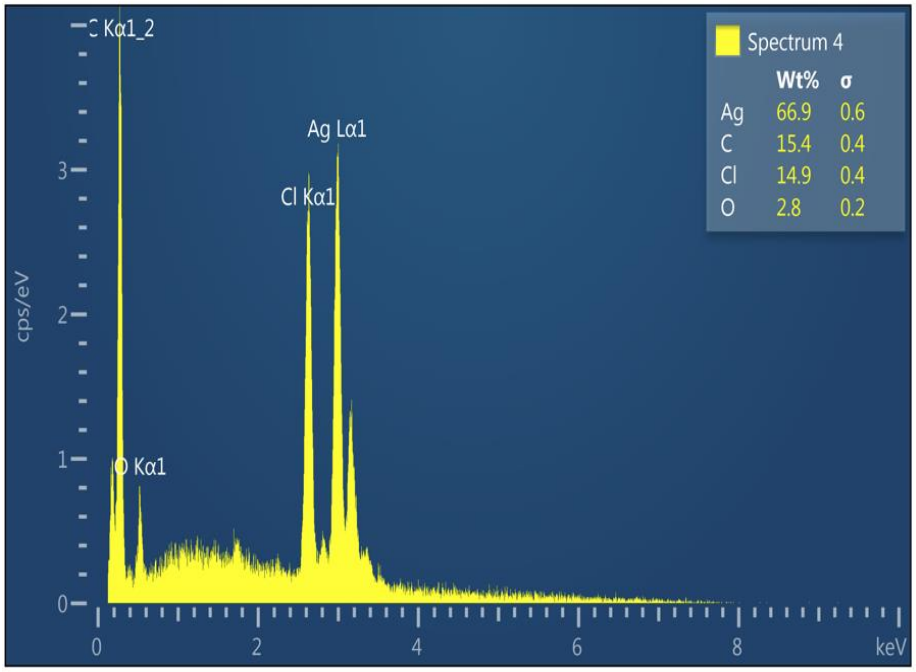

Figure 6.6B

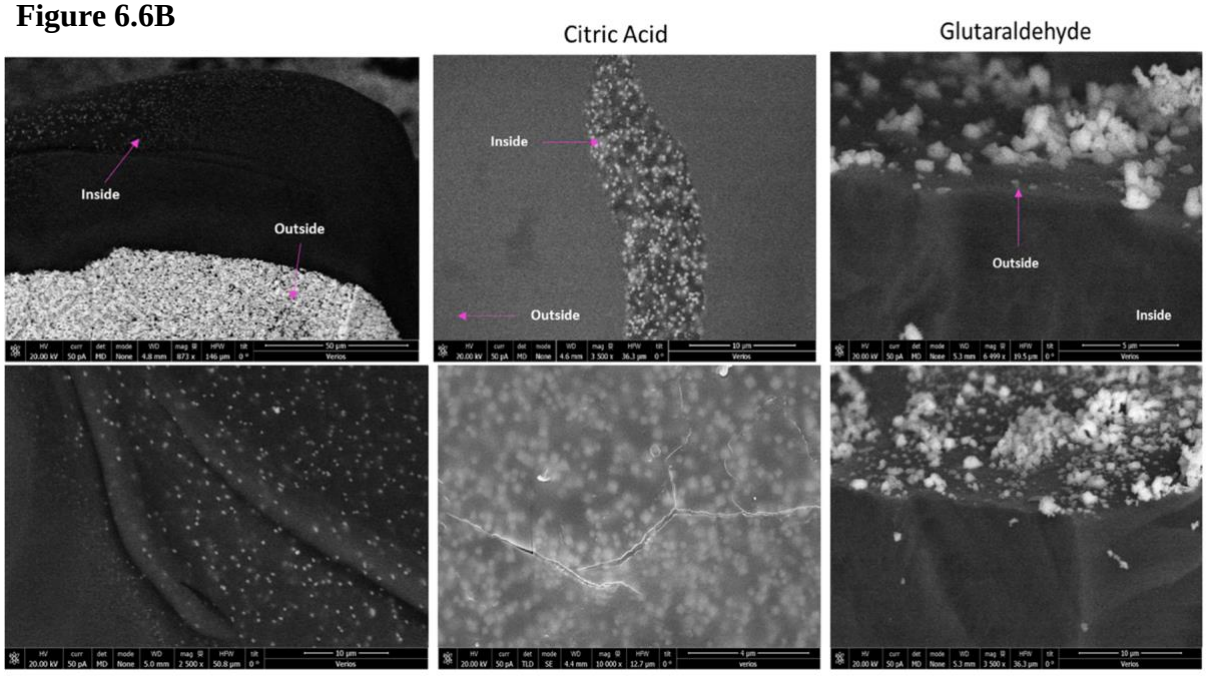

Figure 6.6C

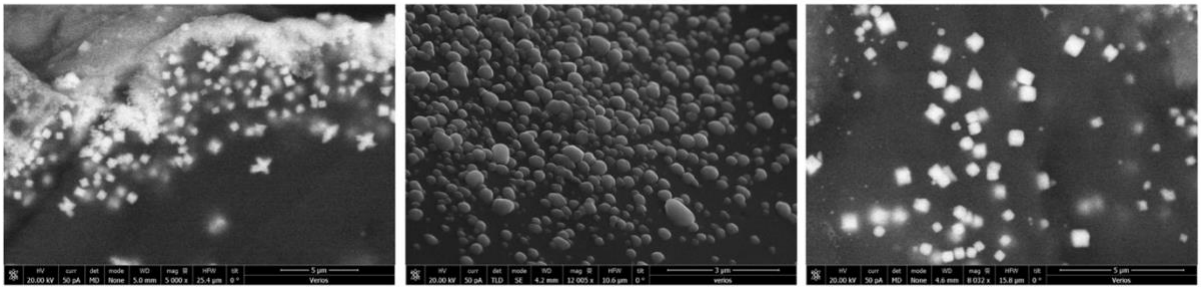

Figure 6.6D

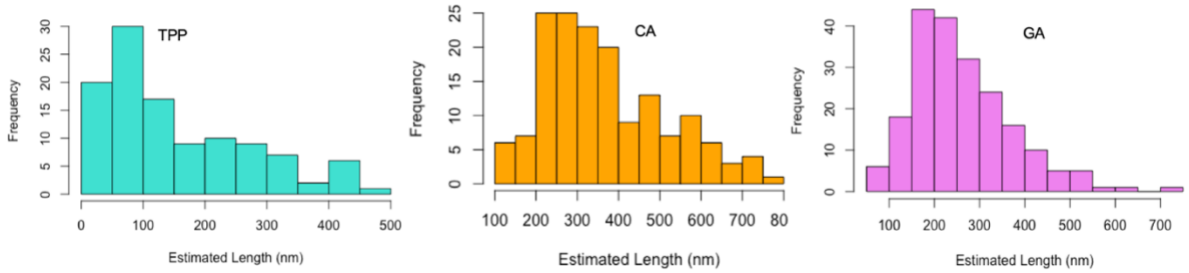

Figure 6. 6 EDX and SEM Images of Ag NP in Three Hydrogel Systems

Figure 6.7

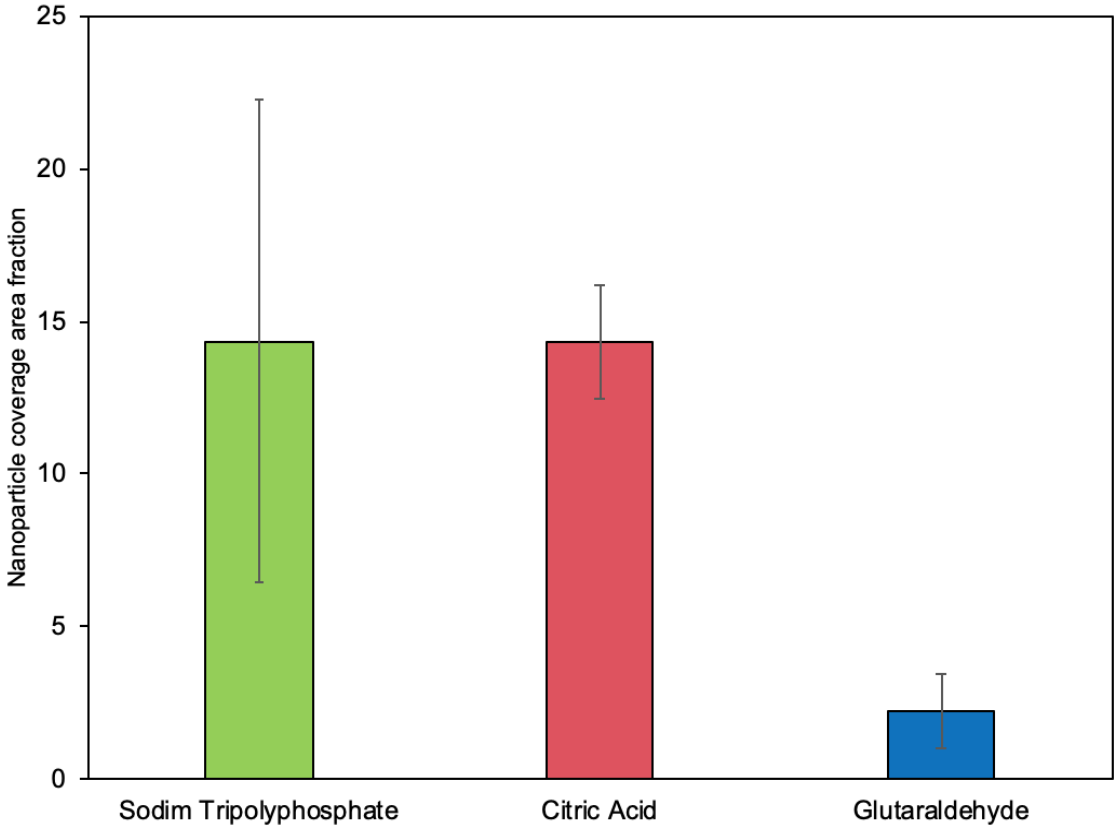

Figure 6. 7 Area coverage of silver nanoparticles synthesize in situ in hydrogels

6.3.3 Mechanical Properties

Figure 6.8A depicts a comparison of the mechanical properties of the hydrogels of HTCC crosslinked by the three crosslinking agents prior to the incorporation of Ag-NPs and shows significantly different responses, as expected based on the large differences in swelling potential presented in **Figure 6.2**. Evaluating the mechanical properties was important because, along with the swelling responses, these traits influence the hydrogel's possible industrial applications. The elastic modulus (G') of hydrogels crosslinked by GA was multiple orders of magnitude greater

than that of hydrogels crosslinked with CA and TPP, where the G' of HTCC crosslinked by TPP was intermediate between the two. Due to their high swelling potential, these preliminary rheological assessments were complemented with nanoscale mechanical measurements of the hydrogels crosslinked by TPP with AFM . AFM is used to characterize soft materials and hydrogels at the micro scale(Lee et al. 2018, Tang et al. 2019) by enabling the evaluation of differences in the mechanical properties resulting from small amounts of incorporated nanoparticles. **Figure 6.8B** shows representative FD curves of the HTCC hydrogels crosslinked by TPP before and after incorporation of Ag-NPs, and their fitting to the Sneddon model, from which the local elastic modulus is estimated (Ochbaum et al. 2020). The 100 FD curves that were used for the analysis of each sample verified that the hydrogels gels did not undergo irreversible deformation, showing no hysteresis between the approach and retraction curves. The local elastic modulus, *E*, that was obtained for each one of the curves of the three hydrogel populations were collected into probability density functions (PDFs), and were fitted with the Gamma distribution, $(\beta^{\alpha}/\Gamma(\alpha))x^{\alpha-1}e^{-\beta x}$, where x is the measured random variable (here *E*), α and β are shape and rate parameters, and $\Gamma(\alpha)$ is the gamma function. Using the two fitted parameters, the mean is given by α/β and the variance by α/β^2. **Figure 6.8C** shows the three PDFs in hierarchical ordered. As can be observed, they span over three orders of magnitude and depicts higher elastic moduli after the incorporation of the nanoparticles.

Figure 6.8A

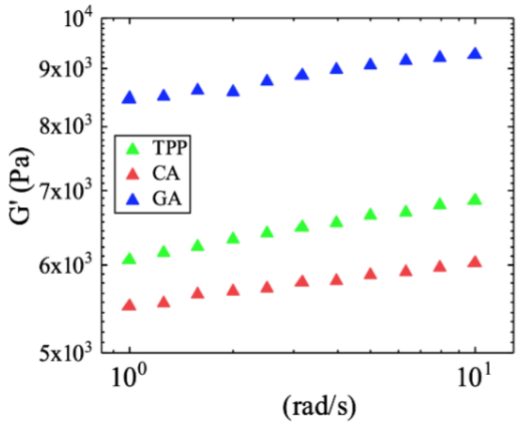

Figure 6.8B

Figure 6.8C

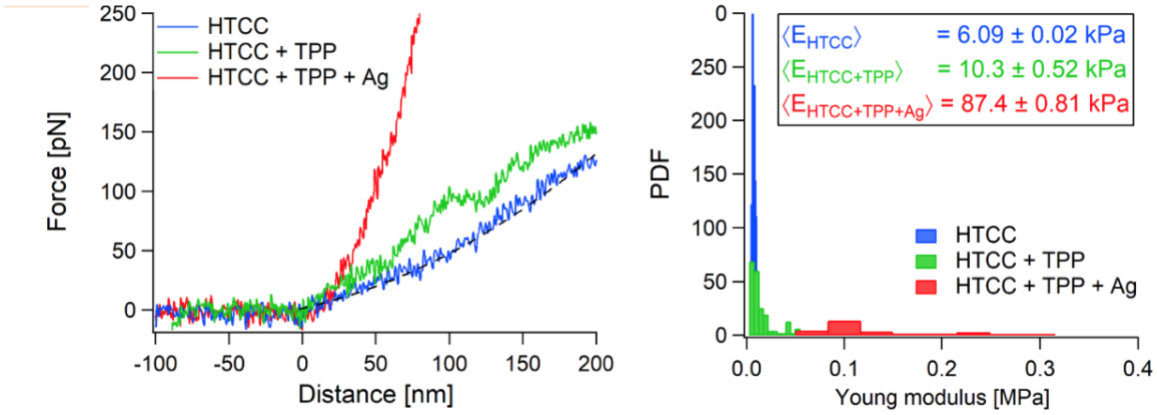

Figure 6. 8 a) Mechanical Properties of hydrogels crosslinked by three crosslinkers, and (b) AFM results for TPP-crosslinked system with Ag NPPs

Figure 6.8A: Comparison of the mechanical properties of the hydrogels of HTCC crosslinked by the three crosslinking agents prior to the incorporation of silver nanoparticles. Results show significantly different responses such that the elastic modulus (G') of hydrogels crosslinked by glutaraldehyde was multiple orders of magnitude greater than that of hydrogels crosslinked with citric acid and sodium tripolyphosphate, where the G' of HTCC crosslinked by sodium tripolyphosphate was intermediate between the two, likely due to differences in swelling. **Figure 6.8B** Representative FD curves of HTCC suspension (blue), HTCC crosslinking by TPP (green) and HTCC crosslinked by TPP incorporating Ag-NPs (red), with a representative fit (black dashed line) to the HTTC trace. **Figure 6.8C**: Probability density functions for the elastic (Young) moduli that were fitted for the three samples. The inset shows mean values with corresponding standard deviations.

6.3.4 Antimicrobial effect of HTCC-Ag hydrogels on intact biofilms

Hydrogels incorporating Ag-NPs crosslinked with all crosslinkers showed good antimicrobial activity against sessile bacteria of both Gram-positive (*Bacillus subtilis*) and Gram-negative (*Pseudomonas aeruginosa*) microorganisms by the disk diffusion method (**Figure 6.9**). These results were verified with the ATP assay, where differences in the effect between the three systems were not statistically significant (**Figure 6.10**). It is noteworthy that the antimicrobial effects on intact biofilms were not different between the hydrogels crosslinked by the three compounds despite the fact that the nanoparticle size distribution and shape were different among the three. This is contrary to what has been reported on the differential effects of Ag-NPs depending on their size and shape(Pal et al. 2007, Carlson et al. 2008), and supports previous observations that the antimicrobial effects of Ag-NPs are caused by interactions with the silver ions released from Ag-NPs rather than the Ag-NPs themselves(Xiu et al. 2011).The stabilization of the nanoparticles provided by the hydrogel scaffold allowed the diffusion of silver ions to occur but prevented direct interaction of the microorganisms with the nanoparticles (Xiu et al. 2011).

Due to the observation that the crosslinking agent had no significant effect on the efficiency of the hydrogels against the two organisms, one system (HTCC- TPP crosslinked with Ag-NP) was selected as a model to test against a wider range of microorganisms (**Figure 6.11**). Results show that the antimicrobial effects of the hydrogel-Ag-NP composites were superior than Ag-NPs on their own as well as to HTCC hydrogels on their own. This is especially evident in the case of *P. aeruginosa* PAO1 which showed virtually zero inhibition by Ag-NPs, chitosan, or crosslinked chitosan but showed a clearance ratio around 68% for the HTCC-Ag composite. *P. aeruginosa* PAO1 has shown resistance to silver ions due to its ability to produce a redox-active

metabolite which reduces silver ions to their elemental form(Muller 2018). This points to a synergistic mechanism whereby the stabilization of the silver nanoparticles provided by the hydrogel allows them to exert greater antimicrobial effects by providing an overall higher silver concentration, exceeding the tolerance level. This may be due to the prevention of the excessive formation of nanoparticle aggregates which have been shown to provide diminished antimicrobial effects(Pal et al. 2007, Xiu et al. 2011, Li et al. 2012, Mohanbaba and Gurunathan 2016, Li et al. 2017, Xie et al. 2018, Jorge de Souza et al. 2019). Additionally, the antimicrobial moieties of the chitosan itself may also play a role in providing this synergy by providing an additional agent.

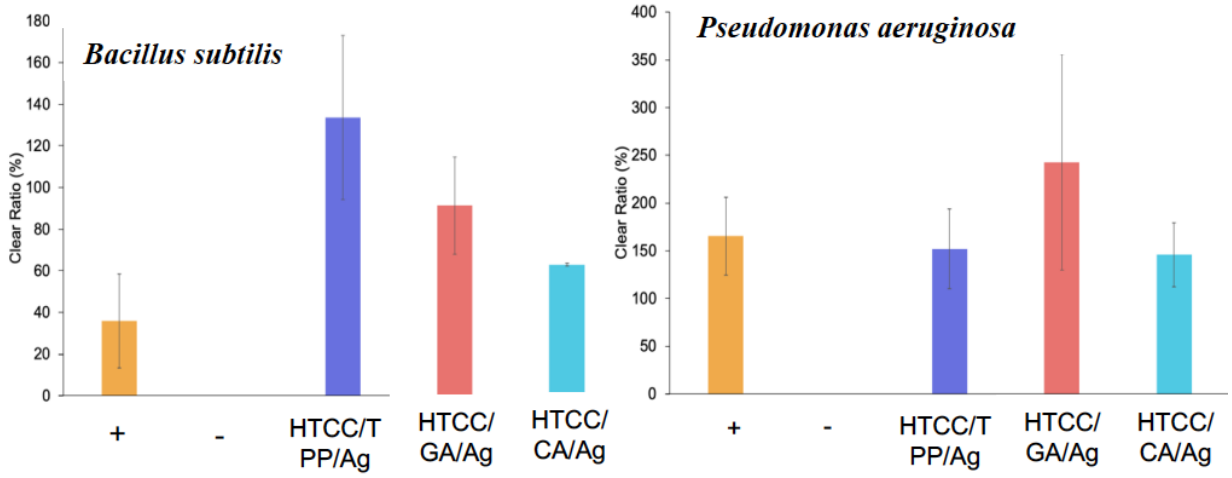

Figure 6. 9 Clear ratio comparison for hydrogels with AgNP crosslinked by the three crosslinking agents

Good antimicrobial capabilities in all cases regardless of crosslinker. (+/- on the x-axis indicate positive control (50% ethanol) and negative control (carrageenan) respectively. For all cases $p<0.05$ compared to the positive control, The differences between the three crosslinked gels are not statistically significant ($p>0.1$).

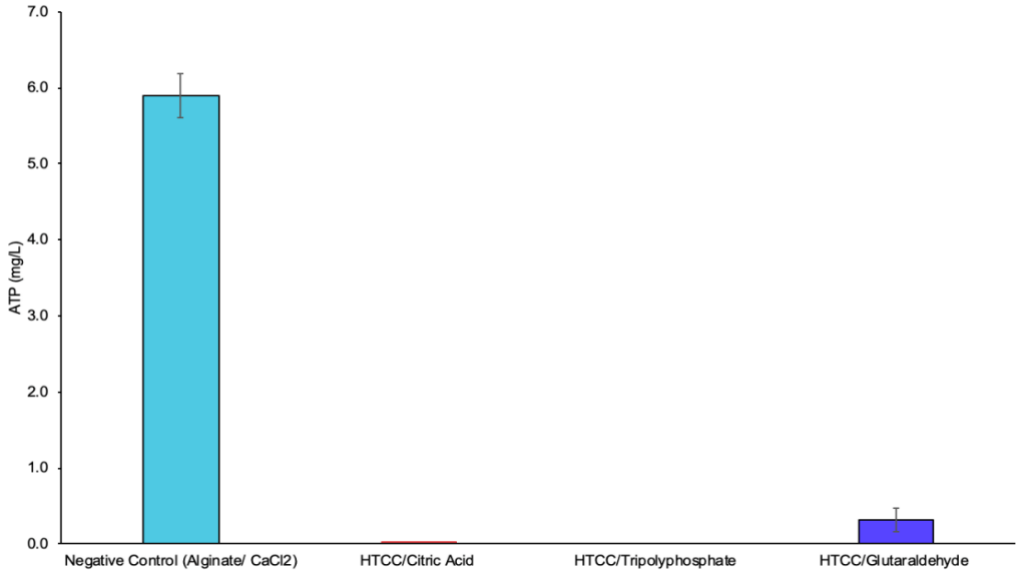

Figure 6. 11 ATP Assay for microorganisms contacted with hydrogels

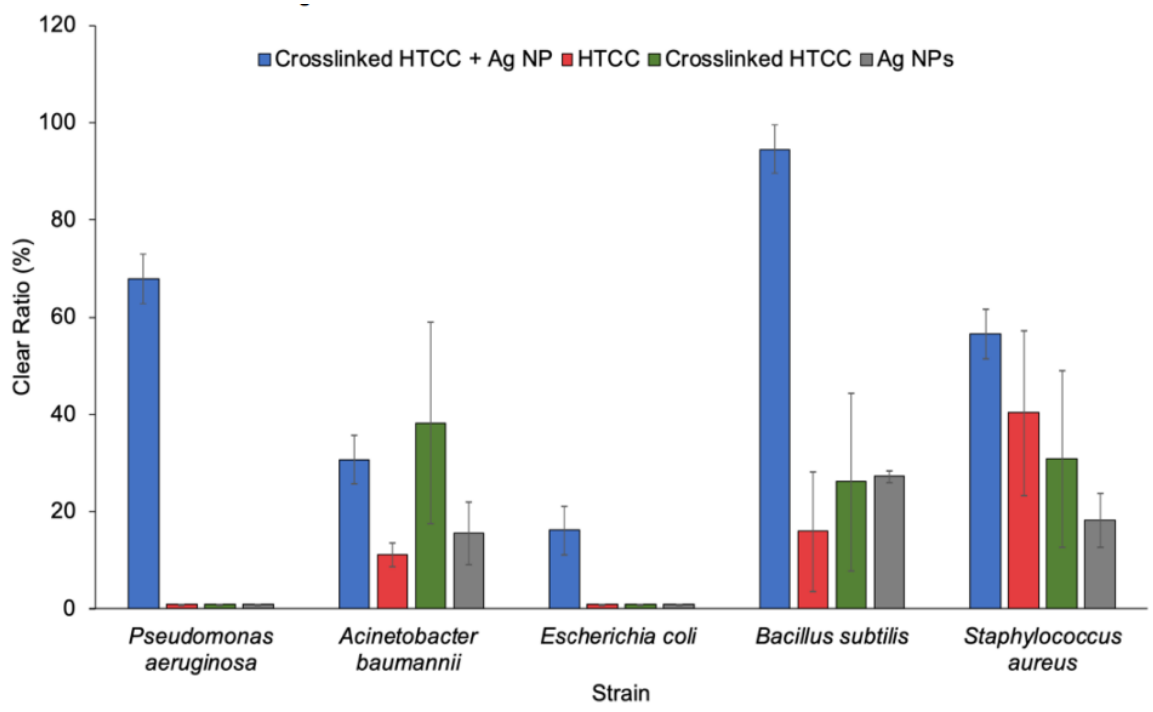

Figure 6. 10 Clear Ratio for Broad-Spectrum Microorganisms Contacted with TPP-Crosslinked Hydrogels

6.3.5 Molecular mechanisms of HTCC-Ag hydrogel antifouling behavior

Figure 6.12 shows that the prevalence of biofilm cells is significantly lower on surfaces containing the HTCC-Ag hydrogels compared to control surfaces. SEM visualizations of the effect of the HTCC-AgNP hydrogels on biofilm cells of a Gram-positive (*Bacillus subtilis)* and one Gram-negative *(Acinetobacter baumannii)* microorganism depict lower attachment of cells onto the treated surfaces. Calculated shape factor values support the observations from SEM images quantitatively since surfaces containing the HTCC-Ag hydrogels have higher shape factors compared to control surfaces (**Figure 6.13**).

Kwok et al.(Kwok et al. 1998) have demonstrated that there is an inverse linear relationship between shape factor and biofilm production(Kwok et al. 1998) whereby shape factor will be lower when more biofilms are present since cells in biofilms are more heterogenous(Kwok et al. 1998). Results from the ATP assay and qPCR on 16S rRNA gene targets for extracted biofilm sample further the evidence for lower biofilm formation on HTCC-Ag hydrogels compared to unmodified surfaces (**Figure 6.14 (All)**). These results also demonstrate that the antifouling capabilities of the HTCC-Ag hydrogels are considerable regardless of the crosslinking agent used in the hydrogel synthesis.

Visualization by SEM revealed single attached cells on HTCC-Ag surfaces, which appeared to be undisturbed in terms of cellular morphology. It was thus important to gage at the mechanism responsible for the HTCC-Ag hydrogels' ability to prevent biofouling. The biofouling prevention ability of the HTCC-Ag hydrogels is further evidenced in **Figure 6.14** depicting the gene transcript of *lasI* in *Pseudomonas aeruginosa* as well as *lasI* gene abundance **Figure 6.15**. Biofilm formation in *P. aeruginosa* depends on four quorum sensing systems, one of which is encoded for in the *las* gene cluster. Quorum sensing in *P. aeruginosa* modulates the

transformation of cells from planktonic state to biofilm state. The *lasI* gene specifically is responsible for the synthesis of N-(3-oxododecanoyl)-L-homo serine lactone, and several studies have shown that a deletion of the *lasI* gene leads to a defective biofilm by causing a loss of exopolysaccharide production (Costerton et al. 1999, Finelli et al. 2003, Abdelraheem et al. 2020).

A lower abundance and transcript of the *lasI* gene in samples of extracted biofilm formed on hydrogels of HTCC-Ag compared to a hydrogel with no antimicrobial capabilities shows that the interaction with the synthesized chitosan-silver composites decreased the quorum sensing abilities of the microorganisms. The observed decrease in biofilm formation was thus at least partially caused by an effect on the quorum sensing system. The lack of statistically significant differences between hydrogels crosslinked with the three compounds indicates that this mechanism takes place regardless of the crosslinking mechanism employed when the hydrogels are first synthesized. This further demonstrates that hydrogel synthesis mechanism may be chosen depending on the desired physical traits without compromising the antimicrobial and antifouling capabilities of the materials.

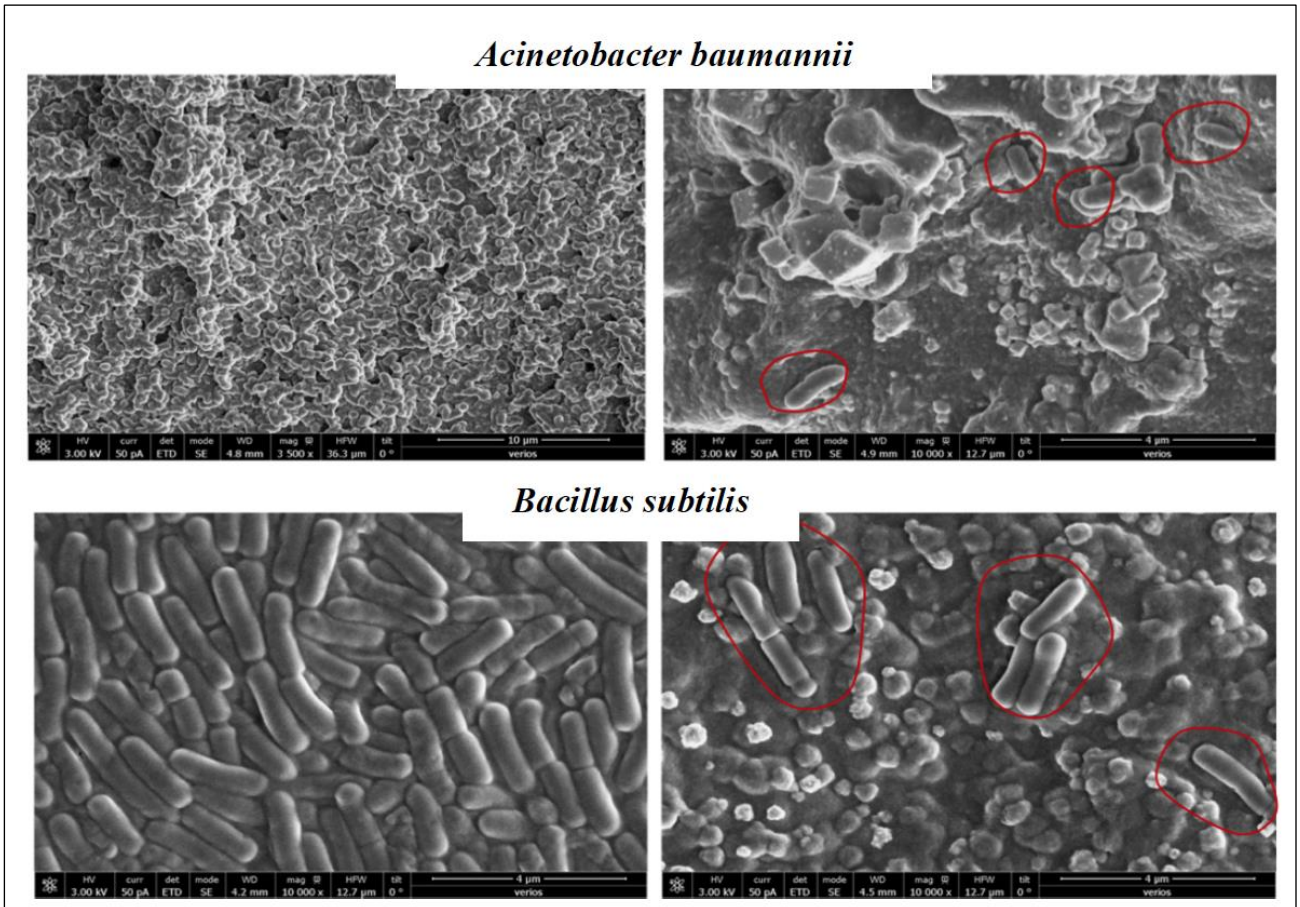

Figure 6. 12 SEM visualization of biofilm formation on the surface of HTCC-Ag hydrogels and HTCC hydrogels without Ag by *Acinetobacter baumanii* and *Bacilus subtilis*

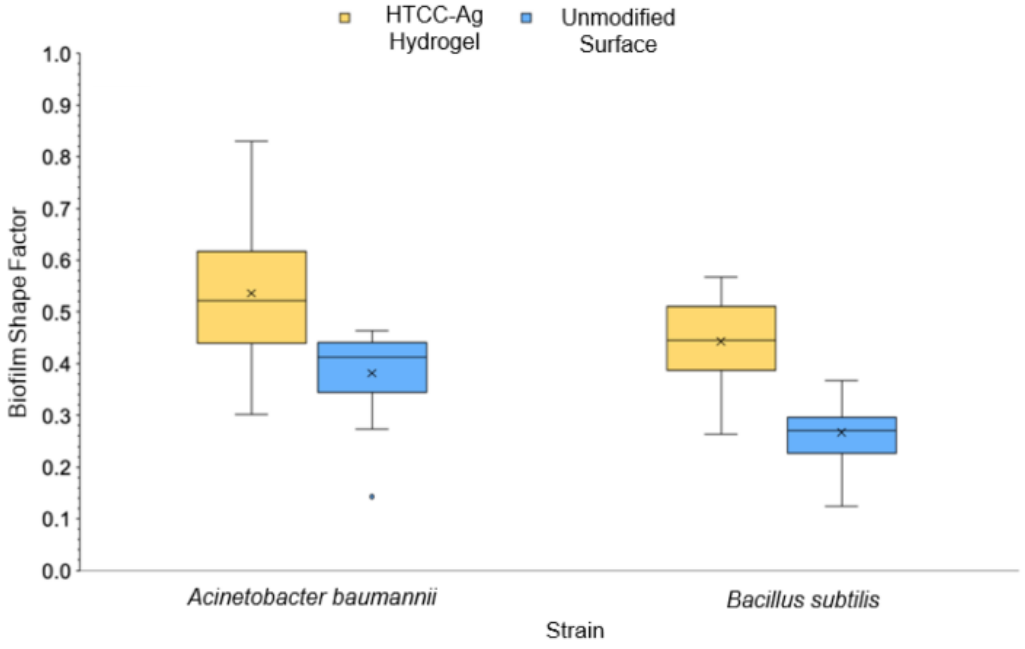

Figure 6. 13 Biofilm shape factor for cells attached to HTCC-Ag hydrogels compared to HTCC hydrogels without Ag

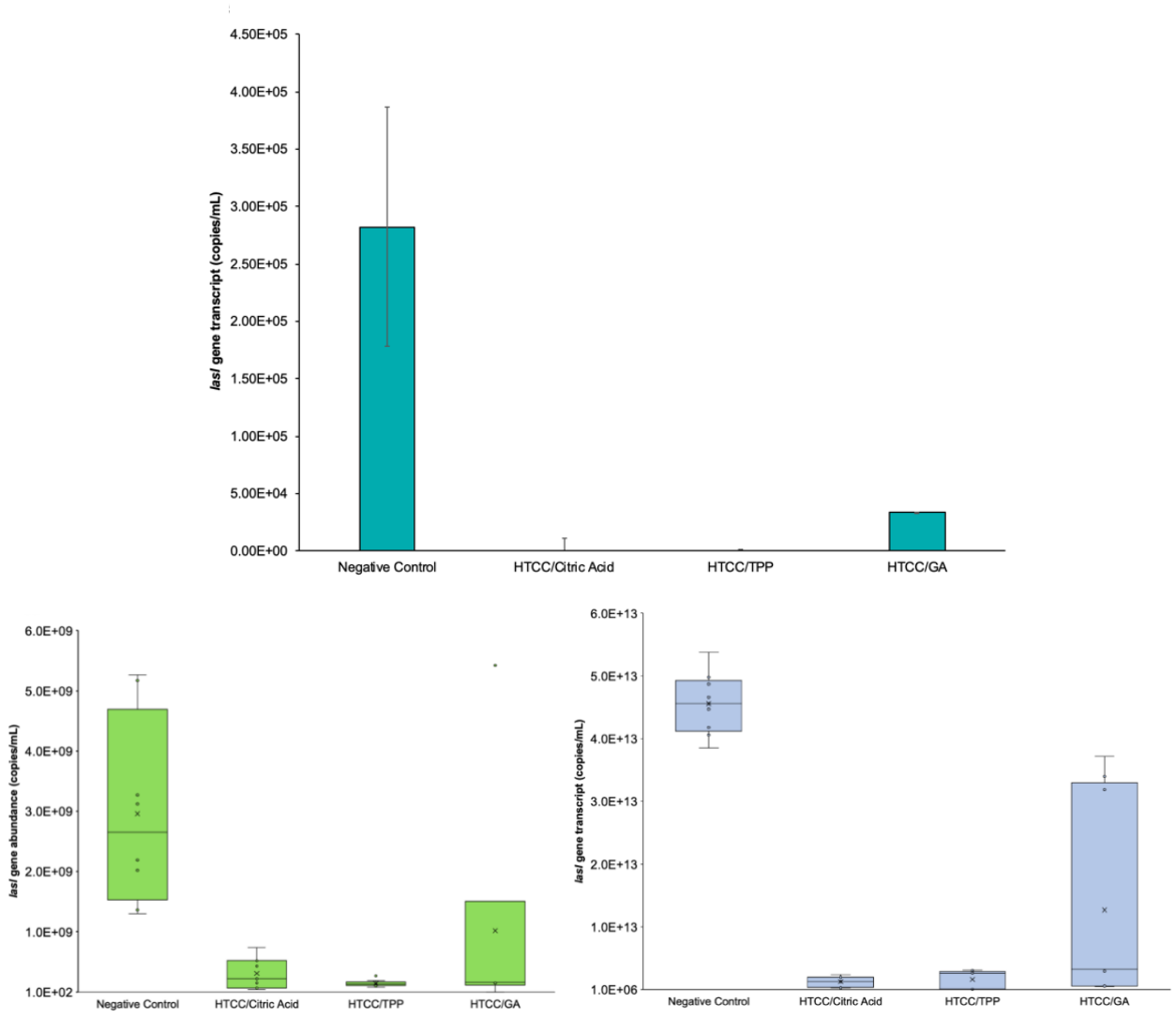

Figure 6. 15 *LasI* gene abundance and expression of detatched biofilms of P. aeruginosa

Figure 6. 14 *LasI* gene expression of P. aeruginosa contacted with HTCC-crosslinked hydrogels

Figure 6.14: *LasI* gene expression of *P. aeruginosa* shows lower expression in detached biofilm of HTCC-Ag hydrogels with the three crosslinkers compared to a control hydrogel. Bars represent mean of three replicates and error bars represent standard deviation (n=3). **Figure 6.15:** *LasI* gene abundance of detached biofilm of *P. aeruginosa* shows lower abundance for HTCC-Ag hydrogels compared to a control inert hydrogel (n=3). Gene abundance of *lasI* gene in suspension of cells in contact with control hydrogel (left) as well as hydrogels crosslinked by citric acid, sodium tripolyphosphate and glutaraldehyde. The differences between the HTCC hydrogels are not statistically significant.

6.3.6 Mechanism of Ag NP action

In accordance with the results presented above, **Figure 6.16** show that the most likely mechanism responsible for the antimicrobial and antifouling effects are interactions with silver ions directly rather than leaching of Ag-NPs. **Figure 6.16** depicts UV-Vis spectra of a control solution of 0.1 M AgNPs as well as the spectra of the wash solutions for the three hydrogel systems. The control spectra depicts a peak around 433 corresponding to the presence of silver nanoparticles since these have a strong absorption peak between 400-450 nm due to the surface Plasmon resonance effect(Li et al. 2012, Yerragopu et al. 2020, Zakia et al. 2020). This confirms that UV-Visible spectra can be used to identify nanoparticles in solution. The fact that no peaks are observed in the wash solutions of the HTCC-AgNP hydrogels is an indication that there was no leaching of the particles into the solution and therefore the antimicrobial effect was not due to interactions between the silver nanoparticles and the microorganisms.

Figure 6.17 support this hypothesis since the concentration of silver ions in the wash solution of the HTCC-AgNP hydrogels with the three crosslinkers was considerable in all cases. There are statistically significant differences in the concentration of silver ions when the hydrogels are crosslinked with CA compared to TPP and GA. The fact that no significant differences in the antimicrobial effects are observed in accordance to this may point to the fact that a lower loading of nanoparticles may be possible to achieve the same effect when crosslinked with TPP and GA. Xiu et al. have shown that the antimicrobial activity of Ag-NPs is due solely to the release of silver ions, and that even relatively low concentrations of released silver ions (µg/L) can account for the observed biological responses(Xiu et al. 2011). This provides the possibility for yet another characteristic of the presented materials that can be tuned and adjusted depending on the desired application.

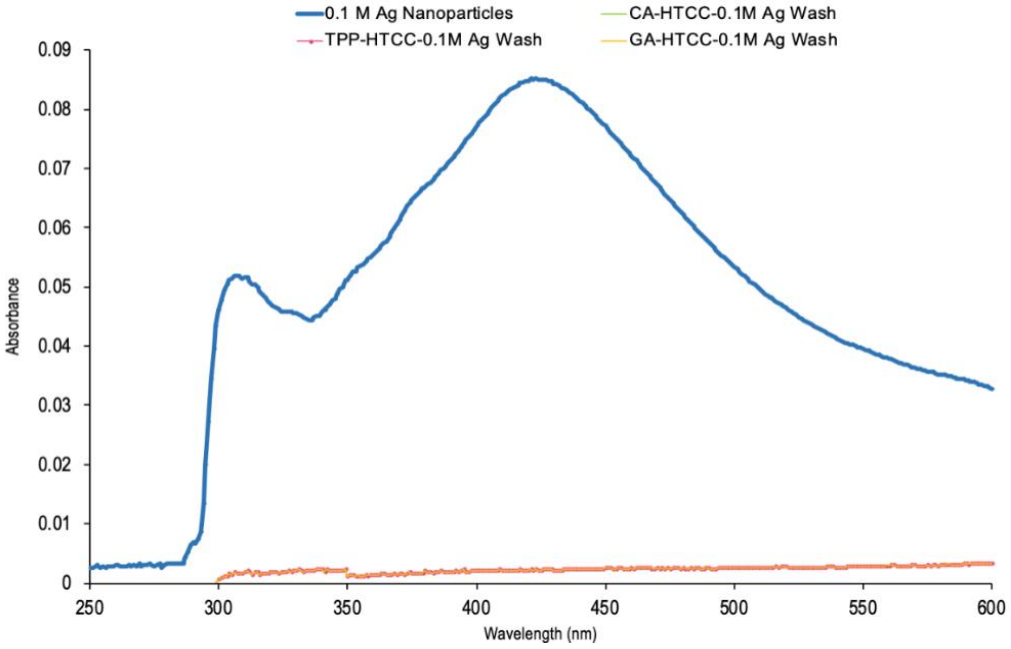

Figure 6. 17 UV-Visible Spectra of silver nanoparticles and wash solutions of synthesized hydrogels

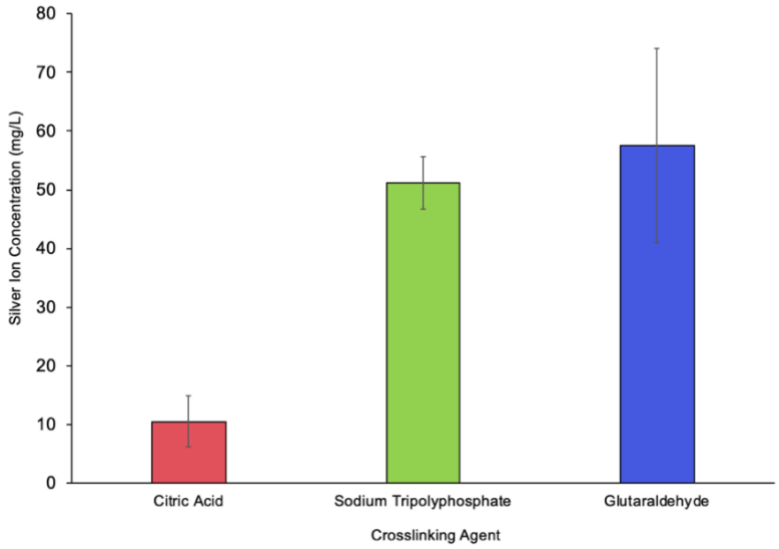

Figure 6. 16 ICP-OES Results of Silver Ions in Hydrogels Wash Solution

6.4 Conclusion

Overall, this study showed that crosslinking agent used in the hydrogel synthesis had an important effect on the physical properties of the hydrogels. The synergistic antimicrobial effect of HTCC hydrogels- Ag-NPs was likely due to both the effectiveness of Ag-NPs as antimicrobials as well as the stabilization provided by the hydrogel structure, which served as a scaffold for effective delivery of silver ions. The promising antimicrobial and antifouling behavior over a range of physical properties provides the possibility for use of each of the hydrogels in different industrial contexts depending on the desired characteristics for each application.

Chapter 7: Conclusions and Future Work

7.1 Summary

This research comprehensively evaluated the design and optimization of interactions between contaminants and surfaces in the context of water and wastewater treatment. Two research avenues were followed, the first involved designing or understanding surfaces for the removal of persistent organic pollutants such as per- and polyfluoroalkyl substances (PFASs) and 1,4-dioxane, while the second involved a focus on biofilm both as a biotechnology resource for water treatment, as well as as an undesirable substance to be removed from functional surfaces.

Modification of the surface of granular activated carbon (GAC) using the cationic polymer polydialydimethyl ammonium chloride (polyDADMAC) was studied as a strategy to improve the removal of the persistent environmental contaminant class per- and polyfluoroalkyl substances (PFASs). Specifically, complex water matrices were used in these studies to simulate challenging conditions that are environmentally relevant. Amending the surface with polyDADMAC concentrations as low as 0.00025% enhanced GAC's adsorption capacity for both short- and long-chained PFASs, even in the presence of competing ions. Regeneration with minimum disruption to the adsorbent's structure was achieved using low-power ultrasound, supporting the consideration of polyDADMAC-modified GAC was an effective, regenerable adsorbent for real environmentally relevant water conditions.

The effect of the carbon/nitrogen (C/N) ratio on biofilm formation by the model heterotrophic organism *Pseudomonas aeruginosa* was evaluated for the benefit that understanding this might have in terms of ideating strategies to either encourage or prevent biofilm formation depending on the desired application. Biofilm composition, in terms of carbohydrates and proteins, was affected as a function of C/N, but no effect was observed in

terms of total biomass attached. The expression of several genes such as *lasI* and *lasR*, involved in quorum sensing, and *rpoS*, involved in stress response, was also differentially affected as a function of C/N. C/N=9 was found to be an important condition, affecting biofilm composition, biofilm gene expression, organic carbon utilization, and biomolecule production.

A multiple lines of evidence approach was developed for the quantification of biofilm on functional and medically relevant surfaces such as catheters. Carbohydrates, proteins, adenosine triphosphate (ATP) and total nucleic acids (total bacterial 16s rRNA) were quantified independently to arrive at converging lines that may be used as evidence for the evaluation of the biofilm presence that might aid in infection diagnosis. Four assays that are not typically used together were proposed for this purpose, namely: Periodic Acid-Schiff Assay for total carbohydrates, Modified Lowry Protein Assay for proteins, BacTiterGlo ATP Assay for ATP, and quantitative polymerase chain reaction for total nucleic acids. The four assays are proposed as a multipronged approach for biofilm quantification in-vitro and from patients.

Antimicrobial hydrogels from the soluble chitosan compound N-(2-hydroxy-3-trimethylammonium)propyl chitosan chloride were synthesized and their physical, chemical, and antimicrobial properties were compared when crosslinked by three different crosslinking agents. The crosslinkers sodium tripolyphosphate (TPP), glutaraldehyde (GA), and citric acid (CA) were compared in terms of their impact on swelling potential, hydrophobicity, and mechanical properties. A range of swelling degrees from 350% to 2350% with GA and TPP respectively were observed. Silver nanoparticles (AgNPs) were synthesized *in situ* leading to improved mechanical properties evidenced by an increase in the Young modulus from 10.3 MPa for TPP-crosslinked systems to 87.4 MPa for TPP-crosslinked /AgNP composites. Broad-spectrum

antimicrobial and antifouling abilities were observed for all systems, suggesting these materials may be used for diverse applications where biofouling control is required.

7.2 Future Work

7.2.1 Surface Modification for Enhanced Removal of Recalcitrant Contaminants

Surface functionalization of adsorbents was shown to be a promising tool for the improved removal of PFASs as well as for the improvement of other surface-mediated treatment strategies such as biofilters. Additionally, the regeneration potential of these adsorbents by low-power ultrasound was shown to be a promising technique, achieving high removal of the contaminants from the surface with minimum disruption to the adsorbent structure. Future research is required to understand the impact of functionalizing other promising surfaces such as carbon nanotubes or water treatment membranes, as well as the potential of these adsorbents and adsorbent regeneration strategies to be used for treatment of other kinds of complex water matrices such as reverse osmosis concentrate brine. Additionally, the impact of improved adsorption of recalcitrant contaminants on the biodegradation or general degradation potentials needs further evaluation.

7.2.2 Biofilm-Mediated Energy Positive Wastewater Treatment and Biofilm Quantification Techniques

The work presented in this dissertation identifies the effect of C/N ratio on biofilm characteristics as well as biofilm-formation mechanisms in a single species system. Additionally, a multipronged culture independent approach was developed in order to quantify biofilms more accurately than the standard approaches. As a first step, future research related to the biofilm work in this chapter should validate the culture-independent biofilm quantification technique developed for catheters and other industrially relevant tubing and validate it for more complex

surfaces such as water treatment membranes. The reason for this is that the mechanisms by which water treatment membranes become fouled are more complicated than the simplifications and assumptions made related to the medically relevant catheter, and it is important to ensure that accurate and reproducible results are obtained for membranes. Additionally, distinctions between the EPS in the cake layer of membrane fouling compared to the tightly bound EPS should be evaluated since this would have important industrially relevant implications. Moreover further development of the culture-independent biofilm quantification method would benefit from gaging at the measured variables that have the greatest effect on the physical and clinical measurable outputs related to fouling (such as pressure increases in membrane systems or infection thresholds in patients). This might be achieved through further statistical analyses and applications of the methodologies in different settings following metrics such as the principal component analyses presented in Chapter 4.

In terms of the effect of influent conditions on the characteristics of biofilm, future work may focus on understanding the effects of nutrient conditions on EPS development and quorum sensing in a real wastewater treatment activated sludge microbial culture, to get a sense of the implications this may have for membrane bioreactor-based treatment systems, or biofilm-based treatment processes such as moving biofilm bioreactors. More complex molecular tools such as metagenomics and metatranscriptomics could also be used to understand the effects of nutrient ratios on microbial community development, or on regulation of a broader range of quorum sensing genes expressed by a wide range of organisms. Following the basis established in this work, future work may focus on understanding whether the observed differences in the biofilm formed in a batch system translate into a flow-through membrane bioreactor considering the added complexities introduced by flow, flux, pressure, aeration, etc. which are relevant for real

wastewater treatment systems. Experiments may focus on identifying whether there are any differences in the composition of the EPS in the tightly bound EPS of fouled membranes compared to the cake layers, as well as gaging at whether there are differences in the visible structure of the biofilm in these two layers, since some could be expected considering the effects of physical processes taking place such as aeration or flux. Growth of algal biofilms on inert surfaces, such as those used in the research in this section, can be evaluated in terms of the effect of carbon, nitrogen, and phosphorous on the development of algal biofilms that are able to remove significant nitrogen and phosphorous from the influent. The relevance of testing the impact of C/N/P in this case, as opposed to C/N only in the case of the prokaryotic biofilms in this section, is that algae growth depends on the assimilation of all three essential nutrients to an ideal proportion known as the Redfield Ratio since the relevance of this in the development of algal biofilms and their nutrient removal and lipid accumulation potentials has not been studied.

8. References

(2019). "Guidance on Natural Organic Matter in Drinking Water Canada https://www.canada.ca/en/health-canada/programs/consultation-organic-matter-drinking-water/document.html Accessed 12/2020."

Abd El-Hady, M. M. and Saeed, S. E. (2020). "Antibacterial Properties and pH Sensitive Swelling of Insitu Formed Silver-Curcumin Nanocomposite Based Chitosan Hydrogel." Polymers **12**(11). 2451. DOI: https://doi.org/10.3390/polym12112451.

Abdelfattah, A., Hossain, M. I. and Cheng, L. (2020). "High-strength wastewater treatment using microbial biofilm reactor: a critical review." World J Microbiol Biotechnol **36** (5).1-10.DOI: https://doi.org/10.1007/s11274-020-02853-y.

Abdelraheem, W. M., Abdelkader, A. E., Mohamed, E. S. and Mohammed, M. S. (2020). "Detection of biofilm formation and assessment of biofilm genes expression in different Pseudomonas aeruginosa clinical isolates." Meta Gene **23**. 100646. DOI: 10.1016/j.mgene.2020.100646.

Adamson, D. T., Pina, E. A., Cartwright, A. E., Rauch, S. R., Hunter Anderson, R., Mohr, T. and Connor, J. A. (2017). "1,4-Dioxane drinking water occurrence data from the third unregulated contaminant monitoring rule." Sci Total Environ **596-597**: 236-245.DOI: 10.1016/j.scitotenv.2017.04.085.

Adamson, D. T., Wilson, J. T., Freedman, D. L., Ramos-Garcia, A. A., Lebron, C. and Danko, A. (2022). "Establishing the prevalence and relative rates of 1,4-dioxane biodegradation in groundwater to improve remedy evaluations." J Hazard Mater **424**(Pt D): 127736.DOI: 10.1016/j.jhazmat.2021.127736.

Alcântara, M. T. S., Lincopan, N., Santos, P. M., Ramirez, P. A., Brant, A. J. C., Riella, H. G. and Lugão, A. B. (2020). "Simultaneous hydrogel crosslinking and silver nanoparticle formation by using ionizing radiation to obtain antimicrobial hydrogels." Radiat Phys Chem **169**.DOI: 10.1016/j.radphyschem.2020.108777. DOI: https://doi.org/10.1016/j.radphyschem.2020.108777

Allesen-Holm, M., Barken, K. B., Yang, L., Klausen, M., Webb, J. S., Kjelleberg, S., Molin, S., Givskov, M. and Tolker-Nielsen, T. (2006). "A characterization of DNA release in *Pseudomonas aeruginosa* cultures and biofilms." Mol Microbiol **59**(4): 1114-1128.DOI: 10.1111/j.1365-2958.2005.05008.x.

Aly, Y. H., Liu, C., McInnis, D. P., Lyon, B. A., Hatton, J., McCarty, M., Arnold, W. A., Pennell, K. D. and Simcik, M. F. (2018). "In Situ Remediation Method for Enhanced Sorption of Perfluoro-Alkyl Substances onto Ottawa Sand." J Environ Eng **144**(9): 04018086-04018081-04018086-04018089.DOI: https://doi.org/10.1061/(ASCE)EE.1943-7870.0001418.

Aly, Y. H., McInnis, D. P., Lombardo, S. M., Arnold, W. A., Pennell, K. D., Hatton, J. and Simcik, M. F. (2019). "Enhanced adsorption of perfluoro alkyl substances for in situ remediation." Environ Sci Water Res Technol **5**(11): 1867-1875.DOI: 10.1039/c9ew00426b.

Amann, R. I., Ludwig, W. and Schleifer, K. H. (1995). "Phylogenetic identification and in situ detection of individual microbial cells without cultivation." Microbiol Rev **59**(1): 143-169. PMCID: PMC239358.

Arens, L., Weißenfeld, F., Klein, C. O., Schlag, K. and Wilhelm, M. (2017). "Osmotic Engine: Translating Osmotic Pressure into Macroscopic Mechanical Force via Poly(Acrylic Acid) Based Hydrogels." Adv Sci **4**(9). 1700112. DOI: https://doi.org/10.1002/advs.201700112.

Ayawei, N., Ebelegi, A. N. and Wankasi, D. (2017). "Modelling and Interpretation of Adsorption Isotherms." J. Chem. **2017**: 3039817.DOI: 10.1155/2017/3039817.

Barzen-Hanson, K. A., Roberts, S. C., Choyke, S., Oetjen, K., McAlees, A., Riddell, N., McCrindle, R., Ferguson, P. L., Higgins, C. P. and Field, J. A. (2017). "Discovery of 40 Classes of Per- and Polyfluoroalkyl Substances in Historical Aqueous Film-Forming Foams (AFFFs) and AFFF-Impacted Groundwater." Environ Sci Technol **51**: 2047-2057.DOI: https://doi.org/10.1021/acs.est.6b05843.

Behzadi, P., Behzadi, E. and Ranjbar, R. (2015). "Urinary tract infections and Candida albicans." Central European journal of urology **68**(1): 96-101.DOI: 10.5173/ceju.2015.01.474.

Bhowmick, R., Ghosal, A., Das, B., Koley, H., Saha, D. R., Ganguly, S., Nandy, R. K., Bhadra, R. K. and Chatterjee, N. S. (2008). "Intestinal Adherence of *Vibrio cholerae* Involves a Coordinated Interaction between Colonization Factor GbpA and Mucin." Infection and Immunity **76**(11): 4968-4977.DOI: 10.1128/iai.01615-07.

Bhumkar, D. R. and Pokharkar, V. B. (2006). "Studies on the Effect of pH on Cross-Linking of Chitosan With Sodium Tripolyphosphate: A Technical Note." AAPS ParmSciTech **7**(2): E138-E146.DOI: https://doi.org/10.1208/pt070250.

Bjarnsholt, T. (2013). "The Role of Bacterial Biofilms in Chronic Infections." APMIS Suppl: 1-51.DOI: https://doi.org/10.1111/apm.12099.

Bock, K. D., Derave, W., Ramaekers, M., Richter, E. A. and Hespel, P. (2007). "Fiber type-specific muscle glycogen sparing due to carbohydrate intake before and during exercise." Journal of Applied Physiology **102**(1): 183-188.DOI: 10.1152/japplphysiol.00799.2006.

Breitbach, M. and Bathen, D. (2001). "Influence of ultrasound on adsorption processes." Ultrason Sonochem **8**(3): 277-283.DOI: 10.1016/s1350-4177(01)00089-x.
Breitbach, M., Bathen, D. and Schmidt-Traub, H. (2003). "Effect of Ultrasound on Adsorption and Desorption Processes." Ind Eng Chem Rest **42**: 5635-5646.

Caló, E. and Khutoryanskiy, V. V. (2015). "Biomedical applications of hydrogels: A review of patents and commercial products." Eur Polym J **65**: 252-267.DOI: 10.1016/j.eurpolymj.2014.11.024.

Carlson, C., Hussain, S. M., Schrand, A. M., Braydich-Stolle, L. K., Hess, K. L., Jones, R. L. and Schlager, J. J. (2008). "Unique Cellular Interaction of Silver Nanoparticles: Size-Dependent Generation of Reactive Oxygen Species." J Phys Chem B **112**: 13608-13619.DOI: https://doi.org/10.1021/jp712087m.

Carmona, P., Tasici, A. M., Sande, S. A., Knudsen, K. D. and Nystrom, B. (2021). "Glyceraldehyde as an Efficient Chemical Crosslinker Agent for the Formation of Chitosan Hydrogels." Gels **7**(4).DOI: 10.3390/gels7040186.

Casolaro, M., Casolaro, I., Akimoto, J., Ueda, M., Ueki, M. and Ito, Y. (2018). "Antibacterial Properties of Silver Nanoparticles Embedded on Polyelectrolye Hydrogels Based on a-Amino Acid Residues." Gels **4**(42).DOI: 10.3390/gels4020042.

CDC (2015). Catheter-associated Urinary Tract Infections. Centers for Disease Control & Prevention, National Center for Emerging and Zoonotic Infectious Diseases, Division of Healthcare Quality Promotion (DHQP).

Chao, Y., Mao, Y., Wang, Z. and Zhang, T. (2015). "Diversity and functions of bacterial community in drinking water biofilms revealed by high-throughput sequencing." Sci Rep **5**.DOI: https://doi.org/10.1038/srep10044.

Chen, G.-Q., Wu, Y.-H., Wang, Y.-H., Chen, Z., Tong, X., Bai, Y., Luo, L.-W., Xi, C. and Hu, H.-Y. (2021). "Effects of microbial inactivation approaches on quantity and properties of extracellular polymeric substances in the process of wastewater treatment and reclamation: A review." J Hazard Mater **413**.DOI: https://doi.org/10.1016/j.jhazmat.2021.125283.

Chen, R., Liu, C., Johnson, N. W., Zhang, L., Mahendra, S., Liu, Y., Dong, Y. and Chen, M. (2019). "Removal of 1,4-dioxane by titanium silicalite-1: Separation mechanisms and bioregeneration of sorption sites." Chem Eng J **371**: 193-202. DOI: 10.1016/j.cej.2019.03.285.

Chen, S., Li, L., Zhao, C. and Zheng, J. (2010). "Surface hydration: Principles and applications toward low-fouling/nonfouling biomaterials." Polymers **51**: 5283-5293.DOI: https://doi.org/10.1016/j.polymer.2010.08.022.

Chen, X., Zhang, Q., Zhu, Y. and Zhao, T. (2021). "Response of wastewater treatment performance, microbial composition and functional genes to different C/N ratios and carrier types in MBBR inoculated with heterotrophic nitrification-aerobic denitrification bacteria." Bioresour Technol **336**.DOI: https://doi.org/10.1016/j.biortech.2021.125339.

Cho, D.-W., Chon, C.-M., Kim, Y., Jeon, B.-H., Schwartz, F. W., Lee, E.-S. and Song, H. (2011). "Adsorption of nitrate and Cr(VI) by cationic polymer-modified granular activated carbon." Chem Eng J **175**: 298-305.DOI: 10.1016/j.cej.2011.09.108.

Chularueangaksorn, P., Tanaja, S., Fuji, S. and Kunacheva, C. (2014). "Adsorption of perfluorooctanoic acid (PFOA) onto anion exchange resin, non-ion exhange resin, and granular-activated carbon by batch and column." Desalin Water Treat **52**(34-36): 6542-6548.DOI: https://doi.org/10.1080/19443994.2013.815589.

Colvin, K. M., Alnabelseya, N., Baker, P., Whitney, J. C., Howell, P. L. and Parsek, M. R. (2013). "PelA Deacetylase Activity Is Required for Pel Polysaccharide Synthesis in *Pseudomonas aeruginosa*." Journal of Bacteriology **195**(10): 2329-2339.DOI: 10.1128/jb.02150-12.

Cordner, A., Goldenman, G., Birnbaum, L. S., Brown, P., Miller, M. F., Mueller, R., Sharyle, P., Salvatore, D. H. and Trasande, L. (2021). "The True Cost of PFAS and the Benefits of Acting Now." Environ Sci Technol **55**(14): 9630-9633.DOI: https://doi.org/10.1021/acs.est.1c03565.

Costerton, J. W., Stewart, P. S. and Greenbert, E. P. (1999). "Bacterial Biofilms: A Common Cause of Persistent Infections." Science **284**.DOI: 10.1126/science.284.5418.1318.

Cramton, S. E., Gerke, C., Schnell, N. F., Nichols, W. W. and Gotz, F. (1999). "The intercellular adhesion (ica) locus is present in *Staphylococcus aureus* and is required for biofilm formation." Infect Immun **67**(10): 5427-5433PMC96900.

Crouzet, M., Le Senechal, C., Brözel, V. S., Costaglioli, P., Barthe, C., Bonneu, M., Garbay, B. and Vilain, S. (2014). "Exploring early steps in biofilm formation: set-up of an experimental system for molecular studies." BMC Microbiol **14**(253).DOI: https://doi.org/10.1186/s12866-014-0253-z.

Cucarella, C., Tormo, M. A., Ubeda, C., Trotonda, M. P., Monzón, M., Peris, C., Amorena, B., Lasa, I. and Penadés, J. R. (2004). "Role of biofilm-associated protein bap in the pathogenesis of bovine *Staphylococcus aureus*." Infection and immunity **72**(4): 2177-2185.DOI: 10.1128/iai.72.4.2177-2185.2004.

Dai, Y., Zhang, N., Xing, C., Cui, Q. and Sun, Q. (2019). "The adsorption, regeneration and engineering applications of biochar for removal organic pollutants: A review." Chemosphere **223**: 12-27.DOI: 10.1016/j.chemosphere.2019.01.161.

Das, T., Sharma, P. K., Krom, B. P., van der Mei, H. C. and Busscher, H. J. (2011b). "Role of eDNA on the adhesion forces between *Streptococcus* mutans and substratum surfaces: influence of ionic strength and substratum hydrophobicity." Langmuir **27**(16): 10113-10118.DOI: 10.1021/la202013m.

Dasgupta, D., Ghosh, R. and Sengupta, T. K. (2013). "Biofilm-Mediated Enhanced Crude Oil Degradation by Newly Isolated Pseudomonas Species." ISRN **2013**.DOI: https://doi.org/10.5402/2013/250749.

Davies, D. (2003). "Understanding biofilm resistance to antibacterial agents." Nat Rev Drug Discov **2**(2): 114-122.DOI: 10.1038/nrd1008.

Davies, D. G., Parsek, M. R., Pearson, J. P., Iglewski, B. H., Costerton, J. W. and Greenbert, E. P. (1998). "The Involvement of Cell-to-Cell Signals in the Development of a Bacterial Biofilm." Science **280**(5361): 295-298.DOI: 10.1126/science.280.5361.295.

de Celis, M., Belda, I., Ortiz-Alvarez, R., Arregui, L., Marquina, D., Serrano, S. and Santos, A. (2020). "Tuning up microbiome analysis to monitor WWTPs' biological reactors functioning." Sci Rep **10**.DOI: https://doi.org/10.1038/s41598-020-61092-1.

De Klevit, T. R., Gillis, R., Marx, S., Brown, C. and Iglewski, B. H. (2001). "Quorum-Sensing Genes in Pseudomonas aeruginosa Biofilms: Their Role and Expression Patterns." Appl Environ Microbiol **67**(4).DOI: https://doi.org/10.1128/AEM.67.4.1865-1873.2001.

Dean, J. A. and Dean, J. (1995). Analytical Chemistry Handbook. New York, NY, McGraw-Hill.
DeLuca, N. M., Angrish, M., Wilkins, A., Thayer, K. and Cohen Hubal, E. A. (2021). "Human exposure pathways to poly- and perfluoroalkyl substances (PFAS) from indoor media: A systematic review protocol." Environ Int **146**.DOI: https://doi.org/10.1016/j.envint.2020.106308.

Doll, K., Jongsthaphongpun, K. L., Stumpp, N. S., Winkel, A. and Stiesch, M. (2016). "Quantifying implant-associated biofilms: Comparison of microscopic, microbiologic and biochemical methods." J Microbiol Methods **130**: 61-68.DOI: 10.1016/j.mimet.2016.07.016.

Douterelo, I., Sharpe, R. and Boxall, J. (2014). "Bacterial community dynamics during the early stages of biofilm formation in a chlorinated experimental drinking water distribution system: implications for drinking water discolouration." J Appl Microbiol **117**(1): 286-301.DOI: https://doi.org/10.1111/jam.12516.

Doyle, R. J. (2000). "Contribution of the hydrophobic effect to microbial infection." Microbes and infection **2**(4): 391-400.DOI: 10.1016/s1286-4579(00)00328-2.

Du, Z., Deng, S., Bei, Y., Huang, Q., Wang, B., Huang, J. and Yu, G. (2014). "Adsorption behavior and mechanism of perfluorinated compounds on various adsorbents--a review." J Hazard Mater **274**: 443-454.DOI: 10.1016/j.jhazmat.2014.04.038.

Smith, E.J., Hamilton-Taylor W.J.D. (2002). "Methods for preparing synthetic freshwaters." Water Res **36**: 1286-1296.

Elieh-Ali-Komi, D. and Hamblin, M. (2016). "Chitin and Chitosan: Production and Application of Versatile Biomedical Nanomaterials." Int J Adv Res **4**(3): 411-427PMC5094803.

EPA (2019). EPA's PFAS Action Plan.

EPA (2022). EPA Announces New Drinking Water Health Advisories for PFAS Chemicals, $1 Billion in Bipartisan Infrastructure Law Funding to Strengthen Health Protections, EPA Office of Water.

Erkhan, H. S. and Engin, G. O. (2019). "Performance and activated sludge characteristics at short solid retention time in a submerged MBR: effects of C/N ratio of wastewater." Environ Technol **40**(16): 2085-2092.DOI: 10.1080/09593330.2018.1437223.

Espartero, L. J. L., Yamada, M., Ford, J., Owens, G., Prow, T. and Juhasz, A. (2022). "Health-related toxicity of emerging per- and polyfluoroalkyl substances: Comparison to legacy PFOS and PFOA." Env Res **212**: 113431.DOI: https://doi.org/10.1016/j.envres.2022.113431.

Fan, X., Li, H.-q., Yang, P. and Lai, B. (2015). "Effect of C/N ratio and aeration rate on performance of internal cycle MBR with synthetic wastewater." Desalination and Water Treat **54**(3).DOI: https://doi.org/10.1080/19443994.2014.884942.

Feneley, R. C. L., Hopley, I. B. and Wells, P. N. T. (2015). "Urinary Catheters: History, Current Status, Adverse Events and Research Agenda." J Med Eng Technol **39**: 459-470.DOI: https://doi.org/10.3109/03091902.2015.1085600.

Finelli, A., Gallant, C. V., Jarvi, K. and Burrows, L. L. (2003). "Use of in-biofilm expression technology to identify genes involved in Pseudomonas aeruginosa biofilm development." J Bacteriol **185**(9): 2700-2710.DOI: 10.1128/JB.185.9.2700-2710.2003.

Flemming, H. C. (2020). "Biofouling and me: My Stockholm syndrome with biofilms." Water Res **173**.DOI: 10.1016/j.watres.2020.115576.

Flemming, H. C. and Wingender, J. (2010). "The biofilm matrix." Nat Rev Microbiol **8**(9): 623-633.DOI: 10.1038/nrmicro2415.

Floyd, K. A., Eberly, A. R. and Hadjifrangiskou, M. (2017). 3 - Adhesion of bacteria to surfaces and biofilm formation on medical devices. Biofilms and Implantable Medical Devices. Y. Deng and W. Lv, Woodhead Publishing**:** 47-95.

Fong, J. N. C. and Yildiz, F. H. (2015). "Biofilm Matrix Proteins." Microbiol Spectr **3**(2).DOI: 10.1128/microbiolspec.MB-0004-2014.

Forbis-Stokes, A. A., Rocha-Melogno, L. and Deshusses, M. A. "Nitrifying trickling filters and denitrifying bioreactors for nitrogen management of high-strength anaerobic digestion effluent." Chemosphere **204**: 119-129.DOI: https://doi.org/10.1016/j.chemosphere.2018.03.137.

Fountoulakis, M., Juranville, J.-F. and Manneberg, M. (1992). "Comparison of the Coomassie brilliant blue, bicinchoninic acid and Lowry quantitation assays, using non-glycosylated and glycosylated proteins." J Biochem Biophys Meth **24**(3): 265-274.DOI: https://doi.org/10.1016/0165-022X(94)90078-7.

Fu, L., Cui, X., Li, Y., Xu, L., Zhang, C., Xiong, R., Zhou, D. and Crittenden, J. C. (2017). "Excessive phosphorus enhances Chlorella regularis lipid production under nitrogen starvation stress during glucose heterotrophic cultivation." Chem Eng J **330**: 566-572.DOI: https://doi.org/10.1016/j.cej.2017.07.182.

Gad, G. F., El-Feky, M. A., El-Rehewy, M. S., Hassan, M. A., Abolella, H. and El-Baky, R. M. (2009). "Detection of i*caA, icaD* genes and biofilm production by *Staphylococcus aureus* and *Staphylococcus epidermidis* isolated from urinary tract catheterized patients." J Infect Dev Ctries **3**(5): 342-351.

Gagliano, E., Sgroi, M., Falciglia, P. P., Vagliasindi, F. G. A. and Roccaro, P. (2020). "Removal of poly- and perfluoroalkyl substances (PFAS) from water by adsorption: Role of PFAS chain length, effect of organic matter and challenges in adsorbent regeneration." Water Res **171**: 115381.DOI: 10.1016/j.watres.2019.115381.

Gedalanga, P. B., Pornwongthong, P., Mora, R., Chiang, S.-Y. D., Baldwin, B., Ogles, D. and Mahendra, S. (2014). "Identification of Biomarker Genes to Predict Biodegradation of 1,4-Dioxane." Appl Environ Microbiol **80**: 3209-3218.DOI: https://doi.org/10.1128/AEM.04162-13.

Gobelius, L., Hedlund, J., Durig, W., Troger, R., Lilja, K., Wiberg, K. and Ahrens, L. (2018). "Per- and Polyfluoroalkyl Substances in Swedish Groundwater and Surface Water: Implications for Environmental Quality Standards and Drinking Water Guidelines." Environ Sci Technol **52**(7): 4340-4349.DOI: 10.1021/acs.est.7b05718.

Gomila, A., Carratalà, J., Eliakim-Raz, N., Shaw, E., Tebé, C., Wolkewitz, M., Wiegand, I., Grier, S., Vank, C., Cuperus, N., Van den Heuvel, L., Vuong, C., MacGowan, A., Leibovici, L., Addy, I., Pujol, M., on behalf of, R. S. G. and Study, S. (2019). "Clinical outcomes of hospitalised patients with catheter-associated urinary tract infection in countries with a high rate of multidrug-resistance: the COMBACTE-MAGNET RESCUING study." Antimicrobial Resistance & Infection Control **8**(1): 198.DOI: 10.1186/s13756-019-0656-6.

Gong, Y., Wang, L., Liu, J., Tang, J. and Zhao, D. (2016). "Removal of aqueous perfluorooctanoic acid (PFOA) using starch-stabilized magnetite nanoparticles." Sci Total Environ **562**: 191-200.DOI: 10.1016/j.scitotenv.2016.03.100.

Goodwin, D. J., Picout, D. R., Ross-Murphy, S. B., Holland, S. J., Martini, L. G. and Lawrence, M. J. (2011). "Ultrasonic degradation for molecular weight reduction of pharmaceutical cellulose ethers." Carbohydr Polym **83**(2): 843-851.DOI: 10.1016/j.carbpol.2010.08.068.

Gregory, J. (2006). Particles in Water: Properties and Processes. England, CRC Press Taylor & Francis Group, LLC.

Griffis, T. J., Chen, Z., Baker, J. M., Wood, J. D., Millet, D. B., Lee, X., Venterea, R. T. and Turner, P. A. (2017). "Nitrous oxide emissions are enhanced in a warmer and wetter world." **114**(45): 12081-12085.DOI: doi: 10.1073/pnas.1704552114.

Gule, N. P., Begum, N. M. and Klumperman, B. (2015). "Advances in biofouling mitigation: A review." Crit Rev Environ Sci Technol **46**(6): 535-555.DOI: 10.1080/10643389.2015.1114444.

Haghighi, F., Mohammadi Sh, R., Mohammadi, P., Eskandari, M. and Hosseinkhani, S. (2012). "The evaluation of *Candida albicans* biofilms formation on silicone catheter, PVC and glass coated with titanium dioxide nanoparticles by XTT method and ATPase assay." Bratisl Lek Listy **113**(12): 707-711.DOI: 10.4149/bll_2012_160.

Haldar, K. and Chakraborty, S. (2019). "Investigation of chemical reaction during sodium alginate drop impact on calcium chloride film." Phys Fluids **31**(7).DOI: 10.1063/1.5100243.

Hamdaoui, O., Naffrechoux, E., Suptil, J. and Fachinger, C. (2005). "Ultrasonic desorption of p-chlorophenol from granular activated carbon." Chem Eng J **106**(2): 153-161.DOI: 10.1016/j.cej.2004.10.010.

Hamdaoui, O., Naffrechoux, E., Tifouti, L. and Petrier, C. (2003). "Effects of ultrasound on adsorption-desorption of p-chlorophenol on granular activated carbon." Ultrason Sonochem **10**(2): 109-114.

Hatch, R. A. and Schiller, N. L. (1998). "Alginate Lyase Promotes Diffusion of Aminoglycosides through the Extracellular Polysaccharide of Mucoid *Pseudomonas aeruginosa*." Antimicrob Agents Chemother **42**(4): 974-977.DOI: 10.1128/aac.42.4.974.

Hatton, J., Holton, C. and DiGuiseppi, B. (2018). "Occurrence and behavior of per- and polyfluoroalkyl substances from aqueous film-forming foam in groundwater systems." Remed J **28**(2): 89-99.DOI: 10.1002/rem.21552.

Heck, K. N., Wang, Y., Wu, G., Wang, F., Tsai, A.-L., Adamson, D. T. and Wong, M. S. (2019). "Effectiveness of metal oxide catalysts for the degradation of 1,4-dioxane." RSC Adv **9**(46): 27042-27049.DOI: 10.1039/c9ra05007h.

Heffernan, B., Murphy, C. D. and Casey, E. (2009). "Comparison of Planktonic and Biofilm Cultures of *Pseudomonas fluorescens* DSM 8341 Cells Grown on Fluoroacetate." Appl Environ Microbiol **75**(9): 2899-2907.DOI: 10.1128/aem.01530-08.

Hekster, F. M., Laane, R. W. P. M. and Voogt, P. d. (2003). "Environmental and Toxicity Effects of Perfluoroalkylated Substances." Rev Environ Contam Toxicol **179**: 99-121.DOI: https://doi.org/10.1007/0-387-21731-2_4.

Herten, M., Bisdas, T., Knaack, D., Becker, K., Osada, N., Torsello, G. B. and Idelevich, E. A. (2017). "Rapid in Vitro Quantification of S. Aureus Biofilms on Vascular Graft Surfaces." Front Microbiol **8**. 2333DOI: https://doi.org/10.3389/fmicb.2017.02333.

Héry-Arnaud, G., Nowak, E., Caillon, J., David, V., Dirou, A., Revert, K., Munck, M. R., Frachon, I., Haloun, A., Horeau-Langlard, D., Le Bihan, J., Danner-Boucher, I., Ramel, S., Pelletier, M. P., Rosec, S., Gouriou, S., Poulhazan, E., Payan, C., Férec, C., Rault, G., Le Gal, G.

and Le Berre, R. (2017). "Evaluation of quantitative PCR for early diagnosis of *Pseudomonas aeruginosa* infection in cystic fibrosis: a prospective cohort study." Clinical Microbiology and Infection **23**(3): 203-207.DOI: https://doi.org/10.1016/j.cmi.2016.11.016.

Hong, P.-N., Matsuura, N., Noguchi, M., Yamamoto-Ikemoto, R. and Honda, R. (2022). "Change of extracellular polymeric substances and microbial community in biofouling mitigation by continuous vanillin dose in membrane bioreactor." J Water Process Eng **47**.DOI: https://doi.org/10.1016/j.jwpe.2022.102644.

Hong, P.-N., Noguchi, M., Matsuura, N. and Honda, R. (2019). "Mechanism of biofouling enhancement in a membrane bioreactor under constant trans-membrane pressure operation." J Membr Sci **592**.DOI: https://doi.org/10.1016/j.memsci.2019.117391.

Hong, P.-N., Taing, C., Phan, P.-T. and Honda, R. (2018). "Polarity-Molecular Weight Profile of Extracellular Polymeric Substances in a Membrane Bioreactor: Comparison between Bulk Sludge and Cake Layers." J Water Environ Technol **16**.DOI: https://doi.org/10.2965/jwet.17-020.

Hossain, M. D., Ngo, H. H. and Guo, W. (2013). "Introductory of Microsoft Excel SOLVER Function- Spreadsheet Method for Isotherm and Kinetics Modelling of Metals Biosorption in Water and Wastewater." JWS **3**: 223-237.

Hossein, M., Chande, O., Ngassapa, F. and Eunice, M. (2022). Exposure to 1,4-dioxane and disinfection by-products due to the reuse of wastewater. Emerging Contaminants in the Environment**:** 87-109.

Houde, M., Martine, J. W., Letcher, R. J., .Solomon, K. R. and Muir, D. C. G. (2006). "Biological Monitoring of Polyfluoroalkyl Substances: A Review." Environ. Sci. Technol. **40**(11): 3463-3473.

Hu, P., Raub, C. B., Choy, J. S. and Luo, X. (2020). "Modulating the properties of flow-assembled chitosan membranes in microfluidics with glutaraldehyde crosslinking." J Mater Chem B **8**(12): 2519-2529.DOI: 10.1039/c9tb02527h.

ITRC. (2021). "1,4-Dioxane Regulatory Framework." 2022, from https://14d-1.itrcweb.org/wp-content/uploads/2021/02/14d_regulatory_framework_021621.pdf.

Jackson, K. D., Starkey, M., Kremer, S., Parsek, M. R. and Wozniak, D. J. (2004). "Identification of *psl*, a Locus Encoding a Potential Exopolysaccharide That Is Essential for *Pseudomonas aeruginosa* PAO1 Biofilm Formation." Journal of Bacteriology **186**(14): 4466-4475.DOI: 10.1128/jb.186.14.4466-4475.2004.

Jamal, M., Ahmad, W., Andleeb, S., Jalil, F., Imran, M., Nawaz, M. A., Hussain, T., Ali, M., Rafiq, M. and Kamil, M. A. (2018). "Bacterial biofilm and associated infections." J Chin Med Assoc **81**(1): 7-11.DOI: 10.1016/j.jcma.2017.07.012.

Johnson, N. W., Gedalanga, P. B., Zhao, L., Gu, B. and Mahendra, S. (2020). "Cometabolic biotransformation of 1,4-dioxane in mixtures with hexavalent chromium using attached and planktonic bacteria." Sci Total Environ **706**. 135734. DOI: 10.1016/j.scitotenv.2019.135734.

Jones, E. R., van Vliet, M. T. H., Qadir, M. and Bierkens, M. F. (2021). "Country-level and gridded estimates of wastewater production, collection, treatment and reuse." Earth Syst Sci Data **13**: 237-254.DOI: https://doi.org/10.5194/essd-13-237-2021.

Jorge de Souza, T. A., Rosa Souza, L. R. and Franchi, L. P. (2019). "Silver nanoparticles: An integrated view of green synthesis methods, transformation in the environment, and toxicity." Ecotoxicol Environ Saf **171**: 691-700.DOI: 10.1016/j.ecoenv.2018.12.095.

Joshi, R. V., Gunawan, C. and Mann, R. (2021). "We Are One: Multispecies Metabolism of a Biofilm Consortium and Their Treatment Strategies." Front Microbiol **12**. 635432. DOI: 10.3389/fmicb.2021.635432.

Kapoor, R. and Yadav, J. S. (2010). "Development of a rapid ATP bioluminescence assay for biocidal susceptibility testing of rapidly growing *Mycobacteria*." J Clin Microbiol **48**(10): 3725-3728.DOI: 10.1128/jcm.01482-10.

Karlapudi, A. P., Venkateswarulu, T. c., Tammineedi, J., Kanaumri, L., Ravuru, K., Dirisala, V. r. and Kodali, V. P. (2018). "Role of biosurfactants in bioremediation of oil pollution-a review." Petroleum **4**(3): 241-249.DOI: https://doi.org/10.1016/j.petlm.2018.03.007.

Karygianni, L., Ren, Z., Koo, H. and Thurnheer, T. (2020). "Biofilm Matrixome: Extracellular Components in Structured Microbial Communities." Trends Microbiol **28**(8): 668-681.DOI: https://doi.org/10.1016/j.tim.2020.03.016.

Kawaguchi, T., Chen, Y. P., Norman, R. S. and Decho, A. W. (2008). "Rapid Screening of Quorum-Sensing Signal N-Acyl Homoserine Lactones by an In Vitro Cell-Free Assay." Appl Environ Microbiol **74**(12). 3667-3671. DOI: https://doi.org/10.1128/AEM.02869-07.

Kesaano, M. and Sims, R. C. (2014). "Algal biofilm based technology for wastewater treatment." Algal Res **5**: 231-240.DOI: https://doi.org/10.1016/j.algal.2014.02.003.

Khouri, J., Penlidis, A. and Moresoli, C. (2019). "Viscoelastic Properties of Crosslinked Chitosan Films." Processes **7**(3).157. DOI: https://doi.org/10.3390/pr7030157.

Kilcoyne, M., Gerlach, J. Q., Farrell, M. P., Bhavanandan, V. P. and Joshi, L. (2011). "Periodic acid-Schiff's reagent assay for carbohydrates in a microtiter plate format." Anal Biochem **416**(1): 18-26.DOI: 10.1016/j.ab.2011.05.006.

Kildeeva, N. R., Perminov, P. A., Vladimirov, L. V., Novikov, V. V. and Mikhailov, S. N. (2009). "About mechanism of chitosan cross-linking with glutaraldehyde." Russ J Bioorg Chem **35**(3): 360-369. DOI: 10.1134/s106816200903011x.

Kim, H., Kim, J. and Ahn, D. (2021). "Effects of carbon to nitrogen ratio on the performance and stability of aerobic granular sludge." Environ Eng Res **26**(1).DOI: https://doi.org/10.4491/eer.2019.284.

Kim, Y.-J., Choi, Y.-J. and Hwang, S.-J. (2021). "Effects of F/M ratio on the EPS production and fouling at MBR." J Korean Soc Water Wastewater **35**(3): 197-204.DOI: https://doi.org/10.11001/jksww.2021.35.3.197.

Knobel, L. L., Bartholomay, R. C., Cecil, L. D., Tucker, B. J. and Wegner, S. J. (1989). Chemical Constituents in the Dissolved and Suspended Fractions of Groundwater from Selected Sites, Idaho Natonal Engineering Laboratory and Vicinity. Idaho, U.S. Geological Survey in cooperation with the U.S. Department of Energy.

Kothawala, D. N., Kohler, S. J., Ostlund, A., Wiberg, K. and Ahrens, L. (2017). "Influence of dissolved organic matter concentration and composition on the removal efficiency of perfluoroalkyl substances (PFASs) during drinking water treatment." Water Res **121**: 320-328.DOI: 10.1016/j.watres.2017.05.047.

Kralik, P. and Ricchi, M. (2017). "A Basic Guide to Real Time PCR in Microbial Diagnostics: Definitions, Parameters, and Everything." Frontiers in Microbiology **8**.108. DOI: 10.3389/fmicb.2017.00108.

Krohn-Molt, I., Wemheuer, B., Alawi, M., Poehlein, A., Gullert, S., Schmeisser, C., Pommerening-Roser, A., Grundhoff, A., Daniel, R., Hanelt, D. and Streit, W. R. (2013). "Metagenome Survey of a Multispecies and Alga-Associated Biofilm Revealed Key Elements of Bacterial-Algal Interactions in Photobioreactors." Appl Environ Microbiol **79**(20). 6196-6206. DOI: https://doi.org/10.1128/AEM.01641-13.

Kwiatkowski, C. F., Andrews, D. Q., Birnbaum, L. S., Bruton, T. A., DeWitt, J. C., Knappe, D. R. U., Maffini, M. V., Miller, M. F., Pelch, K. E., Reade, A., Soehl, A., Trier, X., Venier, M., Wagner, C. C., Wang, Z. and Blum, A. (2020). "Scientific Basis for Managing PFAS as a Chemical Class." Environmental Science & Technology Letters **7**(8): 532-543.DOI: 10.1021/acs.estlett.0c00255.

Kwiatkowski, C. F., Andrews, D. Q., Birnbaum, L. S., Bruton, T. A., DeWitt, J. C., Knappe, D. R. U., Maffini, M. V., Miller, M. F., Pelch, K. E., Reade, A., Soehl, A., Trier, X., Venier, M., Wagner, C. C., Wang, Z. and Blum, A. (2020). "Scientific Basis for Managing PFAS as a Chemical Class." Environ Sci Technol Lett **7**(8): 532-543.DOI: 10.1021/acs.estlett.0c00255.

Kwok, W. K., Picioreanu, C., Ong, S. L., Loosdrecht, M. C. C. v., Ng, W. J. and Heijnen, J. J. (1998). "Influence of Biomass Production and Detachment Forces on Biofilm Structures in a Biofilm Airlift Suspension Reactor." Biotechnol and Bioeng **58**(4). 400-407. DOI: https://doi.org/10.1002/(SICI)1097-0290(19980520)58:4

Lau, C., Anitole, K., Hodes, C., Lai, D., Pfahles-Hutchens, A. and Seed, J. (2007). "Perfluoroalkyl Acids: A Review of Monitoring and Toxicological Findings." Toxicol Sci **99**(2): 366-394.DOI: https://doi.org/10.1093/toxsci/kfm128.

Lee, D., Zhang, H. and Ryu, S. (2018). Elastic Modulus Measurement of Hydrogels, Springer, Cham.

Leyva-Ramos, R., Jacobo-Azuara, A., Diaz-Flores, P. E., Guerrero-Coronado, R. M., Mendoza-Barron, J. and Berber-Mendoza, M. S. (2008). "Adsorption of chromium(VI) from an aqueous solution on a surfactant-modified zeolite." Colloids Surf, A Physicochem Eng Asp **330**(1): 35-41.DOI: 10.1016/j.colsurfa.2008.07.025.

Li, A.-j., Li, X.-y. and Yu, H.-q. (2011). "Effect of the food-to-microorganism (F/M) ratio on the formation and size of aerobic sludge granules." Process Biochem **46**(12): 2269-2276.DOI: https://doi.org/10.1016/j.procbio.2011.09.007.

Li, X., Lenhart, J. J. and Walker, H. W. (2012). "Aggregation Kinetics and Dissolution of Coated Silver Nanoparticles." Langmuir: 1095-1104.DOI: 10.1021/la202328n.

Li, Y., Qin, T., Ingle, T., Yan, J., He, W., Yin, J. J. and Chen, T. (2017). "Differential genotoxicity mechanisms of silver nanoparticles and silver ions." Arch Toxicol **91**(1): 509-519.DOI: 10.1007/s00204-016-1730-y.

Lim, J.-L. and Okada, M. (2005). "Regeneration of granular activated carbon using ultrasound." Ultrason Sonochem **12**(4): 277-282.DOI: 10.1016/j.ultsonch.2004.02.003.

Lim, S.-H. and Hudson, S. M. (2004). "Synthesis of antimicrobial activity of a water-soluble chitosan derivative with a fiber-reactive group." Carbohydr Res **339**: 313-319.DOI: https://doi.org/10.1016/j.carres.2003.10.024.

Lin, M.-F., Lin, Y.-Y. and Lan, C.-Y. (2019). "A method to assess influence of different medical tubing on biofilm formation by *Acinetobacter baumannii*." Journal of Microbiological Methods **160**: 84-86.DOI: https://doi.org/10.1016/j.mimet.2019.03.023.

Liu, C., Hatton, J., Arnold, W. A., Simcik, M. F. and Pennell, K. D. (2020). "In Situ Sequestration of Perfluoroalkyl Substances Using Polymer-Stabilized Powdered Activated Carbon." Environ Sci Technol **54**(11): 6929-6936.DOI: 10.1021/acs.est.0c00155.

Liu, M. Y., Tsang, D. C. W., Hu, J., Ng, K. T. W., Liu, T. and Lo, I. M. C. (2008). "Adsorption of Methylene Blue and Phenol by Wood Waste
Derived Activated Carbon." J Environ Eng **134**(5): 338-345.DOI: 10.1061//ASCE/0733-9372/2008/134:5/338.

Liu, N., Wu, C., Lyu, G. and Li, M. (2021). "Efficient adsorptive removal of short-chain perfluoroalkyl acids using reed straw-derived biochar (RESCA)." Sci Total Environ **798**: 149191.DOI: 10.1016/j.scitotenv.2021.149191.

Liu, S., Gunawan, C., Barraud, N., Rice, S. A., Harry, E. J. and Amal, R. (2016). "Understanding, Monitoring, and Controlling Biofilm Growth in Drinking Water Distribution Systems." Environ Sci Technol **50**(17): 8954-8976.DOI: https://doi.org/10.1021/acs.est.6b00835.

Liu, Y., Johnson, N. W., Liu, C., Chen, R., Zhong, M., Dong, Y. and Mahendra, S. (2019). "Mechanisms of 1,4-dioxane biodegradation and adsorption by bio-zeolite in the presence of chlorinated solvents: experimental and molecular dynamics simulation studies." Environ Sci Technol **53**(24): 14538-14547.DOI: 10.1021/acs.est.9b04154.

Lobo da Costa Lima, J., Rodriguez Alves, L., Luna de Araujo, P. R., Pacifico Bezerra Neto, J. J., Vieira Maciel, M. A. and Camargo de Morais, M. M. (2018). "Biofilm production by clinical isolates of Pseudomonas aeruginosa and structural changes in LasR protein of isolates non biofilm-producing." Braz J Infect Dis **22**: 129-136.DOI: 10.1016/j.bjid.2018.03.003.

López Pérez, D., Baker, P. J., Pintar, A. L., Sun, J., Lin, N. J. and Lin-Gibson, S. (2017). "Experimental and statistical methods to evaluate antibacterial activity of a quaternary pyridinium salt on planktonic, biofilm-forming, and biofilm states." Biofouling **33**(3): 222-234.DOI: 10.1080/08927014.2017.1286476.

Lu, J. and Wang, S. (2010). "Ultrasonic Regeneration of Granular Activated Carbon Used in Water Treatment." **4th International Conference on Bioinformatics and Biomedical Engineering**: 1-3.DOI: 978-1-4244-4713-8/10/$25.00.

Luo, J., Lv, P., Zhang, J., Fane, A. G., McDougald, D. and Rice, S. A. (2017). "Succession of biofilm communities responsible for biofouling of membrane bio-reactors (MBRs)." PLOS One **12**(7).DOI: https://doi.org/10.1371/journal.pone.0179855.

Ly, Q. V., Ngheim, L. D., Cho, J., Maqbool, T. and Hur, J. (2019). "Organic carbon source-dependent properties of soluble microbial products in sequencing batch reactors and its effects on membrane fouling." J Environ Manage **244**: 40-47.DOI: https://doi.org/10.1016/j.jenvman.2019.05.045.

Maan, A. M. C., Hofman, A. H., Vos, W. M. and Kamperman, M. (2020). "Recent Developments and Practical Feasibility of Polymer-Based Antifouling Coatings." Advanced Functional Materials **30**(32).DOI: 10.1002/adfm.202000936.

Magin, C. M., Cooper, S. P. and Brennan, A. B. (2010). "Non-toxic antifouling strategies." Mater Today **13**(4): 36-44.DOI: https://doi.org/10.1016/S1369-7021(10)70058-4.

Mahendra, S. and Alvarez-Cohen, L. (2006). "Kinetics of 1,4-dioxane biodegradation by monooxygenase-expressing bacteria." Environ Sci Technol **40**: 5435-5442.DOI: https://doi.org/10.1021/es060714v.

Mahendra, S., Grostern, A. and Alvarez-Cohen, L. (2013). "The impact of chlorinated solvent co-contaminants on the biodegradation kinetics of 1,4-dioxane." Chemosphere **91**(1): 88-92.DOI: 10.1016/j.chemosphere.2012.10.104.

Mahendra, S., Petzold, C. J., Baidoo, E. E., Keasling, J. D. and Alvarez-Cohen, L. (2007). "Identification of the intermediates of in vivo oxidation of 1,4-dioxane by monooxygenase-containing Bacteria." Environ Sci Technol **41**: 7330-7336.DOI: https://doi.org/10.1021/es0705745.

Maimaiti, A., Deng, S., Meng, P., Wang, W., Wang, B., Huang, J., Wang, Y. and Yu, G. (2018). "Competitive adsorption of perfluoroalkyl substances on anion exchange resins in simulated AFFF-impacted groundwater." Chem Eng J **348**: 494-502.DOI: 10.1016/j.cej.2018.05.006.

Malesevic, M., Di Lorenzo, F., Filipic, B., Stanisavljevic, N., Novovic, K., Senerovic, L., Polovic, N., Molinaro, A., Kojic, M. and Jovcic, B. (2019). "Pseudomonas aeruginosa quorum sensing inhibition by clinical isolate Delftia tsuruhatensis 11304: involvement of N-octadecanoylhomoserine lactones." Sci Rep **9**(1): 16465.DOI: 10.1038/s41598-019-52955-3.

Mandakhalikar, K. D., Rahmat, J. N., Chiong, E., Neoh, K. G., Shen, L. and Tambyah, P. A. (2018). "Extraction and quantification of biofilm bacteria: Method optimized for urinary catheters." Scientific Reports **8**(1): 8069.DOI: 10.1038/s41598-018-26342-3.

Mandakhalikar, K. D., Rahmat, J. N., Chiong, E., Neoh, K. G., Shen, L. and Tambyah, P. A. (2018). "Extraction and Quantification of Biofilm Bacteria: Method Optimized for Urinary Catheters." Sci Rep **8**.DOI: https://doi.org/10.1038/s41598-018-26342-3.

Mangwani, N., Kumari, S. and Das, S. (2015). "Involvement of quorum sensing genes in biofilm development and degradation of polycyclic aromatic hydrocarbons by a marine bacterium Pseudomonas aeruginosa N6P6." Appl Microbiol Biotechnol **99**: 10283-10297.DOI: https://doi.org/10.1007/s00253-015-6868-7.

Marchant, R. and Banat, I. M. (2012). "Microbial biosurfactants: challenges and opportunities for future exploitation." Trends Biotechnol **30**(11): 558-565.DOI: https://doi.org/10.1016/j.tibtech.2012.07.003.

Masuko, T., Minami, A., Iwasaki, N., Majima, T., Nishimura, S.-I. and Lee, Y. C. (2005). "Carbohydrate analysis by a phenol–sulfuric acid method in microplate format." Analytical Biochemistry **339**(1): 69-72.DOI: https://doi.org/10.1016/j.ab.2004.12.001.

McElroy, A. C., Hyman, M. R. and Knappe, D. R. U. (2019). "1,4-Dioxane in drinking water: emerging for 40 years and still unregulated." Curr Opin Environ Sci Health **7**: 117-125.DOI: 10.1016/j.coesh.2019.01.003.

Mekkawy, A. I., El-Mokhtar, M. A., El-Shanawany, S. M. and Ibrahim, E. H. (2018). "Silver Nanoparticle-loaded Hydrogels, A Potential Treatment for Resistant Bacterial Infection and Wound Healing: A Review." Br J Pharm Res **14**(2): 1-19.DOI: 10.9734/BJPR/2016/30525.

Mempin, R., Tran, H., Chen, C., Gong, H., Kim Ho, K. and Lu, S. (2013). "Release of extracellular ATP by bacteria during growth." BMC Microbiology **13**(1): 301.DOI: 10.1186/1471-2180-13-301.

Meng, F., Zhang, S., Oh, Y., Zhou, Z., Shin, H.-S. and Chae, S.-R. (2017). "Fouling in membrane bioreactors: An updated review." Water Res **114**: 151-180.DOI: https://doi.org/10.1016/j.watres.2017.02.006.

Meonteiro Jr., O. A. C. and Airoldi, C. (1999). "Some studies of crosslinking chitosan-glutaraldehyde interaction in a homogenous system." Int J Biol Macromol **26**(2-3): 119-128.DOI: https://doi.org/10.1016/S0141-8130(99)00068-9.

Merino, N., Qu, Y., Deeb, R. A., Hawley, E. L., Hoffmann, M. R. and Mahendra, S. (2016). "Degradation and Removal Methods for Perfluoroalkyl and Polyfluoroalkyl Substances in Water." Environ Eng Sci **33**(9): 615-649.DOI: 10.1089/ees.2016.0233.

Miqueleto, A. P., Dolosic, C. C., Pozzi, E., Foresti, E. and Zaiat, M. (2010). "Influence of carbon sources and C/N ratio on EPS production in anaerobic sequencing batch biofilm reactors for wastewater treatment." Bioresour Technol **101**(4).DOI: https://doi.org/10.1016/j.biortech.2009.09.026.

Mittal, R., Aggarwal, S., Sharma, S., Chhibber, S. and Harjai, K. (2009). "Urinary tract infections caused by Pseudomonas aeruginosa: A minireview." Journal of Infection and Public Health **2**(3): 101-111.DOI: https://doi.org/10.1016/j.jiph.2009.08.003.

Mohanbaba, S. and Gurunathan, S. (2016). Differential biological activities of silver nanoparticles against Gram-negative and Gram-positive bacteria. Nanobiomaterials in Antimicrobial Therapy**:** 193-227. DOI: https://doi.org/10.1016/B978-0-323-42864-4.00006-3

Mohod, A. V. and Gogate, P. R. (2011). "Ultrasonic degradation of polymers: effect of operating parameters and intensification using additives for carboxymethyl cellulose (CMC) and polyvinyl alcohol (PVA)." Ultrason Sonochem **18**(3): 727-734.DOI: 10.1016/j.ultsonch.2010.11.002.

Mohr, T., DiGuiseppi, W., Anderson, J. K., Hatton, J., Bishop, J., Selcoe, B. and Kappleman, W. (2020). Environmental Investigation and Remediation. Boca Raton, CRC Press.

Monsigny, M., Petit, C. and Roche, A.-C. (1988). "Colorimetric determination of neutral sugars by a resorcinol sulfuric acid micromethod." Analytical Biochemistry **175**(2): 525-530.DOI: https://doi.org/10.1016/0003-2697(88)90578-7.

Mpongwana, N. (2022). "Exploiting Biofilm Characteristics to Enhance Biological Nutrient Removal in Wastewater Treatment Plants." Appl Sci **12**(15).DOI: https://doi.org/10.3390/app12157561.

Mukherjee, S. (2019). "Bacterial quorum sensing in complex and dynamically changing environments." Nat Rev Microbiol **17**: 371-382.DOI: https://doi.org/10.1038/s41579-019-0186-5.

Muller, M. (2018). "Bacterial Silver Resistance Gained by Cooperative Interspecies Redox Behavior." Antimicrob Agents Chemother **62**(8): e00672-00618.DOI: https://doi.org/10.1128/AAC.00672-18.

Munoz-Pinto, D. J., Grigoryan, B., Long, J., Grunlan, M. and Hahn, M. S. (2012). "J Biomed Mater Res A." 2855-2860.DOI: https://doi.org/10.1002/jbm.a.34289.

Mwangi, I. W., Ngila, J. C. and Ndungu, P. (2012). "A new spectrophotometric method for determination of residual polydiallyldimethylammonium chloride flocculant in treated water based on a diazotization-coupled ion pair." Water SA **38**(5). 707-714. DOI: 10.4314/wsa.v38i5.8.

Mwangi, I. W., Ngila, J. C., Ndungu, P. and Msagati, T. A. M. (2013). "Method Development for the Determination of Diallyldimethylammonium Chloride at Trace Levels by Epoxidation Process." Water Air Soil Pollut **224**: 1638.DOI: 10.1007/s11270-013-1638-6.

Myers, M. A., Johnson, N. W., Marin, E. Z., Pornwongthong, P., Liu, Y., Gedalanga, P. B. and Mahendra, S. (2018). "Abiotic and bioaugmented granular activated carbon for the treatment of 1,4-dioxane-contaminated water." Environ Pollut **240**: 916-924.DOI: 10.1016/j.envpol.2018.04.011.

Nagler, M., Insam, H., Pietramellara, G. and Ascher-Jenull, J. (2018). "Extracellular DNA in natural environments: features, relevance and applications." Appl Microbiol Biotechnol **102**(15): 6343-6356.DOI: 10.1007/s00253-018-9120-4.

Nguyen, L. N., Truong, M. V., Nguyen, A. Q., Johir, M. A. H., Commault, A. S., Ralph, P. J., Semblante, G. U. and Ngheim, L. D. (2020). "A sequential membrane bioreactor followed by a membrane microalgal reactor for nutrient removal and algal biomass production." Environ Sci Water Res Technol **6**: 189-196.DOI: 10.1039/C9EW00851A

Noble, J. E. and Bailey, M. J. A. (2009). Chapter 8 Quantitation of Protein. Methods in Enzymology. R. R. Burgess and M. P. Deutscher, Academic Press. **463:** 73-95.

Nuñes, K. G. P., L. W. Sfreddo, Rosset, M. and L. A. Feris (2020). "Efficiency evaluation of thermal, ultrasound and solvent techniques in activated carbon regeneration." Environ Technol: 1-12.DOI: 10.1080/09593330.2020.1746839.

O'Toole, G. A. (2011). "Microtiter dish biofilm formation assay." Journal of visualized experiments(47): 2437.DOI: 10.3791/2437.

Ochbaum, G., Chetrit, E., Berkovich, R. and Bitton, R. (2020). "Effect of the C-terminal amino acid of the peptide on the structure and mechanical properties of alginate-peptide hydrogels across length-scales." Soft Matter **16**(26): 6155-6162.DOI: 10.1039/d0sm00329h.
Ochoa-Herrera, V. and Sierra-Alvarez, R. (2008). "Removal of perfluorinated surfactants by sorption onto granular activated carbon, zeolite and sludge." Chemosphere **72**(10): 1588-1593.DOI: 10.1016/j.chemosphere.2008.04.029.

Okshevsky, M. and Meyer, R. L. (2015). "The role of extracellular DNA in the establishment, maintenance and perpetuation of bacterial biofilms." Crit Rev Microbiol **41**(3): 341-352.DOI: 10.3109/1040841X.2013.841639.

Okshevsky, M., Regina, V. R. and Meyer, R. L. (2015). "Extracellular DNA as a target for biofilm control." Curr. Opin. Biotechnol. **33**: 73-80.DOI: https://doi.org/10.1016/j.copbio.2014.12.002.

Ou, A. and Bo, I. (2017). "Chitosan Hydrogels and their Glutaraldehyde-Crosslinked Counterparts as Potential Drug Release and Tissue Engineering Systems- Synthesis, Characterization, Swelling Kinetics and Mechanics." J Phys Chem Biophys **7**(3): 1-9.DOI: 10.4172/2161-0398.1000256.

Pal, S., Tak, Y. K. and Song, J. M. (2007). "Does the antibacterial activity of silver nanoparticles depend on the shape of the nanoparticle? A study of the Gram-negative bacterium Escherichia coli." Appl Environ Microbiol **73**(6): 1712-1720.DOI: 10.1128/AEM.02218-06.

Pamp, S. J. and Tolker-Nielsen, T. (2007). "Multiple Roles of Biosurfactants in Structural Biofilm Development by *Pseudomonas aeruginosa*." J Bacteriol **189**(6). 2531-2539. DOI: https://doi.org/10.1128/JB.01515-06.

Panchavinin, S., Tobino, T., Hara-Yamamura, H., Matsuura, N. and Honda, R. (2019). "Candidates of quorum sensing bacteria in activated sludge associated with N-acyl homoserine lactones." Chemosphere **236** 124292.DOI: https://doi.org/10.1016/j.chemosphere.2019.07.023.

Papenfort, K. (2016). "Quorum sensing signal–response systems in Gram-negative bacteria." Nat Rev Microbiol **14**: 576-588.DOI: https://doi.org/10.1038/nrmicro.2016.89.

Patel, J. D., Colton, E., Ebert, M. and Anderson, J. M. (2012). "Gene expression during *S. epidermidis* biofilm formation on biomaterials." J Biomed Mater Res A **100**(11): 2863-2869.DOI: 10.1002/jbm.a.34221.

Peeters, E., Nelis, H. J. and Coenye, T. (2008). "Comparison of multiple methods for quantification of microbial biofilms grown in microtiter plates." Journal of Microbiological Methods **72**(2): 157-165.DOI: https://doi.org/10.1016/j.mimet.2007.11.010.

Percival, S. L., Suleman, L., Vuotto, C. and G., D. (2015). "Healthcare-Associated Infections, Medical Devices and Biofilms: Risk, Tolerance and Control." J Med Microbiol **64**: 323-334.DOI: https://doi.org/10.1099/jmm.0.000032.

Petrovich, M., Chia-Yun, W., Rosenthal, A., Chen, K.-F., Packman, A. I. and Wells, G. F. (2017). "Nitrosomonas europaea biofilm formation is enhanced by Pseudomonas aeruginosa." FEMS Microbiol Ecol **93**(5).DOI: https://doi.org/10.1093/femsec/fix047.

Pfotenhauer, D., Sellers, E., Olson, M., Praedel, K. and Shafer, M. (2022). "PFAS concentrations and deposition in precipitation: An intensive 5-month study at National Atmospheric Deposition Program – National trends sites (NADP-NTN) across Wisconsin, USA." Atmos Environ **291.** 119368. DOI: https://doi.org/10.1016/j.atmosenv.2022.119368.

Pica, N. E., Miao, Y., Johnson, N. W., Ramos, P., Mahendra, S. and Blotevogel, J. (2021). "Bioelectrochemical treatment of 1,4-dioxane in the presence of chlorinated solvents: design, process, and sustainability considerations." ACS Sustain Chem Eng **9**(8): 3172-3182.DOI: 10.1021/acssuschemeng.0c08152.

Pietramellara, G., Ascher, J., Borgogni, F., Ceccherini, M. T., Guerri, G. and Nannipieri, P. (2009). "Extracellular DNA in soil and sediment: fate and ecological relevance." Biol. Fertil. Soils **45**(3): 219-235.DOI: 10.1007/s00374-008-0345-8.

Pinzon, N. M. (2009). "Analysis of rhamnolipid biosurfactants by methylene blue complexation." Appl Microbiol Biotechnol **82**: 975-981.DOI: https://doi.org/10.1007/s00253-009-1896-9.

Polasko, A. L., Miao, Y., Kwok, I., Park, K., Park, J. O. and Mahendra, S. (2021). "Vinyl chloride and 1,4-dioxane metabolism by *Pseudonocardia dioxanivorans* CB1190." J Hazard Mater Lett **2**. 100039. DOI: 10.1016/j.hazl.2021.100039.

Polasko, A. L. R., Pia, Kaner, R. B. and Mahendra, S. (2021). "A Multipronged Approach for Systematic in vitro Quantification of Catheter-Associated Biofilms." J Haz Mat Lett.**2**. 100032. DOI: 10.1016/j.hazl.2021.100032.

Prakash Singh, M. and Greenstein, M. (2006). "A simple, rapid, sensitive method detecting homoserine lactone (HSL)-related compounds in microbial extracts." J Microbiol Methods **65**(1): 32-37.DOI: https://doi.org/10.1016/j.mimet.2005.06.003.

Ramachandran, S., Nandhakumar, S. and Dhanaraju, M. D. (2011). "Formulation and Characterization of Glutaraldehyde Cross-Linked Chitosan Biodegradable Microspheres Loaded with Famotidine." Trop J Pharm Res **10**(3): 309-316.DOI: 10.4314/tjpr.v10i3.13.

Ramos-Garcia, A. A., Walecka-Hutchison, C. and Freedman, D. L. (2022). "Effect of biostimulation and bioaugmentation on biodegradation of high concentrations of 1,4-dioxane." Biodegradation **33**(2): 157-168.DOI: 10.1007/s10532-022-09971-4.

Randrianjatovo-Gbalou, I., Girbal-Neuhauser, E. and Marcato-Romain, C. E. (2016). "Quantification of biofilm exopolysaccharides using an in situ assay with periodic acid-Schiff reagent." Anal Biochem **500**: 12-14.DOI: 10.1016/j.ab.2016.01.008.

Rao, X., Huang, X., Zhou, Z. and Lin, X. (2013). "An improvement of the 2ˆ(–delta delta CT) method for quantitative real-time polymerase chain reaction data analysis." Biostat Bioinforma Biomath **3**(3): 71-85. PMCID: PMC4280562

Rasamiravaka, T., Labtani, Q., Duez, P. and El Jaziri, M. (2015). "The Formation of Biofilms by Pseudomonas aeruginosa: A Review of the Natural and Synthetic Compounds Interfering with Control Mechanisms." Biomed Res Int **2015**.DOI: 10.1155/2015/759348.

Rashid, M. H. and Kornberg, A. (2000). "Inorganic polyphosphate is needed for swimming, swarming, and twitching motilities of *Pseudomonas aeruginosa*." PNAS **97**(9): 4885-4890.DOI: 10.1073/pnas.060030097.

Razali, M. A. A., Sanusi, N., Ismail, H., Othman, N. and Ariffin, A. (2012). "Application of response surface methodology (RSM) for optimization of cassava starch grafted polyDADMAC synthesis for cationic properties." Starke **64**(12): 935-943.DOI: 10.1002/star.201200007.

Rege, S. U., Yang, R. T. and Cain, C. A. (1998). "Desorption by Ultrasound: Phenol on Activated Carbon and Polymeric Resin." AIChE Journal **44**(7): 1519-1528.DOI: https://doi.org/10.1002/aic.690440706

Richards, C., O'Connor, N., Jose, D., Barrett, A. and Regan, F. (2020). "Selection and optimization of protein and carbohydrate assays for the characterization of marine biofouling." Analytical Methods **12**(17): 2228-2236.DOI: 10.1039/D0AY00272K.

Rittmann, B. E. a. M., Perry (2018). Environmental Biotechnology: Principles and Applications, McGraw-Hill Higher Education.

Roberts, G. A. F. and Taylor, K. E. (1989). "The formation of gels by reaction of chitosan with glutaraldehyde." Makromol Chem **190**: 951-960.DOI: https://doi.org/10.1002/macp.1989.021900504.

Romling, U., Kjelleberg, S., Normark, S., Nyman, L., Uhlin, B. E. and Akerlund, B. (2014). "Microbial biofilm formation: a need to act." J Intern Med **276**(2): 98-110.DOI: 10.1111/joim.12242.

Ross, I., McDonough, J., Miles, J., Storch, P., Kochunarayanan, P. T., Kalve, E., Hurst, J., Dasgupta, S. S. and Burdick, J. (2018). "A review of emerging technologies for remediation of PFASs." Remediation Journal **28**(2): 101-126.DOI: 10.1002/rem.21553.

Roy, R., Tiwari, M., Donelli, G. and Tiwari, V. (2018). "Strategies for combating bacterial biofilms: A focus on anti-biofilm agents and their mechanisms of action." Virulence **9**(1): 522-554.DOI: 10.1080/21505594.2017.1313372.

Saidulu, D., Mujumder, A. and Kumar Gupta, A. (2021). "A systematic review of moving bed biofilm reactor, membrane bioreactor, and moving bed membrane bioreactor for wastewater

treatment: Comparison of research trends, removal mechanisms, and performance." J Environ Chem Eng **9**(5).DOI: https://doi.org/10.1016/j.jece.2021.106112.

Sánchez, M.-C., Llama-Palacios, A., Marín, M.-J., Figuero, E., León, R., Blanc, V., Herrera, D. and Sanz, M. (2013). "Validation of ATP bioluminescence as a tool to assess antimicrobial effects of mouthrinses in an *in vitro* subgingival-biofilm model." Med Oral Patol Oral Cir Bucal. **18**(1): e86-e92.DOI: 10.4317/medoral.18376.

Schittenhelm, N. and Kulicke, W.-M. (2000). "Producing homologous series of molar masses for establishing structure-property relationships with the aid of ultrasonic degradation." Macromol. Chem. Phys. **201**: 1976-1984. DOI: https://doi.org/10.1002/1521-3935(20001001)201:15%3C1976::AID-MACP1976%3E3.0.CO;2-0

Schueller, B. S. and Yang, R. T. (2001). "Ultrasound Enhanced Adsorption and Desorption of Phenol on Activated Carbon and Polymeric Resin." Ind Eng Chem Rest **40**: 4912-4918.DOI: https://doi.org/10.1021/ie010490j.

Schwarz, F., Sculean, A., Romanos, G., Herten, M., Horn, N., Scherbaum, W. and Becker, J. (2005). "Influence of different treatment approaches on the removal of early plaque biofilms and the viability of SAOS2 osteoblasts grown on titanium implants." Clinical Oral Investigations **9**(2): 111-117.DOI: 10.1007/s00784-005-0305-8.

Senthil Muthu Kumar, T., Senthilkumar, K., Ratanit, M., Rajini, N., Canunpanich, N., Hariram, N., Pornwongthong, P. and Siengchin, S. (2021). "Influence of Titanium Dioxide Particles on the Filtration of 1,4-Dioxane and Antibacterial Properties of Electrospun Cellulose Acetate and Polyvinylidene Fluoride Nanofibrous Membranes." J Polym Environ **29**: 775-784.DOI: https://doi.org/10.1007/s10924-020-01919-0.

Sheik, A. R., Muller, E. E. and Wilmes, P. (2014). "A hundred years of activated sludge: time for a rethink." Front Microbiol **7**. 47. DOI: https://doi.org/10.3389/fmicb.2014.0004.

Shen, Q., Gao, J., Liu, J., S, L., Liu, Z., Wang, Y., Guo, B., Zhuang, X. and Zhuang, G. (2016). "A New Acyl-homoserine Lactone Molecule Generated by Nitrobacter winogradskyi." Sci Rep **6**. 1-11.DOI: https://doi.org/10.1038/srep22903.

Shen, Y., Yang, T., Zhu, W. and Zhao, Y. (2017). "Wastewater treatment and biofuel production through attached culture of Chlorella vulgaris in a porous substratum biofilm reactor." J Appl Phycol **29**: 833-841.DOI: https://doi.org/10.1007/s10811-016-0981-6.

Shnit-Orland, M. and Kushmaro, A. (2009). "Coral mucus-associated bacteria: a possible first line of defense." FEMS Microbiol Ecol **67**(3): 371-380.DOI: https://doi.org/10.1111/j.1574-6941.2008.00644.x.

Simmer, R., Mathieu, J., da Silva, M. L. B., Lashmit, P., Gopishetty, S., Alvarez, P. J. J. and Schnoor, J. L. (2020). "Bioaugmenting the poplar rhizosphere to enhance treatment of 1,4-dioxane." Sci Total Environ **744**.DOI: 10.1016/j.scitotenv.2020.140823.

Singh, A. K., Prakash, P., Achra, A., Singh, G. P., Das, A. and Singh, R. K. (2017). "Standardization and Classification of *In Vitro* Biofilm Formation by Clinical Isolates of *Staphylococcus* aureus." J Glob Infect Dis **9**(3): 93-101.DOI: 10.4103/jgid.jgid_91_16.

Singh Kalra, S., Cranmer, B., Dooley, G., Hanson, A. J., Maraviov, S., Mohanty, S., Blotevogel, J. and Mahendra, S. (2021). "Sonolytic Destruction of Per- and Polyfluoroalkyl Substances in Groundwater, Aqueous Film-Forming Foams, and Investigation Derived Waste." Chem Eng J.**425.** 131778**.** DOI: 10.1016/j.cej.2021.131778.

Sodha, K. H., Jadav, J. K., Gajera, H. P. and Rathod, K. J. (2015). "Characterization of Silver Nanoparticles Synthesized by Different Chemical Reduction Methods." Int J Pharm Bio **6**(4): 199-208.

Speranza, A., Calzoni, G. L. and Pacini, E. (1997). "Occurrence of mono- or disaccharides and polysaccharide reserves in mature pollen grains." Sex Plant Reprod **10**(2): 110-115.DOI: 10.1007/s004970050076.

Stauder, M., Huq, A., Pezzati, E., Grim, C. J., Ramoino, P., Pane, L., Colwell, R. R., Pruzzo, C. and Vezzulli, L. (2012). "Role of GbpA protein, an important virulence-related colonization factor, for *Vibrio cholerae's* survival in the aquatic environment." Environ Microbiol Rep **4**(4): 439-445.DOI: https://doi.org/10.1111/j.1758-2229.2012.00356.x.

Stenehjem, E., Rimland, D., Crispell, E. K., Stafford, C., Gaynes, R. and Satola, S. W. (2012). "Cepheid Xpert *MRSA* cycle threshold in discordant colonization results and as a quantitative measure of nasal colonization burden." J clin microbiol **50**(6): 2079-2081.DOI: 10.1128/JCM.06690-11.

Stepanović, S., Vuković, D., Dakić, I., Savić, B. and Švabić-Vlahović, M. (2000). "A Modified Microtiter-Plate Test for Quantification of Staphylococcal Biofilm Formation." J Microbiol Methods **40**(2): 175-179.DOI: https://doi.org/10.1016/S0167-7012(00)00122-6.

Stepanović, S., Vuković, D., Hola, V., Di Bonaventura, G., Djukić, S., Cirković, I. and Ruzicka, F. (2017). "Quantification of Biofilm in Microtiter Plates: Overview of Testing Conditions and Practical Recommendations for Assessment of Biofilm Production by *Staphylococci.*" APMIS **115** (8): 891-899.DOI: https://doi.org/10.1111/j.1600-0463.2007.apm_630.x.

Stickler, D. J. (2014). "Clinical complications of urinary catheters caused by crystalline biofilms: something needs to be done." J. Intern. Med **276**(2): 120-129.DOI: https://doi.org/10.1111/joim.12220.

Stoppel, W. L., White, J. C., Horava, S. D., Henry, A. C., Roberts, S. C. and Bhatia, S. R. (2014). "Terminal sterilization of alginate hydrogels: efficacy and impact on mechanical properties." J Biomed Mater Res B Appl Biomater **102**(4): 877-884.DOI: 10.1002/jbm.b.33070.

Tang, G., Galluzzi, M., Zhang, B., Shen, Y. L. and Stadler, F. J. (2019). "Biomechanical Heterogeneity of Living Cells: Comparison between Atomic Force Microscopy and Finite Element Simulation." Langmuir **35**(23): 7578-7587.DOI: 10.1021/acs.langmuir.8b02211.

Tanner, W. D., VanDerslice, J. A., Goel, R. K., Leecaster, M. K., Fisher, M. A., Olstadt, J., Gurley, C. M., Morris, A. G., Seely, K. A., Chapman, L., Korando, M., Shabazz, K.-A., Stadsholt, A., VanDeVelde, J., Braun-Howland, E., Minihane, C., Higgins, P. J., Deras, M., Jaber, O., Jette, D. and Gundlapalli, A. V. (2019). "Multi-state study of Enterobacteriaceae harboring extended-spectrum beta-lactamase and carbapenemase genes in U.S. drinking water." Sci Rep **9** (1). 1-8. .DOI: https://doi.org/10.1038/s41598-019-40420-0.

Tempe, J., Petit, A., Holsters, M., van Montagu, M. and Schell, J. (1997). "Thermosensitive step associated with transfer of the Ti plasmid during conjugation: Possible relation to transformation in crown gall." PNAS **74**(7): 2848-2849.DOI: https://doi.org/10.1073/pnas.74.7.2848.

Tessmer, C. H., Vidic, R. D. and Uranowski, L. J. (1997). "Impact of Oxygen-Containing Surface Functional Groups on Activated Carbon Adsorption of Phenols." Environ. Sci. Technol. **31**(7): 1872-1878.DOI: 10.1021/es960474r.

Thérien-Aubin, H., Chen, L. and Ober, C. K. (2011). "Fouling-resistant polymer brush coatings." Polymer **52**(24): 5419-5425.DOI: 10.1016/j.polymer.2011.09.017.

Trevisani, L., Sartori, S., Rossi, M. R., Bovolenta, R., Scoponi, M., Gullini, S. and Abbasciano, V. (2005). "Degradation of polyurethane gastrostomy devices: what is the role of fungal colonization?" Dig Dis Sci **50**(3): 463-469.DOI: 10.1007/s10620-005-2459-2.

Tripathi, S., Chandra, R., Purchase, D., Bilal, M., Mythili, R. and Yadav, S. (2022). "Quorum sensing - a promising tool for degradation of industrial waste containing persistent organic pollutants." Environ Pollut **292**. 267-279. DOI: https://doi.org/10.1016/j.envpol.2021.118342.

Tseng, L. Y., Gori, R. and Rosso, D. (2015). "Effects of Activated Sludge Process Conditions on the Production of Extracellular Polymeric Substances: Results of Yearlong Monitoring in a Warm Climate." Environ Eng Sci **32**(7). 939-945. DOI: https://doi.org/10.1089/ees.2014.0523.

Vajihinejad, V., Gumfekar, S. P., Bazoubandi, B., Najafabadi, Z. R. and Soares, J. B. P. (2018). "Water Soluble Polymer Flocculants: Synthesis, Characterization, and Performance Assessment." Macromol Mater Eng **304**(2). 1800526. DOI: 10.1002/mame.201800526.

Vasudevan, R. (2014). "Biofilms: Microbial Cities of Scientific Significance." J Microbiol Exp **1**(3). 00014. DOI: 10.15406/jmen.2014.01.00014.

Verderosa, A. D., Totsika, M. and Fairfull-Smith, K. E. (2019). "Bacterial Biofilm Eradication Agents: A Current Review." Front Chem **7**. 824. DOI: 10.3389/fchem.2019.00824.

Verrecht, B., Judd, S., Guglielmi, G., Brespols, C. and Mulder, J. W. (2008). "An aeration energy model for an immersed membrane bioreactor." Water Res **42**(19): 4761-4770.DOI: https://doi.org/10.1016/j.watres.2008.09.013.

Vinardell, S., Astals, S., Peces, M., Cardete, M. A., Fernandez, I., Mata-Alvarez, J. and Dosta, J. (2020). "Advances in anaerobic membrane bioreactor technology for municipal wastewater treatment: A 2020 updated review." Renew Sust Energ Rev **130.** 109936**.**.DOI: https://doi.org/10.1016/j.rser.2020.109936.

Vo, H. N. P., Nguyen, T. M. H., Ngo, H. H., Guo, W. and Shukla, P. (2021). "Biochar sorption of perfluoroalkyl substances (PFASs) in aqueous film-forming foams-impacted groundwater: Effects of PFASs properties and groundwater chemistry." Chemosphere **286**(Pt 1): 131622.DOI: 10.1016/j.chemosphere.2021.131622.

Vu, C. T. and Wu, T. (2020). "Recent progress in adsorptive removal of per- and poly-fluoroalkyl substances (PFAS) from water/wastewater." Crit Rev Environ Sci Technol **50**: 1-40.DOI: 10.1080/10643389.2020.1816125.

Ward, A. J., Lewis, D. M. and Green, F. B. (2014). "Anaerobic digestion of algae biomass: A review." Algal Res **5**: 204-214.DOI: https://doi.org/10.1016/j.algal.2014.02.001.

Watanabe, N., Takata, M., Takemine, S. and Yamamoto, K. (2018). "Thermal mineralization behavior of PFOA, PFHxA, and PFOS during reactivation of granular activated carbon (GAC) in nitrogen atmosphere." Environ Sci Pollut Res Int **25**(8): 7200-7205.DOI: 10.1007/s11356-015-5353-2.

Wellinghausen, N., Siegel, D., Winter, J. and Gebert, S. (2009). "Rapid diagnosis of candidaemia by real-time PCR detection of *Candida* DNA in blood samples." J Med Microbiol **58**(Pt 8): 1106-1111.DOI: 10.1099/jmm.0.007906-0.

Westreich, P., Mimna, R., Brewer, J. and Forrester, F. (2018). "The removal of short-chain and long-chain perfluoroalkyl acids and sulfonates via granular activated carbons: A comparative column study." Remed J **29**(1): 19-26.DOI: 10.1002/rem.21579.

Whiteley, M., Parsek, M. R. and Greenbert, E. P. (2000). "Regulation of Quorum Sensing by *RpoS* in *Pseudomonas aeruginosa.*" J Bacteriol **182**(15). 4356-4360. .DOI: https://doi.org/10.1128/JB.182.15.4356-4360.2000.

Wong, E., Vaaje-Kolstad, G., Ghosh, A., Hurtado-Guerrero, R., Konarev, P. V., Ibrahim, A. F. M., Svergun, D. I., Eijsink, V. G. H., Chatterjee, N. S. and van Aalten, D. M. F. (2012). "The *Vibrio cholerae* Colonization Factor GbpA Possesses a Modular Structure that Governs Binding to Different Host Surfaces." PLOS Pathogens **8**(1): e1002373.DOI: 10.1371/journal.ppat.1002373.

Wu, L., Ning, D., Zhang, B., Li, Y., Zhang, P., Shan, X., Zhang, Q., Brown, M. R., Li, Z., Van Nostrand, J. D., Ling, F., Xiao, N., Zhang, Y., Vierheilig, J., Wells, G. F., Yang, Y., Deng, Y.,

Tu, Q., Wang, A., Zhang, T., He, Z., Keller, J., Nielsen, P. H., Alvarez, P. J. J., Criddle, C. S., Wagner, M., Tiedje, J. M., He, Q., Curtis, T. P., Stahl, D. A., Alvarez-Cohen, L., Rittmann, B. E., Wen, X. and Zhou, J. (2019). "Global diversity and biogeography of bacterial communities in wastewater treatment plants." Nat Microbiol **4**: 1183-1195.DOI: https://doi.org/10.1038/s41564-019-0426-5.

Xie, Y., Liao, X., Zhang, J., Yang, F. and Fan, Z. (2018). "Novel chitosan hydrogels reinforced by silver nanoparticles with ultrahigh mechanical and high antibacterial properties for accelerating wound healing." Int J Biol Macromol **119**: 402-412.DOI: 10.1016/j.ijbiomac.2018.07.060.

Xiu, Z. M., Ma, J. and Alvarez, P. J. (2011). "Differential effect of common ligands and molecular oxygen on antimicrobial activity of silver nanoparticles versus silver ions." Environ Sci Technol **45**(20): 9003-9008.DOI: 10.1021/es201918f.

Xu, H., Deng, Y., Li, X., Liu, Y., Huang, S., Yang, Y., Wang, Z. and Hu, C. (2021). "Effect of Increasing C/N Ratio on Performance and Microbial Community Structure in a Membrane Bioreactor with a High Ammonia Load." IJERPH **18**(15). 8070..DOI: https://doi.org/10.3390/ijerph18158070.

Xu, H., Wang, C., Liang, Z., He, L. and Wu, W. (2014). "The structure and component characteristics of partial nitrification biofilms under autotrophic and heterotrophic conditions." Appl Microbiol Biotechnol **99**: 3673-3683.DOI: https://doi.org/10.1007/s00253-014-6300-8.

Xu, J. H., Gao, N. Y., Deng, Y., Sui, M. H. and Tang, Y. L. (2011). "Perchlorate removal by granular activated carbon coated with cetyltrimethyl ammonium bromide." J Colloid Interface Sci **357**(2): 474-479.DOI: 10.1016/j.jcis.2011.01.017.

Yan, Z., Huang, M., Melander, C. and Kjellerup, B. V. (2020). "Dispersal and inhibition of biofilms associated with infections." Journal of Applied Microbiology **128**(5): 1279-1288.DOI: https://doi.org/10.1111/jam.14491.

Yang, L., Barken, K. B., Skindersoe, M. E., Christensen, A. B., Givskov, M. and Tolker-Nielsen, T. (2007). "Effects of iron on DNA release and biofilm development by *Pseudomonas aeruginosa*." Microbiology **153**(5): 1318-1328.DOI: https://doi.org/10.1099/mic.0.2006/004911-0.

Ye, F., Ye, Y. and Li, Y. (2011). "Effect of C/N ratio on extracellular polymeric substances (EPS) and physicochemical properties of activated sludge flocs." J Hazard Mater **188**(1-3): 37-43.DOI: https://doi.org/10.1016/j.jhazmat.2011.01.043.

Yeh, S. B., Chen, C. S., Chen, W. Y. and Huang, C. J. (2014). "Modification of silicone elastomer with zwitterionic silane for durable antifouling properties." Langmuir **30**(38): 11386-11393.DOI: 10.1021/la502486e.

Yeon, K.-M., Cheong, W.-S., Oh, H.-S., Lee, W.-N., Hwang, B.-K., Lee, C.-H., Beyanal, H. and Lewandowski, Z. (2009). "Quorum Sensing: A New Biofouling Control Paradigm in a Membrane Bioreactor for Advanced Wastewater Treatment." Environ Sci Technol **43**(2): 380-385.DOI: https://doi.org/10.1021/es8019275.

Yerragopu, P. S., Hiregoudar, S., Nidoni, U., Ramappa, K. T., Sreenivas, A. G. and Doddagoudar, S. R. (2020). "Chemical Synthesis of Silver Nanoparticles Using Tri-sodium Citrate, Stability Study and Their Characterization." Int Res J Pure Appl Chem **21**(3): 37-50.DOI: 10.9734/IRJPAC/2020/v21i330159.
Yin, W., Wang, Y., Liu, L. and He, J. (2019). "Biofilms: The Microbial "Protective Clothing" in Extreme Environments." Internat j molec sci **20**(14): 3423.DOI: 10.3390/ijms20143423.

Zabed, H. M., Qi, X., Yun, J. and Zhang, H. (2019). Anaerobic Digestion of Microalgae Biomass for Methane Production. Microalgae Biotechnology for Development of Biofuel and Wastewater Treatment, Springer, Singapore.

Zakia, M., Koo, J. M., Kim, D., Ji, K., Huh, P., Yoon, J. and Yoo, S. I. (2020). "Development of silver nanoparticle-based hydrogel composites for antimicrobial activity." Green Chem Lett Rev **13**(1): 34-40.DOI: 10.1080/17518253.2020.1725149.

Zeng, X., Guo, X., Su, G., Danquah, M. K., Zhang, S., Lu, Y., Sun, Y. and Lin, L. (2015). "Bioprocess considerations for microalgal-based wastewater treatment and biomass production." Renewable and Sustainable Energy Reviews **42**: 1385-1392.DOI: 10.1016/j.rser.2014.11.033.

Zhang, D. Q., Zhang, W. L. and Liang, Y. N. (2019). "Adsorption of perfluoroalkyl and polyfluoroalkyl substances (PFASs) from aqueous solution - A review." Sci Total Environ **694**: 133606.DOI: 10.1016/j.scitotenv.2019.133606.

Zhang, S., Gedalanga, P. B. and Mahendra, S. (2016). "Biodegradation kinetics of 1,4-dioxane in chlorinated solvent mixtures." Environ Sci Technol **50**(17): 9599-9607.DOI: 10.1021/acs.est.6b02797.

Zhao, K., Tseng, B. S., Beckerman, B., Jin, F., Gibiansky, M. L., Harrison, J. J., Luijten, E., Parsek, M. R. and Wong, G. C. L. (2013). "Psl trails guide exploration and microcolony formation in *Pseudomonas aeruginosa* biofilms." Nature **497**(7449): 388-391.DOI: 10.1038/nature12155.

Zou, X., Zhao, X. and Ye, L. (2015). "Synthesis of cationic chitosan hydrogel and its controlled glucose-responsive drug release behavior." Chemical Engineering Journal **273**: 92-100.DOI: 10.1016/j.cej.2015.03.075.

Zuo, P., Metz, J., Yu, P. and Alvarez, P. J. J. (2022). "Biofilm-responsive encapsulated-phage coating for autonomous biofouling mitigation in water storage systems." Water Res **224**. 119070. DOI: https://doi.org/10.1016/j.watres.2022.119070.